letnik/volume **52** - št./no. **3/06** - str./pp. **141-206**
Ljubljana, mar./Mar. 2006, zvezek/issue **491**

STROJNIŠKI VESTNIK

JOURNAL OF MECHANICAL ENGINEERING

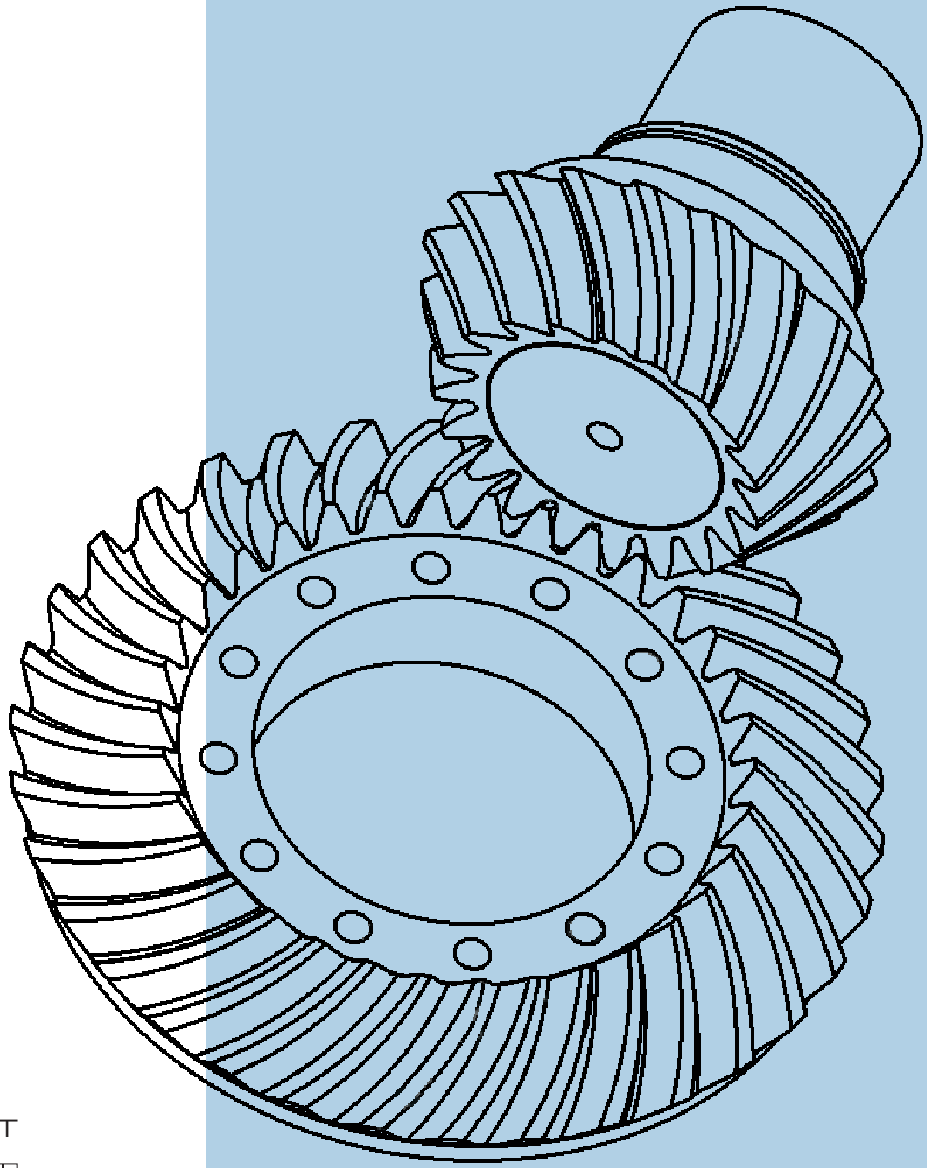

cena 800 SIT

9 770039 248001

ISSN 0039-2480

Vsebina - Contents

Strojniški vestnik - Journal of Mechanical Engineering
letnik - volume 52, (2006), številka - number 3
Ljubljana, marec - March 2006
ISSN 0039-2480

Izhaja mesečno - Published monthly

Strojniški vestnik - Journal of Mechanical Engineering 52(2006)3, 142-160
UDK - UDC 004.94:621.039.58
Izvirni znanstveni članek - Original scientific paper (1.01)

Simuliranje preizkusa težke nesreče Phebus FPT1 s programom MELCOR

Simulation of the Phebus FPT1 Severe Accident Experiment with the MELCOR Computer Code

Matjaž Leskovar - Borut Mavko
(Institut Jožef Stefan, Ljubljana)

V okviru sodelovanja v Mednarodnem standardnem problemu OECD št. 46 smo z dvema verzijama programa MELCOR 1.8.5 (QZ in RE) simulirali ključne pojave v gorivnem svežnju in primarnem krogu naprave Phebus med fazo degradacije sredice pri preizkusu Phebus FPT1. Pri razvoju vhodnega modela smo upoštevali priporočila glede nodalizacije in uporabe privzetih parametrov, ki so podana v specifikacijah ISP-46. Posebno pozornost smo namenili modeliranju specifičnosti naprave Phebus.

Primerjava rezultatov izračunov s preizkusnimi meritvami je pokazala dobro ujemanje termohidravličnih spremenljivk in zadovoljivo ujemanje končnih izpustov za večino radioaktovnih snovi, medtem ko je odlaganje v uparjalniku precenjeno. Ključni dogodki so napovedani ob pravih časih. Razlike med rezultati simuliranj z obema različicama programa MELCOR so zanemarljive za termohidravlične spremenljivke, majhne za izpuste radioaktovnih snovi in časovno napoved ključnih dogodkov, vendar pomembne za odlaganje radioaktovnih snovi in degradacijo sredice. V splošnem se rezultati novejše različice RE programa MELCOR 1.8.5 bolje ujemajo z meritvami preizkusa.

(Ključne besede: nezgode reaktorjev, modeliranje, simuliranje, PHEBUS, MELCOR)

As part of the OECD International Standard Problem No. 46, the thermal-hydraulic, fuel-degradation and aerosol phenomena, which occurred in the bundle and circuit of the Phebus facility during the degradation phase of the Phebus FPT1 experiment, were simulated with two versions of MELCOR 1.8.5 (QZ and RE). The input model was developed by strictly following the recommendations on noding and the use of the default parameters provided in the ISP-46 Specification Report. Special attention was given to the modelling of the specifics of the Phebus facility.

A comparison of the simulation results and the experimental measurements showed good agreement for the thermal-hydraulic variables and satisfactory agreement for the total releases for most radio-nuclides, whereas the radio-nuclide depositions in the steam generator were overestimated. The timing of the key events was relatively well predicted. The differences between the simulation results of both MELCOR versions were negligible for the thermal-hydraulic variables, small for the radio-nuclide releases and the timing of the key events, but significant for the radio-nuclide depositions and the bundle degradation. In general, the results of the newer MELCOR 1.8.5 version RE show better agreement with the experimental measurements.

(Keywords: reactor accident, modelling, simulation, PHEBUS, MELCOR)

0 UVOD

V programu Phebus FP [1] raziskujejo ključne pojave med hipotetično težko nesrečo v lahkovodnem jedrskem reaktorju s serijo integralnih preizkusov. Naprava Phebus, ki je na Institutu za zaščito pred sevanjem in za nuklearno varnost ("Institut de

0 INTRODUCTION

The Phebus FP program [1] investigates the key phenomena involved in light-water-reactor severe-accident sequences through a series of in-pile integral experiments. The Phebus facility, which is located at the "Institut de radioprotection et de

radioprotection et de sûreté nucléaire" - IRSN), v Cadarache-u, Francija, je sestavljena iz pomanjšane reaktorske sredice, pomanjšanega primarnega kroga z uparjalnikom in pomanjšanega zadrževalnega hrama. Phebus FPT1 [2], drugi preizkus v vrsti, je bil izbran kot osnova za Mednarodni standardni problem OECD št. 46 (MSP-46 ali ISP-46) ([3] in [4]). Preizkus omogoča ocenjevanje zmožnosti sistemskih programov, namenjenih modeliranju težkih nesreč, za celostno obravnavo pojavov, ki zajemajo degradacijo sredice do poznih faz (nastanek bazena taline), nastanek vodika, izpust in transport razcepkov, pojave v primarnem krogu in zadrževalnem hramu ter kemijo joda.

Glavni namen MSP-46 je oceniti zmožnost računalniških programov za celostno modeliranje fizikalnih pojavov med težko nesrečo, od začetnih faz degradacije sredice do obnašanja sproščenih razcepkov v zadrževalnem hramu. Računalniške programe naj bi uporabljali podobno, kakor se uporabljajo pri izračunih za jedrske elektrarne. To pomeni uporabo standardnih modelov in opcij, kolikor je mogoče, ter podobno natančen opis naprave Phebus, kakor se uporablja za opis jedrskih elektrarn. Priporočila glede ustrezne nodalizacije naprave Phebus so predstavljena v specifikacijah MSP-46 [3], kjer je predpisano tudi, na koliko vozlišč je treba razdeliti posamezne dele naprave.

Sodelujoči pri MSP-46 so uporabljali različne računalniške programe, s katerimi so simulirali napravo Phebus v celoti ali njen del [3]. Odsek za reaktorsko tehniko Instituta "Jožef Stefan" je sodeloval v MSP-46 z dvema različicama programa MELCOR 1.8.5 (QZ in RE) ([5] in [6]) (gorivni sveženj in primarni krog) in s programom CONTAIN 2.0 [7] (zadrževalni hram).

1 PREIZKUS

1.1 Naprava Phebus

Preizkusni del naprave Phebus predstavlja v razmerju okoli 1/5000 pomanjšani francoski 900 MW tlačnovodni jedrski reaktor [2]. Na sliki 1 je prikazana shema ključnih delov naprave Phebus.

Reaktorska sredica je 1 m visok gorivni sveženj iz 20 gorivnih palic, ki je obdan s keramičnim izolacijskim ovojem, in je znotraj tlačne cevi (sl. 2). V središču gorivnega svežnja je palica, to je reaktorska krmilna palica. Preizkusna sredica, obdana z večplastno cevjo, je vstavljena v tlačno cev, ki poteka skozi središče bistveno večje 40 MW pogonske

sûreté nucléaire" (IRSN) in Cadarache, France, incorporates scaled-down representations of the reactor core, the primary circuit including the steam generator, and the containment. Phebus FPT1 [2], the second experiment in the series, was selected as the basis for the OECD International Standard Problem No. 46 (ISP-46) ([3] and [4]). The experiment provides the opportunity to assess the capability of systems-level severe-accident modelling codes in an integral manner, covering core degradation through to the late phase (melt-pool formation), hydrogen production, fission-products release and transport, circuit and containment phenomena, and iodine chemistry.

The general objective of the ISP-46 is to assess the capability of the computer codes to model, in an integrated way, the physical processes taking place during a severe accident in a pressurized water reactor, from the initial stages of core degradation through to the behaviour of the released fission products in the containment. The codes are supposed to be used in a similar manner as they would be used for plant studies, employing standard models and options as far as possible, with representations of the facility and similar details as used for plant studies. The recommendations for the appropriate noding of the Phebus facility are given in the ISP-46 specification [3], where the number of nodes in different parts of the facility is prescribed.

A number of codes were used by the ISP-46 participants, simulating the Phebus facility as a whole or part of it [3]. The Jo□ef Stefan Institute Reactor Engineering Division participated in the ISP-46 with two versions of the MELCOR 1.8.5 computer code (QZ and RE) ([5] and [6]) (bundle and circuit part) and with the CONTAIN 2.0 computer code [7] (containment part).

1 EXPERIMENT

1.1 Phebus facility

The overall scaling factor of the Phebus facility test train is approximately 1/5000 with respect to the French 900-MW pressurized-water reactor [2]. In Fig. 1 a schematic view of the essential part of the Phebus facility is presented.

The degrading reactor core is represented by a 20-rod, 1-m-high, test-fuel bundle surrounded by an insulating ceramic shroud fitted inside a pressure tube (Fig. 2). A rod simulating the reactor control-rod system occupies the central position. The test device is inserted into a pressurized-water loop,

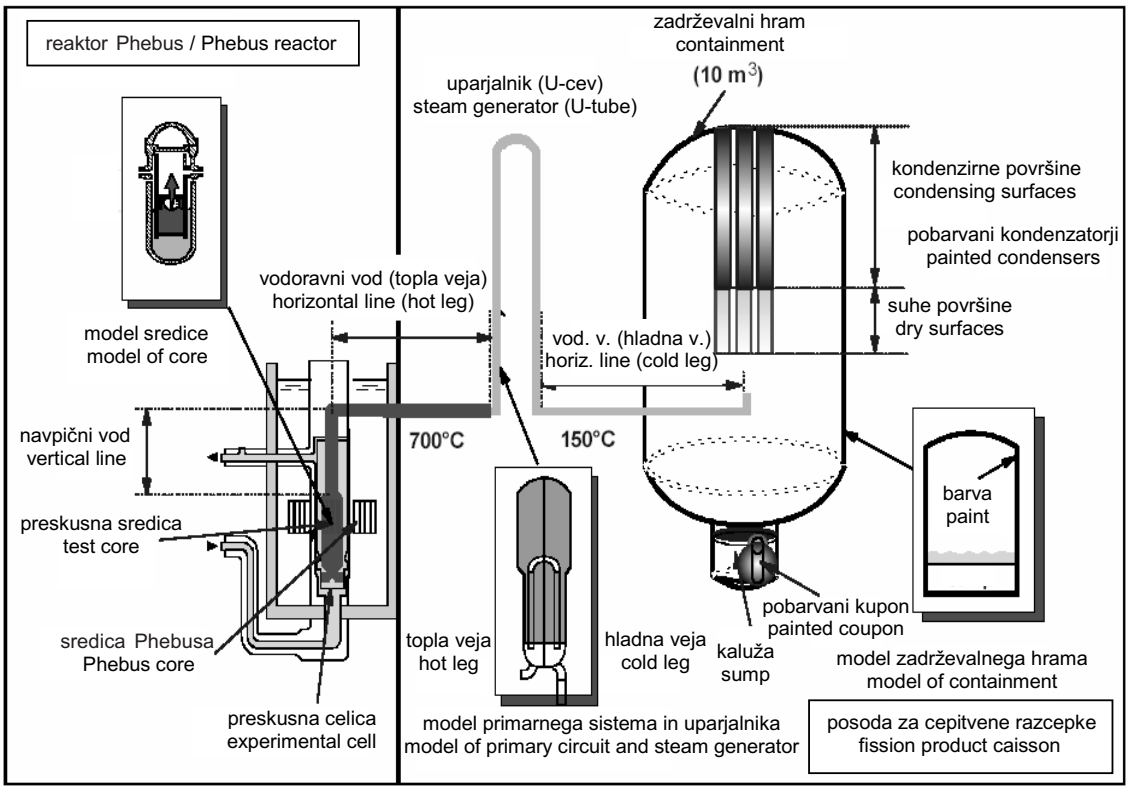

Sl. 1. *Shema naprave Phebus*
Fig. 1. *Schematic representation of the Phebus facility*

sredice Phebus. Zgornji predel nad preizkusnim gorivnim svežnjem je povezan s preizkusnim primarnim krogom, v katerem je cev v obliki narobe obrnjene črke U, pomeni pa uparjalnik tlačnovodnega reaktorja. Primarni cevovod je povezan s posodo s prostornino 10 m^3, to je zadrževalni hram (simulacija zloma v hladni veji), kamor med preizkusom odtekajo mešanica pare in vodika ter radioaktivne razpršene snovi. Posoda zadrževalnega hrama vsebuje ustrezno pomanjšane pobarvane površine in z vodo napolnjeno kalužo za raziskovanje obnašanja joda v dejanskih okoliščinah.

1.2 Opis preizkusa

Preizkusni gorivni sveženj FPT1 je vseboval 18 gorivnih palic tlačnovodnega reaktorja, ki so bile poprej obsevane do povprečne zgorelosti 23,4 GWd/tU, dve instrumentacijski sveži gorivni palici in eno krmilno palico iz srebra, indija in kadmija. Pred začetkom preizkusa so v napravi Phebus gorivni sveženj okoli 7 dni obsevali pri povprečni moči svežnja okoli 205 kW, da bi v gorivu ustvarili kratkožive razcepke. Po tej pripravljalni fazi so

located at the centre of the 40-MW Phebus driver core. The upper plenum above the test-fuel bundle is connected to an experimental circuit, including an inverted U-tube that simulates a PWR steam generator. At the outlet of the circuit, the steam-hydrogen mixture and the radioactive aerosols are injected into a 10 m^3 vessel simulating the containment building of a reactor (cold-leg break simulation). The containment vessel includes scaled painted surfaces and a water-filled sump to investigate the iodine behaviour under realistic conditions.

1.2 Experiment description

The FPT1 test bundle, which included 18 PWR fuel rods previously irradiated to an average burn-up level of 23.4 GWd/tU, two instrumented fresh fuel rods and one silver-indium-cadmium control rod, was pre-irradiated for approximately 7 days with an average bundle power of approximately 205 kW in the Phebus reactor before the experimental phase of the test itself in order to generate short-lived fission products in the fuel. After the pre-

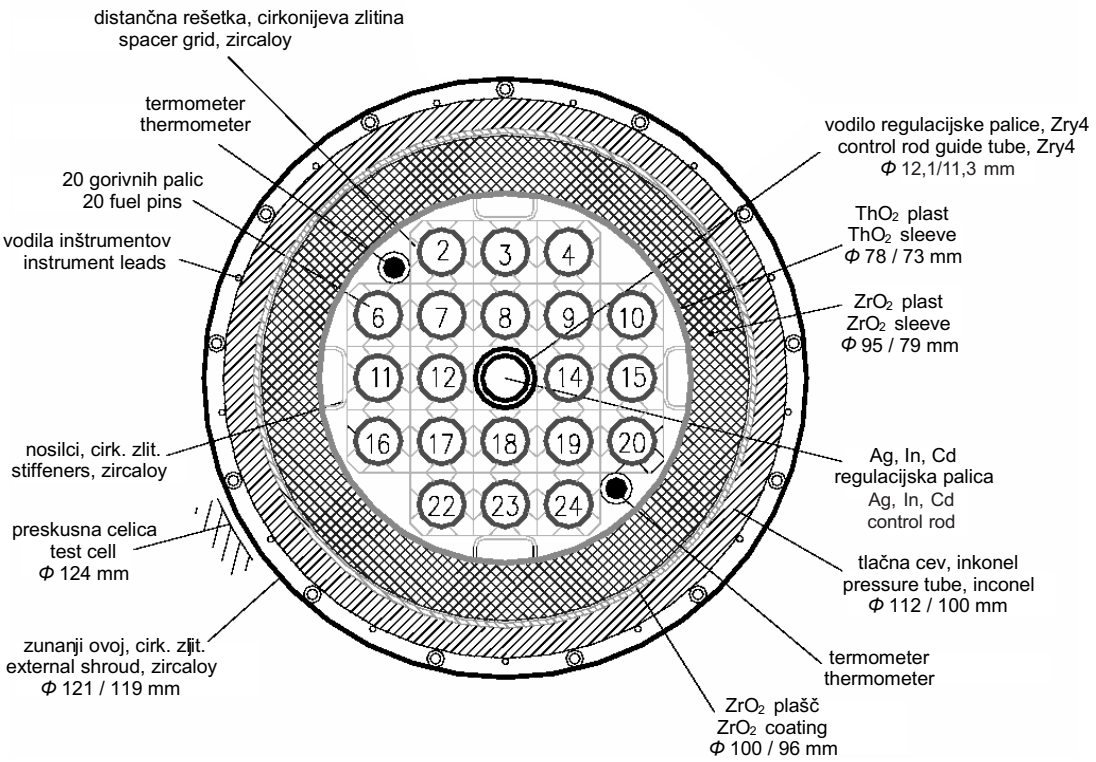

Sl 2. *Prečni prerez FPT1 reaktorske posode z gorivnim svežnjem*
Fig. 2. *Radial configuration of the FPT1 bundle*

potrebovali 36 ur za zmanjšanje zastrupitve reaktorja s ksenonom, za posušitev gorivnega svežnja z nevtralnim plinom ter za nastavitev začetnih pogojev. Dejanski preizkus se je začel z vbrizgavanjem pare v gorivni sveženj in s postopnim dvigovanjem jedrske moči sredice.

Med fazo degradacije gorivnega svežnja, ki je trajala približno 5 ur, so vhodni tok vodne pare, ki so jo v preizkusni cevovod vbrizgavali s spodnje strani, spreminjali od 0,5 do 2,2 g/s in tako ustvarili razmere za oksidacijo, pri tem pa so moč gorivnega svežnja postopoma povečevali od 0,65 kW do 36,5 kW (sl. 3). Fazo degradacije gorivnega svežnja lahko razdelimo na dve obdobji. Prvo obdobje je bilo namenjeno toplotni umeritvi svežnja in meritvam faktorja sklopitve med preizkusnim svežnjem in pogonsko sredico. V tem obdobju, ki je trajalo okoli 7900 s, so moč svežnja in tok pare spreminjali po korakih, da bi preverili toplotni odziv svežnja. Drugo obdobje, ki je trajalo od približno 7900 s do približno 17000 s, predstavlja dejanski temperaturni prehodni pojav in fazo degradacije gorivnega svežnja. Faza degradacije gorivnega svežnja je bila posebej posvečena izpustom razcepkov in snovem goriva, struktur in krmilne palice, da bi lahko raziskovali

conditioning phase, a period of 36 hours was necessary to bring down the reactor xenon poisoning, to dry the bundle using a neutral gas and to establish the initial conditions. The experiment itself then began by injecting steam into the bundle and gradually increasing the core nuclear power.

The fuel-degradation phase lasted about 5 hours, during which time the inlet-steam flow rate injected at the bottom of the test train varied from 0.5 to 2.2 g/s, providing oxidising conditions, while the bundle power was progressively increased from 0.65 kW up to 36.5 kW (Fig. 3). The bundle degradation phase consisted of two main periods. The first one, devoted to the thermal calibration of the bundle and to the measurement of the coupling factor between the experimental bundle and the driver core, lasted app. 7900 s. During this period, the bundle power and the steam flow rate were changed step by step in order to check the thermal response of the bundle. The second period was the real temperature transient and degradation phase of the test, lasting from app. 7900 s to app. 17000 s. The degradation phase was especially devoted to the release of fission products, and bundle, structure and control rod materials in order to study their

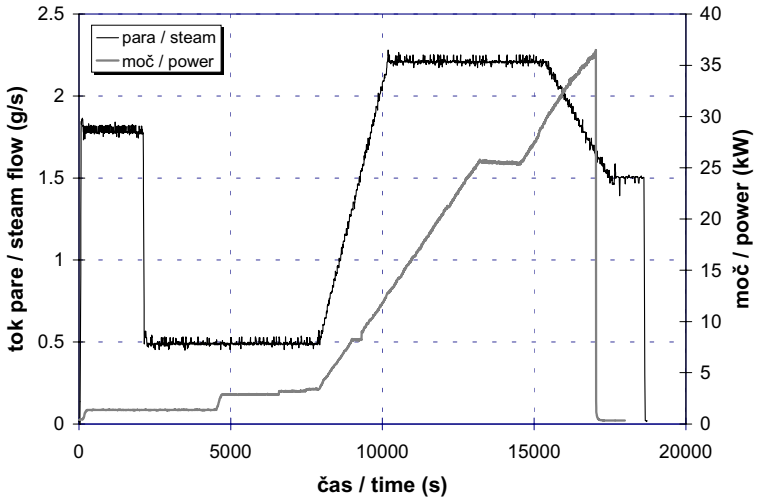

Sl. 3. *Vstopni tok pare in moč gorivnega svežnja v FPT1*
Fig. 3. *Inlet steam flow history and bundle power in FPT1*

njihov prenos in zadrževanje v preizkusnem primarnem krogu.

Po fazi degradacije se je preizkus nadaljeval z razpršeno, izpiralno in kemijsko fazo, ki pa jih v prispevku ne obravnavamo.

2 OPIS MODELA NAPRAVE PHEBUS

2.1 Program MELCOR

MELCOR je popolnoma integriran, inženirski računalniški program, ki modelira napredovanje težkih nesreč v lahkovodnih jedrskih reaktorjih [8]. MELCOR razvijajo v "Sandia National Laboratories" za upravni organ ZDA kot orodje za oceno tveganja jedrskih elektrarn. Simulirni program MELCOR je sestavljen iz tako imenovanih modulov, ki modelirajo reaktor ali preizkusno napravo na prilagojen način. Moduli so razdeljeni po pojavih in ne po področjih. Tako je na primer mehanika tekočin v vseh delih modela opisana z istim naborom enačb, izračuni pa potekajo sočasno.

S programom MELCOR je mogoče modelirati naslednje pojave med nezgodo:

- termohidravlični odziv primarnega reaktorskega hladilnega sistema, reaktorske votline, zadrževalnega hrama in izolacijskih zgradb;
- odkrivanje sredice (izguba hladiva), segrevanje goriva, oksidacija srajčk, degradacija goriva (deformacija gorivnih palic) ter taljenje in porušitev sredice;
- segrevanje spodnjega dela reaktorske posode zaradi porušitve sredice, toplotne in mehanične

transport and retention in the experimental circuit.

After the degradation phase the experiment continued with the aerosol phase, the washing phase and the chemistry phase, which are not treated in this paper.

2 MODEL DESCRIPTION OF PHEBUS FACILITY

2.1 MELCOR code

MELCOR is a fully integrated, engineering-level computer code that models the progression of severe accidents in light-water-reactor nuclear power plants [8]. MELCOR is being developed at Sandia National Laboratories for the U.S. Nuclear Regulatory Commission as a plant-risk assessment tool. The MELCOR simulation code is composed of several so-called "packages" that model a reactor or experimental facility in a modular fashion. The modularisation is by phenomena, not by region. For example, fluid-dynamics calculations for all parts of the model are solved simultaneously, using the same set of fluid equations in all regions.

With MELCOR, the following phenomena occurring during an accident can be modelled:

- the thermal-hydraulic response of the primary-reactor coolant system, the reactor cavity, the containment, and the confinement buildings,
- core uncovering (loss of coolant), fuel heat up, cladding oxidation, fuel degradation (loss of rod geometry), and core-material melting and relocation,
- the heat up of the reactor vessel's lower head from relocated fuel materials and the thermal and mechanical loading and failure of the vessel lower

obremenitve sten reaktorske posode ter odpoved reaktorske posode, izliv taline iz reaktorske posode v reaktorsko votlino;
- interakcija taline z betonom in nastajanje razpršin;
- nastajanje vodika v reaktorski posodi in zunaj nje, prenos in gorenje vodika;
- izpust razcepkov (razpršine in hlapi), njihov prenos in odlaganje;
- obnašanje radioaktivnih razpršin v zadrževalnem hramu;
- vpliv varnostnih sistemov na termohidravlični odziv in obnašanje radioaktivnih snovi.

Za modeliranje preizkusa Phebus FPT1 smo od 25 modulov, ki so na voljo v programu MELCOR 1.8.5, uporabili naslednjih 17 modulov: CVH – hidrodinamika, CVT – termodinamika, FL – tokovne poti, HS – toplotna telesa, COR – sredica, DCH – razpadna toplota, RN – radioaktivne snovi, MP – snovske lastnosti, NCG – nekondenzirajoči plini, EOS – enačba stanja, H20 – lastnosti vode, CF – krmilne funkcije, TF – tabelne funkcije, EDF – zunanje datoteke s podatki, EXEC – izvršilni modul, UTIL – podporni modul, PROG – knjižnice.

2.2 Termohidrodinamična nodalizacija in modeliranje

Termohidrodinamično nodalizacijo primarnega kroga, ki je predstavljena na sliki 4, smo napravili v skladu s specifikacijami ISP-46 [3], v katerih je predpisano, katero območje naprave Phebus naj obravnavamo in na koliko vozlišč je treba razdeliti posamezne dele naprave. Nadzorne prostornine so označene s CV-xxx, tokovne poti s FL-xxx in toplotna telesa s HS-xxxxx. Geometrijske podatke za vhodni model smo dobili v podatkovni knjigi FPT1 [9], poročilu specifikacij ISP-46 [3] in končnem poročilu FPT1 [2]. Podatke za vhodni tok pare, temperaturo pare in tlak pare smo dobili v končnem poročilu FPT1 [2].

2.3 Vozliščenje gorivnega svežnja in modeliranje

Vozliščenje reaktorske posode in gorivnega svežnja je predstavljena na sliki 5. Nadzorne prostornine so označene s CV-xxx, celice sredice s COR-xxx in toplotna telesa s HS-xxxxx. Enajst osnih ravni na grelnem območju od višine –7,987 m do višine –6,987 m, označenih s COR-x04 do COR-x14, smo določili v skladu s specifikacijami ISP-46 [3]. Gorivni sveženj smo modelirali z dvema prečnima obročema. V prvem prečnem obroču so krmilna

head, and the transfer of core materials to the reactor-vessel cavity,
- the core-concrete interaction and ensuing aerosol generation,
- the in-vessel and ex-vessel hydrogen production, transport, and combustion,
- the fission products' release (aerosol and vapour), transport, and deposition,
- the behaviour of radioactive aerosols in the reactor-containment building,
- the impact of engineering safety features on thermal-hydraulic and radio-nuclide behaviour.

For the modelling of experiment FPT1 from 25 packages, which are available in the MELCOR 1.8.5 computer code, the following 17 packages were used: CVH – hydrodynamics, CVT – thermodynamics, FL – flow paths, HS – heat structures, COR – core, DCH – decay heat, RN – radio-nuclides, MP – material properties, NCG – non-condensable gases, EOS – equation of state, H2O – water properties, CF – control functions, TF – tabular functions, EDF – external data files, EXEC – executive package, UTIL – utility package, PROG – libraries.

2.2 Hydrodynamic nodalization and modelling

The hydrodynamic nodalization of the bundle and circuit was done according to the ISP-46 specification [3], where the number of nodes in different parts of the Phebus facility and the computational domain is prescribed, and is presented in Fig. 4. The control volumes are denoted with CV-xxx, the flow paths with FL-xxx, and the heat structures with HS-xxxxx. The geometric data for the input model was obtained from the FPT1 Data Book [9], the ISP-46 Specification Report [3] and the FPT1 Final Report [2]. The inlet-steam flow rate, the steam temperature and the steam pressure were obtained from the FPT1 Final Report [2].

2.3 Core nodalization and modelling

The core nodalization of the bundle is presented in Fig. 5. The control volumes are denoted with CV-xxx, the core cells with COR-xxx, and the heat structures with HS-xxxxx. The 11 axial levels in the heated length from level –7.987 m to level –6.987 m denoted with COR-x04 to COR-x14 were defined according to the ISP-46 specification [3]. The bundle was modelled with two radial rings. In the first radial ring there are the control rod, the control-rod

palica, vodilo krmilne palice in 8 notranjih obsevanih gorivnih palic. V drugem prečnem obroču pa je 10 zunanjih obsevanih gorivnih palic, 2 sveži gorivni palici in nosilci. Ker so sveže in obsevane gorivne palice v istih celicah drugega prečnega obroča, jih ne moremo obravnavati ločeno. Zato smo lahko v vhodnem modelu upoštevali le povprečne lastnosti svežih in obsevanih gorivnih palic in zato smo lahko izračunali le povprečne rezultate. Kot podporno

guide tube and the inner 8 irradiated fuel rods. In the second radial ring there are the outer 10 irradiated fuel rods, the 2 fresh-fuel rods and the stiffeners. Since the fresh and irradiated fuel rods are both in the same core cells of the second radial ring they cannot be treated separately. Therefore, in the input model only the average properties of the fresh and irradiated fuel rods could be considered, and for the same reason only the average results can be calcu-

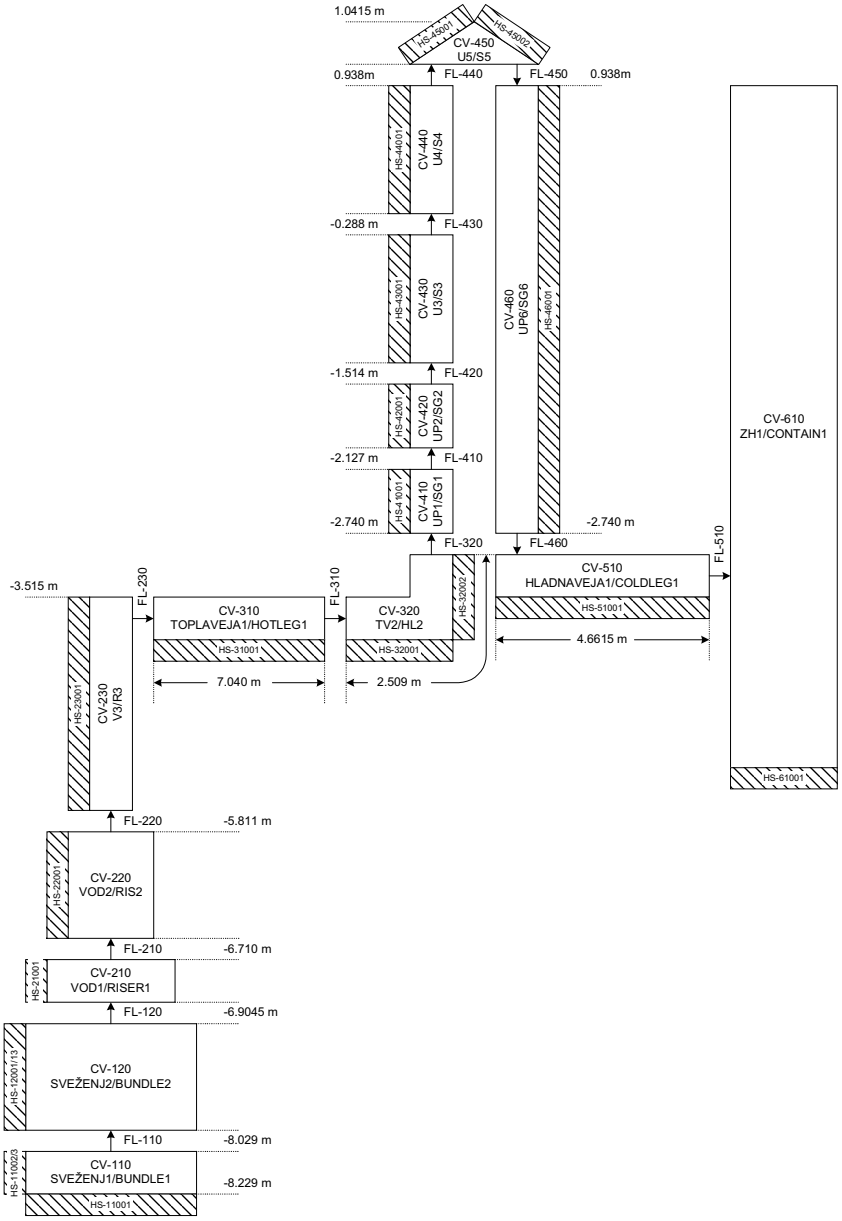

Sl. 4. *Termohidrodinamična nodalizacija primarnega kroga in nodalizacija toplotnih teles*
Fig. 4. *Thremalhydrodynamic and heat structure nodalization of the bundle and circuit*

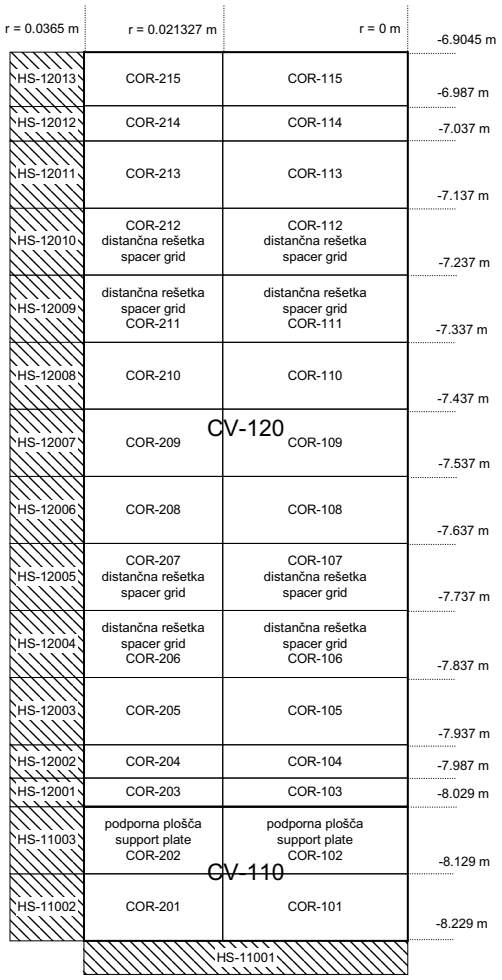

Sl. 5. *Nodalizacija reaktorske posode z gorivnim svežnjem in nodalizacija toplotnih teles*
Fig. 5. *Core and heat structure nodalization of the bundle*

strukturo smo modelirali podporno ploščo goriva in obe distančni rešetki, kot nepodporno strukturo pa krmilno palico, vodilo krmilne palice, nosilce ter vzmeti v krmilni in gorivnih palicah. Podporno ploščo in obe distančni rešetki smo razporedili v oba prečna obroča v skladu s površino obročev. Cev, ki obdaja gorivni sveženj, smo obravnavali kot toplotno telo.

2.4 Vozliščenje toplotnih teles in modeliranje

Podatke za snovi, iz katerih je cev, ki obdaja gorivni sveženj, smo dobili iz poročila specifikacij MSP-46 [3]. Vse druge snovske lastnosti smo dobili iz baze podatkov v MELCOR modulu snovskih lastnosti (MP). Zunanjo temperaturo cevi, ki obdaja gorivni sveženj, smo ustalili na 438 K, kar je v skladu s poročilom specifikacij MSP-46. Po specifikacijah ISP-46 naj bi

lated. As a supporting structure the fuel-supporting plate and the two spacer grids were modelled, and as a non-supporting structure the control rod, the control-rod guide tube, the stiffeners and the springs in the control and fuel rods were modelled. The support plate and the two spacer grids were distributed in both radial rings according to the rings' surface area. The shroud was considered as a heat structure.

2.4 Heat structure nodalization and modelling

The data for the shroud materials was taken from the ISP-46 specification report [3]. All other material properties were taken from the MELCOR material properties package database (MP). The outside temperature of the shroud was fixed at the constant temperature of 438 K, obtained from the ISP-46 specification report. The temperature evolution of the circuit walls should be, accord-

potek temperature notranje strani cevi primarnega kroga predpisali na podlagi preizkusnih podatkov. V modulu MELCOR toplotnih teles (HS) temperature ni mogoče predpisati na notranji strani cevi, ampak jo je mogoče predpisati le na zunanji strani cevi. Da bi lahko čim bolj natančno predpisali temperaturo na notranji strani cevi primarnega kroga, smo primarni krog obdali z umetnimi tankimi (1 mm) toplotnimi telesi iz nerjavnega jekla. Ker ima nerjavno jeklo veliko toplotno prevodnost, je tako razlika temperatur na notranji in zunanji strani toplotnega telesa zanemarljiva. Temperaturo na zunanji strani teh umetnih toplotnih teles (in s tem posredno temperaturo na notranji strani cevi) smo predpisali na podlagi razpoložljivih preizkusnih podatkov.

2.5 Modeliranje radioaktivnih snovi

Začetno količino radionaktivnih snovi smo določili iz končnega poročila FPT1 [2]. Elemente radioaktivnih snovi smo razvrstili v privzete vnaprej določene skupine radioaktivnih snovi modula MELCOR radioaktivnih snovi (RN) v skladu s privzetimi sestavami [8]. V modulu RN je privzetih 16 skupin radioaktivnih snovi, ki so poimenovane po reprezentativni radioaktivni snovi. V vhodnem modelu smo določili, da takoj po izpustu skupina "jod" reagira s skupino "cezij" in ustvari skupino "cezijev jodid".

V modulu RN so na voljo trije modeli izpustov: CORSOR, CORSOR-M in CORSOR-BOOTH [8]. Simuliranja smo opravili z vsemi tremi modeli in izkazalo se je, da model CORSOR-BOOTH napove večinoma premajhne izpuste, medtem ko modela CORSOR in CORSOR-M napovesta za nekatere radioaktivne snovi kar dobre rezultate. Izpuste nekaterih radioaktivnih snovi je bolje napovedal model CORSOR, medtem ko je druge bolje napovedal model CORSOR-M. Zaradi različnega obnašanja za različne radioaktivne snovi se je bilo težko odločiti, kateri model je v splošnem boljši. Na koncu smo se odločili, da bomo simuliranja opravili z modelom CORSOR-M, ker so rezultati v povprečju za spoznanje boljši. Izpusta strukturnih snovi (tj. snovi, ki niso gorivo), ki pomembno vplivajo na kemijo in zaradi tega tudi na izvorni člen, ni bilo mogoče izračunati, ker v programu MELCOR ni ustreznega modela za izračun izpusta strukturnih snovi.

2.6 Modeliranje specifičnosti naprave Phebus

Pri visokih temperaturah je toplotno sevanje pomemben način prenosa toplote v sredici, saj se

ing to the ISP-46 specification, derived from the experimental data. In the MELCOR heat-structure package (HS) it is not possible to define the pipe's inside-wall temperature directly, but it is possible to define the pipe's outside-wall temperature. To be able to determine the circuit's inside-wall temperature as accurately as possible, artificially thin (1-mm) heat structures made of stainless steel were provided along the circuit. Since the heat conductivity of stainless steel is high, the difference between the inside and outside temperature of the heat structure is negligible. The outside temperature of these artificial heat structures (and so, indirectly, the circuit's inside-wall temperature) was derived from the available experimental data.

2.5 Radio-nuclide modelling

The initial radio-nuclide inventory was derived from the FPT1 Final Report [2]. The radio-nuclide elements were grouped into the predetermined, default radio-nuclide classes of the MELCOR radio-nuclide package (RN) according to the default compositions [8]. In the RN package there are 16 default classes, which are named by their representative radio-nuclide. In the input model it was defined that immediately after the release the iodine class reacts with the caesium class and forms the caesium-iodine class.

In the RN package three different radio-nuclide release models are available: CORSOR, CORSOR-M and CORSOR-BOOTH [8]. Simulations were performed with all three models and it turned out that the CORSOR-BOOTH model mostly predicts releases that are too low, whereas the CORSOR and CORSOR-M models give, for some radio-nuclide classes, relatively good results. The CORSOR model gave better predictions for the releases of some radio-nuclide classes whereas the CORSOR-M model gave better predictions for some others. Due to the different behaviour for different radio-nuclide classes it was difficult to decide which model is generally better. In the end it was decided to perform the simulations with the CORSOR-M model since the results are, on average, slightly better. The structural material (i.e., the non-fuel material) release, which significantly influences the chemistry and consequently also the source term, could not be calculated since MELCOR has no appropriate structural-material release model.

2.6 Modelling of specifics of Phebus facility

At high temperatures the thermal radiation becomes an important mode of heat transfer within

izsevani toplotni tok zvečuje s četrto potenco absolutne temperature. Prenos toplote s sevanjem med različnimi deli sredice in med sredico ter okoliškimi strukturami je odvisen od geometrijske oblike sredice, emisijskega koeficienta površin in tekočine, v katerem je sredica. V splošnem lahko prenos toplote s sevanjem med ploskvama *i* in *j* izračunamo s z naslednjo enačbo:

the core, since the radiated heat flux rises with the fourth power of the absolute temperature. The heat transferred by thermal radiation between the different parts of the core and between the core and the surrounding structures depends on the core geometry, the emissivity of the surfaces and the medium surrounding the core. In general, the heat-transfer rate from surface *i* to surface *j* can be calculated with the following equation:

$$q_{ij} = A_i F_{ij} \tau_{ij} \left(J_i - J_j \right), \tag{1}$$

kjer so A_i površina ploskve *i*, F_{ij} geometrijski faktor pogleda s ploskve *i* na ploskev *j*, τ_{ij} prepustnost sevanja med ploskvama *i* in *j* ter J_i celoten sevalni tok s ploskve *i*. Celoten sevalni tok s ploskve *i* izračunamo kot vsoto odbitega in izsevanega sevalnega toka:

where A_i is the area of surface *i*, F_{ij} is the geometric view factor from surface *i* to surface *j*, τ_{ij} is the radiation transmittance between the surfaces *i* and *j*, and J_i is the radiosity of surface *i*. The radiosity, which is defined as the total radiation flux leaving the surface *i* – both reflected and emitted – is calculated as:

$$J_i = \left(1 - \varepsilon_i\right) G_i + \varepsilon_i E_{bi}, \tag{2}$$

kjer so ε_i emisijski koeficient ploskve *i*, G_i vpadni sevalni tok na ploskev *i* in $E_{bi} = \sigma T_i^4$ toplotni sevalni tok s ploskve *i*, če bi ploskev *i* sevala kot črno telo.

V modulu MELCOR sredice (COR) se emisijski koeficient površin sredice ε_i in prepustnost sevanja skozi medij τ_{ij} določata z ustreznimi odvisnostmi ob upoštevanju stanja degradirane sredice, geometrijski faktor pogleda F_{ij} pa lahko uporabnik določi sam. V modulu COR vsaka gorivna palica ni modelirana posebej, ampak so gorivne palice združene v prečne obroče sredice, prenos toplote s sevanjem pa se modelira med sosednjima prečnima obročema. Tako pomeni geometrijski faktor povprečno vidljivost gorivnih palic v dveh sosednjih prečnih obročih. Zaradi prečnega temperaturnega gradienta v prečnih obročih sredice je razlika temperatur gorivnih palic ob meji dveh sosednjih prečnih obročev manjša od razlike povprečnih temperatur gorivnih palic v sosednjih prečnih obročih. Ker izračun prenosa toplote s sevanjem temelji na povprečnih temperaturah v posameznih prečnih obročih, ne pa na temperaturah gorivnih palic ob robu prečnega obroča, je tako izračunan prenos toplote s sevanjem precenjen. To odstopanje je mogoče do neke mere izravnati z ustreznim zmanjšanjem geometrijskega faktorja pogleda. Tako dobljeni faktor, ki je prilagojen načinu modeliranja prenosa toplote s sevanjem v modulu COR, imenujemo sevalni izmenjalni količnik.

Optimalna vrednost sevalnega izmenjalnega količnika je odvisna od velikosti sredice in njenega

where ε_i is the emissivity of surface *i*, G_i is the radiation flux incident on surface *i* and $E_{bi} = \sigma T_i^4$ is the blackbody emissive power of surface *i*.

In the MELCOR core package (COR), the emissivity of the core surfaces ε_i and the radiation transmittance of the media τ_{ij} are calculated using appropriate correlations considering the state of the degraded core, whereas the geometric view factor F_{ij} can be set by the user. In the COR package each fuel rod is not modelled separately, but the fuel rods are grouped in radial core rings, and the heat transfer by thermal radiation is modelled between adjacent radial rings. So, the geometric view factor presents an average view of fuel rods in two adjacent radial rings. Due to the radial temperature gradient in the radial core rings, the difference between the fuel-rod temperatures at the boundary of two adjacent radial rings is smaller than the difference between the average fuel-rod temperatures in adjacent radial rings. Since the calculation of the heat transfer by thermal radiation is based on the average fuel-rod temperatures in the radial rings and not on the fuel-rod temperatures at the boundary of the radial ring, the so-calculated heat transfer by thermal radiation is overestimated. This overestimation can be, to a certain degree, compensated by reducing the geometric view factor. The so-established factor, which takes into account the specific treatment of heat transfer by thermal radiation in the COR package, is called the radiative exchange factor.

The optimum value of the radiative exchange factor depends on the core size and the nodalization.

vozliščenja. Zaradi majhne velikosti gorivnega svežnja v napravi Phebus je v vsakem obroču vozliščene sredice le ena prečna »plast« gorivnih palic. Tako ima »povprečna« gorivna palica v obroču precej boljšo vidljivost sosednjega obroča, kakor bi jo imela v primeru reaktorske sredice v naravni velikosti. Poleg tega gorivne palice v notranjem obroču ne vidijo le gorivnih palic v zunanjem obroču, ampak vidijo neposredno tudi cev, ki obdaja gorivni sveženj. Zato je treba sevalni izmenjalni količnik za sevanje v prečni smeri med dvema sosednjima prečnima obročema sredice (privzeta vrednost: 0,25) občutno povečati.

Na slikah 6 do 8 so prikazani izračuni temperatur cevi MELCOR 1.8.5 RE okoli gorivnega svežnja, srajčke in goriva za različne sevalne izmenjalne količnike (0,25; 0,5; 0,75) v primerjavi s preizkusnimi meritvami (FPT1). Valovanje (sl. 7) in nenadne spremembe (sl. 8) v preizkusnih krivuljah so posledica odpovedi termočlenov. Nenaden padec

Because of the small size of the bundle in Phebus, each ring of the core nodalization contains only one radial layer of fuel rods. Thus, the "average" rod in a ring has a much better view of the adjacent ring than would be the case in a full-scale reactor core. In addition, the fuel rods in the inner ring can see not only the fuel rods in the outer ring but also directly the shroud. Therefore the radiative exchange factor for radiation radially outward from the cell boundary to the next adjacent cell (default value: 0.25) has to be significantly increased.

In Figures 6 to 8 the MELCOR 1.8.5 RE calculated temperatures of the shroud, clad and fuel are presented for different radiative exchange factors (0.25, 0.5, 0.75) in comparison with the experimental measurements (FPT1). The fluctuations (Fig. 7) or abrupt changes (Fig. 8) in the experimental curves are due to the failure of thermocouples. The abrupt fall in the calculated curves (Fig. 7 and 8) indicates a component failure, since in MELCOR it is defined

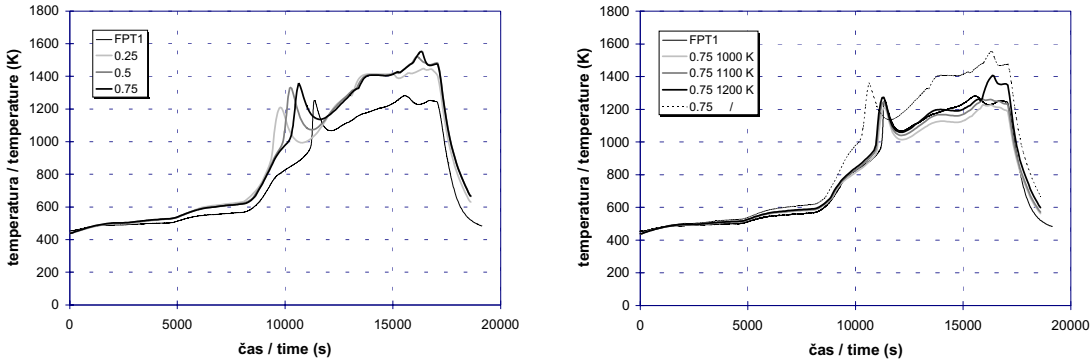

Sl. 6. *Temperatura na notranji strani cevi okoli gorivnega svežnja na višini 800 mm za različne sevalne izmenjalne količnike (levo) in za različne temperature zapiranja parnih rež (desno)*

Fig. 6. *Inside shroud temperature at level 800 mm for different radiative exchange factors (left) and for different steam gaps closure temperatures (right)*

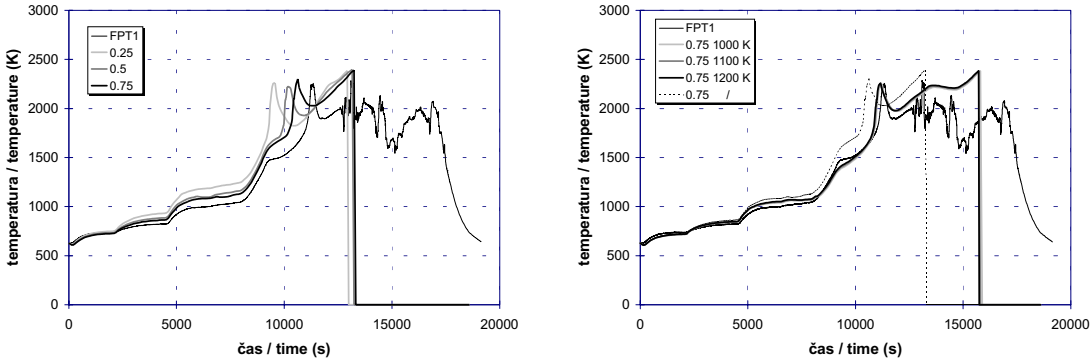

Sl. 7. *Temperatura srajčke v zunanjem obroču sredice na višini 600 mm za različne sevalne izmenjalne količnike (levo) in za različne temperature zapiranja parnih rež (desno)*

Fig. 7. *Clad temperature in outer core ring at level 600 mm for different radiative exchange factors (left) and for different steam gaps closure temperatures (right)*

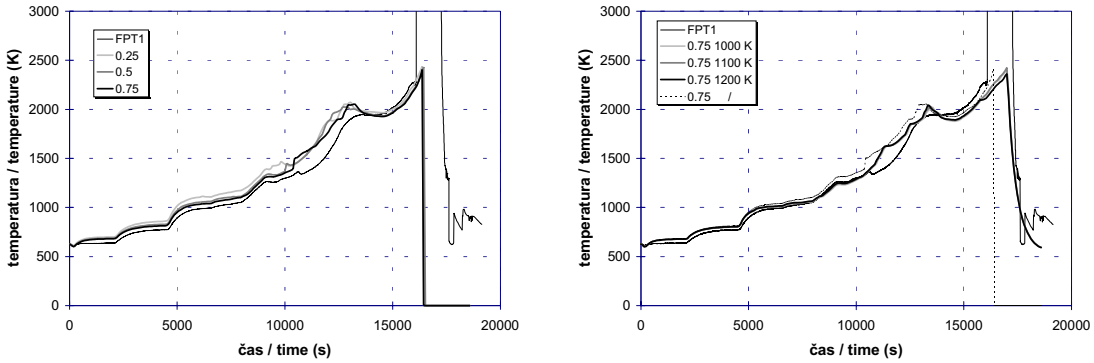

Sl. 8. *Temperatura goriva v zunanjem obroču sredice na višini 300 mm za različne sevalne izmenjalne količnike (levo) in za različne temperature zapiranja parnih rež (desno)*

Fig. 8. *Fuel temperature in outer core ring at level 300 mm for different radiative exchange factors (left) and for different steam gaps closure temperatures (right)*

(sl. 7, 8) v preizkusnih krivuljah pa označuje porušitev komponente, saj je v programu MELCOR definirano, da je temperatura komponente, ki je v celici ni, 0 K. Kakor je bilo pričakovati, se temperatura srajčke in goriva zmanjša, če sevalni izmenjalni količnik povečamo (sl. 7, 8), saj se več toplote odvaja s sevanjem. Posledično se tudi temperaturni vrh srajčke, ki je posledica eksotermne oksidacije cirkonija, pojavi kasneje (sl. 7). Če povečujemo sevalni izmenjalni količnik, se krivulje temperatur približujejo preizkusnim meritvam, vendar tudi za ocenjeno vrednost sevalnega izmenjalnega količnika 0,75, ujemanje še vedno ni zadovoljivo.

Na sliki 6 vidimo, da je izračunana temperatura na notranji strani cevi, ki obdaja gorivni sveženj, precenjena, kar kaže, da bi lahko bila toplotna prevodnost cevi podcenjena. In res, v večplastni cevi sta dve 0,5 mm debeli parni reži - med plastema ThO_2 in ZrO_2 ter med plastjo ZrO_2 in ZrO_2 plaščem (sl. 2), ki močno vplivata na toplotno prevodnost cevi. Med segrevanjem cevi se zaradi toplotnega raztezanja notranjih toplejših plasti debelini obeh parnih rež zmanjšujeta, dokler se obe parni reži popolnoma ne zapreta in pride do neposrednega stika posameznih plasti. Ob neposrednem stiku posameznih plasti cevi se toplotna prevodnost cevi občutno poveča. Ker v programu MELCOR zapiranja obeh parnih rež ni mogoče neposredno simulirati, smo zapiranje parnih rež modelirali s temperaturno odvisno dejansko toplotno prevodnostjo pare v obeh režah:

that the temperature of a component that does not exist in the considered cell is 0 K. As expected the temperature of the clad and fuel decreases when the radiative exchange factor is increased (Fig. 7 and 8), since more heat is transferred by radiation. Consequently, the clad-temperature peak caused by the zirconium's exothermic oxidation reaction also occurs at a later time (Fig. 7). When the radiative exchange factor is increased the temperature curves move towards the experimental measurements, but also for an estimated value of the radiative exchange factor of 0.75 the agreement is still not satisfactory.

In Fig. 6 we see that the calculated inside-shroud temperature is overestimated, which is an indication that the shroud's heat conductivity could be underestimated. Indeed, in the shroud there are two 0.5-mm-thick steam gaps – between the ThO_2 and ZrO_2 sleeves and between the ZrO_2 sleeve and the ZrO_2 spray coating (Fig. 2) – which significantly influence the shroud's heat conductivity. During the shroud's heating up the thickness of both steam gaps reduces due to the thermal expansion of the inner hotter sleeves until both steam gaps completely close and there is a direct contact between the different shroud layers. At a direct contact between the shroud layers the heat conductivity of the shroud significantly increases. Since in MELCOR it is not possible to simulate the closure of the two steam gaps directly, we decided to model the steam-gaps closure with the temperature-dependent effective thermal conductivity of the steam in both gaps:

$$\lambda_{effective} = \begin{cases} \min\left(10\frac{\mathrm{W}}{\mathrm{mK}}, \lambda_{steam}\left(1-\frac{T-300\mathrm{K}}{T_{close}-300\mathrm{K}}\right)^{-1}\right) & \text{èe/if } T < T_{close} \\ 10\frac{\mathrm{W}}{\mathrm{mK}} & \text{èe/if } T \geq T_{close} \end{cases} \quad (3),$$

ki temelji na predpostavki, da se med dvigom temperature od 300 K do T_{close} debelini obeh parnih rež linearno zmanjšujeta do popolnega zaprtja. Zaprti parni reži smo modelirali kot reži, v katerih je para z zelo veliko dejansko toplotno prevodnostjo $\lambda_{effective} = 10\,\mathrm{W/mK}$, ki tako ne zmanjšujeta več toplotne prevodnosti večplastne cevi. Na slikah 6 do 8 je prikazan vpliv predpostavljene temperature T_{close} (1000 K, 1100 K, 1200 K, brez zapiranja rež), pri kateri se parni reži popolnoma zapreta, na rezultate simuliranj s programom MELCOR 1.8.5 RE. Vidimo, da model zapiranja parnih rež občutno izboljša rezultate simuliranj in da se rezultati simuliranj pri temperaturi zapiranja parnih rež 1100 K skoraj popolnoma ujemajo z izmerjenimi temperaturami.

3 REZULTATI SIMULIRANJ

Opravili smo dve primerjalni simuliranji z različnima različicama programa MELCOR, to je z različico MELCOR 1.8.5 QZ (v nadaljevanju QZ), ki smo jo posodobili z najnovejšim uradnim popravkom (oznaka "Patch 185003"), kar je zadnja uradna izvedba, ter z izboljšano verzijo MELCOR 1.8.5 RE (v nadaljevanju RE), ki smo jo prejeli na uporabniški delavnici "MELCOR Users' Workshop 2002". Glavne razlike med različicama RE in QZ, ki zadevajo simuliranje preizkusa Phebus FPT1, so naslednje: v izvedbi RE so izboljšali doslednost hidrodinamičnega modula in modula sredice (CVH/COR), odpravili so nekaj programerskih hroščev v modulu sredice (COR) in v modulu radioaktivnih snovi (RN) so izboljšali interpolacijo koeficientov razpršin.

Simuliranji smo opravili pri ocenjeni vrednosti sevalnega izmenjalnega količnika za sevanje v prečni smeri med dvema sosednjima celicama sredice 0,75 in pri vrednosti temperature zapiranja parnih rež T_{close} = 1100K, kjer so se rezultati izračunov najbolje ujemali z meritvami. Kakor je prikazano na slikah 6 do 8, je tako mogoče dobiti dobro ujemanje temperaturnih razmer v gorivnem svežnju s preizkusnimi meritvami, kar je potrebno, če želimo ocenjevati zmožnost programa MELCOR za napovedovanje drugih preizkusnih rezultatov, to so nastanek vodika, izpust in odlaganje razcepkov, degradacija sredice idr. Ker so razlike med QZ in RE izračuni temperatur cevi okoli gorivnega svežnja, srajčke in goriva zanemarljivi, teh rezultatov za simuliranje QZ ne bomo opisovali.

Na sliki 9 sta prikazana preizkusni (FPT1) in simulirani (QZ, RE) masni tok vodika. Vodik nastane med oksidacijo cirkonijevih srajčk gorivnih palic v

which is based on the assumption that during the temperature rise from 300 K to T_{close} the thickness of both steam gaps linearly reduces until complete closure occurs. The closed steam gaps were modelled as gaps filled with steam that has a very high effective heat conductivity $\lambda_{effective} = 10\,\mathrm{W/mK}$, so that the gaps do not reduce the heat conductivity of the multi-layer shroud anymore. In Figures 6 to 8 the influence of the assumed steam gaps' closure temperature T_{close} (1000 K, 1100 K, 1200 K, no gaps closure) on the MELCOR 1.8.5 RE simulation results is presented. We see that the steam gaps' closure model significantly improves the simulation results, and that the results for the steam gaps' closure temperature 1100 K are in nearly perfect agreement with the measured temperatures.

3 SIMULATION RESULTS

Two simulations were performed with different versions of MELCOR, i.e., with the MELCOR 1.8.5 QZ version (denoted QZ) updated with the newest patch (label "Patch 185003"), which is the latest official version, and with the improved MELCOR 1.8.5 RE version (denoted RE), which was distributed at the MELCOR Users' Workshop 2002. The main differences between the RE and QZ versions, which affect the Phebus FPT1 experiment simulation, are that in the RE version the consistency of the hydrodynamics package and the core package (CVH/COR) was improved, that some core-package (COR) bugs were fixed, and that in the radio-nuclide package (RN) the aerosol-coefficient interpolation was improved.

The simulations were performed with the estimated value of the radiative exchange factor for radiation radially outward from the cell boundary to the next adjacent cell 0.75 and the best fit steam gaps closure temperature 1100 K. In this way, as shown in Figures 6 to 8, a good agreement of the temperature conditions in the bundle with the experimental measurements was achieved, which is needed to be able to assess the capability of MELCOR to predict other experimental results, like the hydrogen generation, the fission-products release and deposition, the core degradation, etc. Since the differences between the QZ and RE calculated temperatures of the shroud, clad and fuel are negligible, these QZ simulation results will not be presented.

Fig. 9 shows the experimental (FPT1) and simulated (QZ, RE) hydrogen mass-flow rate. Hydrogen is generated during the oxidation of the zirconium fuel

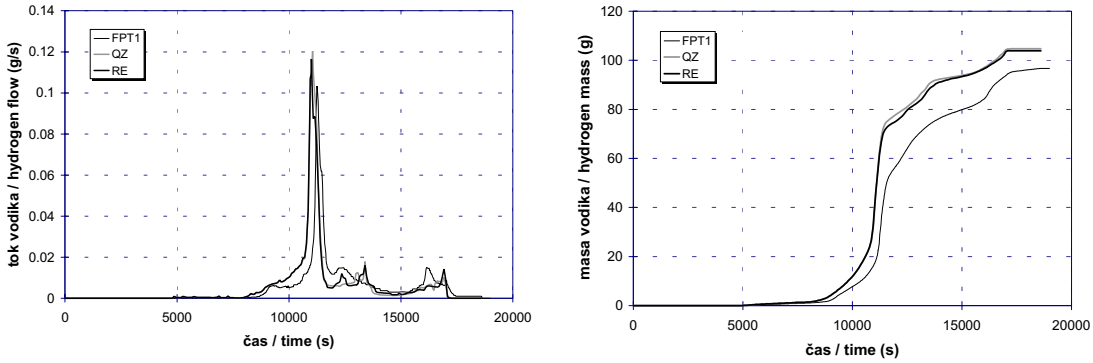

Sl. 9. *Masni tok vodika na izhodu sredice (levo) in skupna masa vodika (desno)*
Fig. 9. *Hydrogen mass flow rate at core exit (left) and total mass of hydrogen (right)*

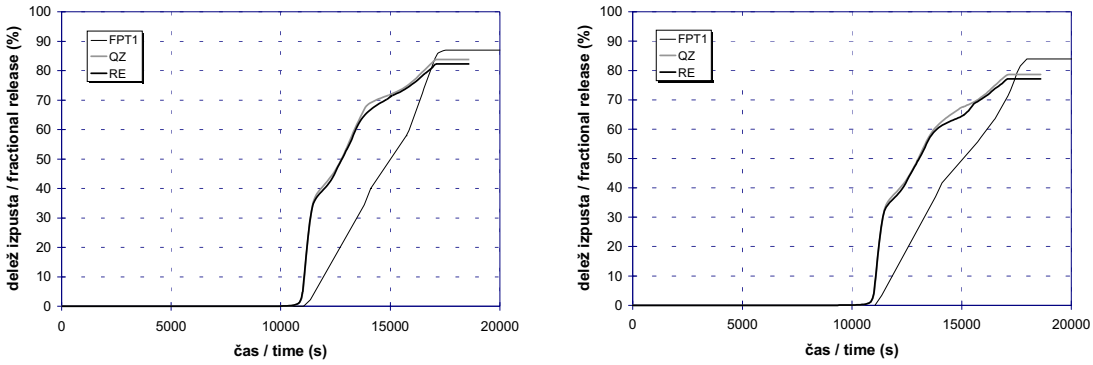

Sl. 10. *Delež izpusta I (levo) in Cs (desno) iz sredice glede na začetno stanje*
Fig. 10. *Fractional release of I (left) and Cs (right) initial inventory*

ozračju vodne pare, do katere pride v večji meri pri temperaturah nad 1100 K. Med oksidacijo cirkonijevih srajčk se sprošča toplota, zaradi česar se cirkonijeve srajčke dodatno segrevajo (sl. 7), kar lahko zaradi pozitivne povratne zanke privede do samostojnega stopnjevanja oksidacijskega postopka, kar se je zgodilo pri preizkusu FPT1 (sl. 9). Med degradacijo sredice se spreminja velikost površine cirkonijevih srajčk, ki je v stiku z vodno paro, ter debelina oksidne plasti, ki prekriva cirkonijeve srajčke, kar pomembno vpliva na nastanek vodika. Oboje je v modulu MELCOR sredice (COR) ustrezno upoštevano. Na sliki 9 vidimo, da je izračunan vrh masnega toka vodika nekoliko precenjen in da se pojavi nekoliko prezgodaj. Eden izmed razlogov za to bi lahko bila predpostavka, da naj bi bile srajčke na začetku simuliranja popolnoma neoksidirane, kar je splošna praksa, medtem ko so bile srajčke verjetno nekoliko oksidirane že pred pričetkom preizkusa. Kot posledica precenjenega masnega toka vodika, je tudi skupna masa vodika precenjena (sl. 9), a je še vedno v okviru natančnosti preizkusne meritve ±10 %. Razlike med simuliranji QZ in RE so majhne.

rods' cladding in the steam atmosphere, which occurs to a greater extent at temperatures over 1100 K. During the zirconium-cladding oxidation heat is released, thereby additionally heating up the zirconium cladding (Fig. 7), which can lead, due to the positive feedback, to a self-excursion of the oxidation process, as happened in the experiment FPT1 (Fig. 9). During the core degradation the area of the zirconium cladding in contact with the steam and the thickness of the oxide layer covering the zirconium cladding are changing, which significantly influences the hydrogen generation. In the MELCOR core package (COR) both processes are appropriately considered. In Fig. 9 we see that the hydrogen mass-flow-rate peak is slightly overestimated, and that it occurs slightly too early. One of the reasons for this could be that it was presumed that at the beginning of the simulation the cladding is completely unoxidized, as is an overall practice, whereas the cladding was probably somewhat oxidized already before the experiment started. As a consequence of the overestimated hydrogen mass-flow rate also the total hydrogen mass is overestimated (Fig. 9), but is still inside the experimental measurement accuracy band of ±10 %. The differences between the QZ and RE simulations are small.

Na sliki 10 je prikazan delež izpusta joda in cezija. Za izračun izpustov smo v modulu MELCOR radioaktivnih snovi (RN) izbrali model CORSOR-M, ki temelji na eksperimentalnih meritvah in predpostavlja, da je hitrost izpusta posamezne radioaktivne snovi preprosta funkcija temperature [8]. Končni deleži izpustov so kar dobro napovedani, medtem ko so začetni izpusti precenjeni. Iz preglednice 1, ki prikazuje rezultate ključnih dogodkov, je razvidno, da niso izpusti vseh radioaktivnih snovi napovedani tako dobro. Izračun RE napove v splošnem nekoliko večje izpuste iz gorivnega svežnja kakor izračun QZ (za nekatere radioaktivne snovi je prav nasprotno).

Preglednica 1 prikazuje rezultate obeh simuliranj za ključne dogodke v primerjavi s preizkusnimi meritvami. Vidimo, da je ujemanje časovnih napovedi ključnih dogodkov s preizkusnimi meritvami kar dobro in da so razlike med obema simuliranjema majhne. Končni deleži izpustov iz gorivnega svežnja in cevovoda so zadovoljivo napovedani za večino radioaktivnih snovi, toda za nekatere, npr. rutenij in uran, so razlike med izračuni in meritvami več velikostnih razredov. V splošnem lahko ugotovimo, da se rezultati novejše različice RE programa MELCOR bolje ujemajo s preizkusnimi meritvami.

In Fig. 10 the fractional releases of iodine and caesium are presented. For the calculation of the releases in the MELCOR radio-nuclide package (RN) the CORSOR-M model was chosen. In the CORSOR-M model, which is based on experimental data, it is presumed that the fractional release rate of a particular radio-nuclide is a simple function of temperature [8]. The final fractional releases are relatively well predicted, whereas the initial releases are overestimated. From Table 1, showing the results for key events, it is evident that not all radio-nuclide class releases were predicted as well. The RE simulation predicts, in general, slightly lower bundle releases than the QZ simulation (for some radio-nuclide classes it is just the opposite).

Table 1 provides the results of both simulations for some key events in comparison with the experimental measurements. We see that the timing of key events is relatively well predicted and that the differences between both simulations are small. The total fractional releases from the bundle and circuit are satisfactory for most radio-nuclides, but for some, like ruthenium and uranium, the difference between the simulation results and the experimental measurements is more orders of magnitude. In general, one can state that the results of the newer MELCOR version RE are in better agreement with the experimental measurements.

Preglednica 1. *Ključni dogodki za simuliranji MELCOR 1.8.5 QZ in RE v primerjavi s preizkusnimi meritvami*
Table 1. *Key events for MELCOR 1.8.5 QZ and RE simulations in comparison with experimental measurements*

Pojav / Event		**FPT1** [2,3]		**QZ**		**RE**	
Prva porušitev srajčk / First cladding rupture		5700 s		5332 s		5332 s	
Začetek oksidacije srajčk Start of cladding oxidation		~ 8580 s		8415 s		8415 s	
Začetek izpusta razcepkov iz goriva Start of fission products release from fuel		11170 s		10810 s		10806 s	
Prvo premikanje goriva / First fuel movement		~ 11000 s		11039 s		11025 s	
Prvi oksidacijski temperaturni vrh First oxidation temperature peak		11260 s		11058 s		11046 s	
Končni odstotek izpusta iz svežnja in cevovoda Total percentage release from bundle and circuit		sveženj bundle	cevovod circuit	sveženj bundle	cevovod circuit	sveženj bundle	cevovod circuit
žlahtni plin / noble gas	Xe	77,4	77,4	84,3	84,3	82,7	82,7
hlapljivi razcepki volatile fission products	I	87,0 ± 4,0	64,1	83,9	43,5	82,3	51,3
	Cs	84,0 ± 0,8	43,8	78,6	35,1	77,2	44,7
	Te	83,0 ± 1,0	52,5	76,5	32,6	78,2	48,6
	Mo	56,0 ± 4,0	23,0	13,2	4,26	14,8	8,62
slabo hlapljivi razcepki low volatile fission products	Ba	< 5	0,65	3,21	1,06	3,08	1,42
	Ru	< 5	0,50	5,16E-4	1,64E-4	5,21E-4	2,99E-4
gorivni sveženj / fuel bundle	U	> 0,14	0,119	1,98E-2	4,03E-3	2,09E-2	1,06E-2

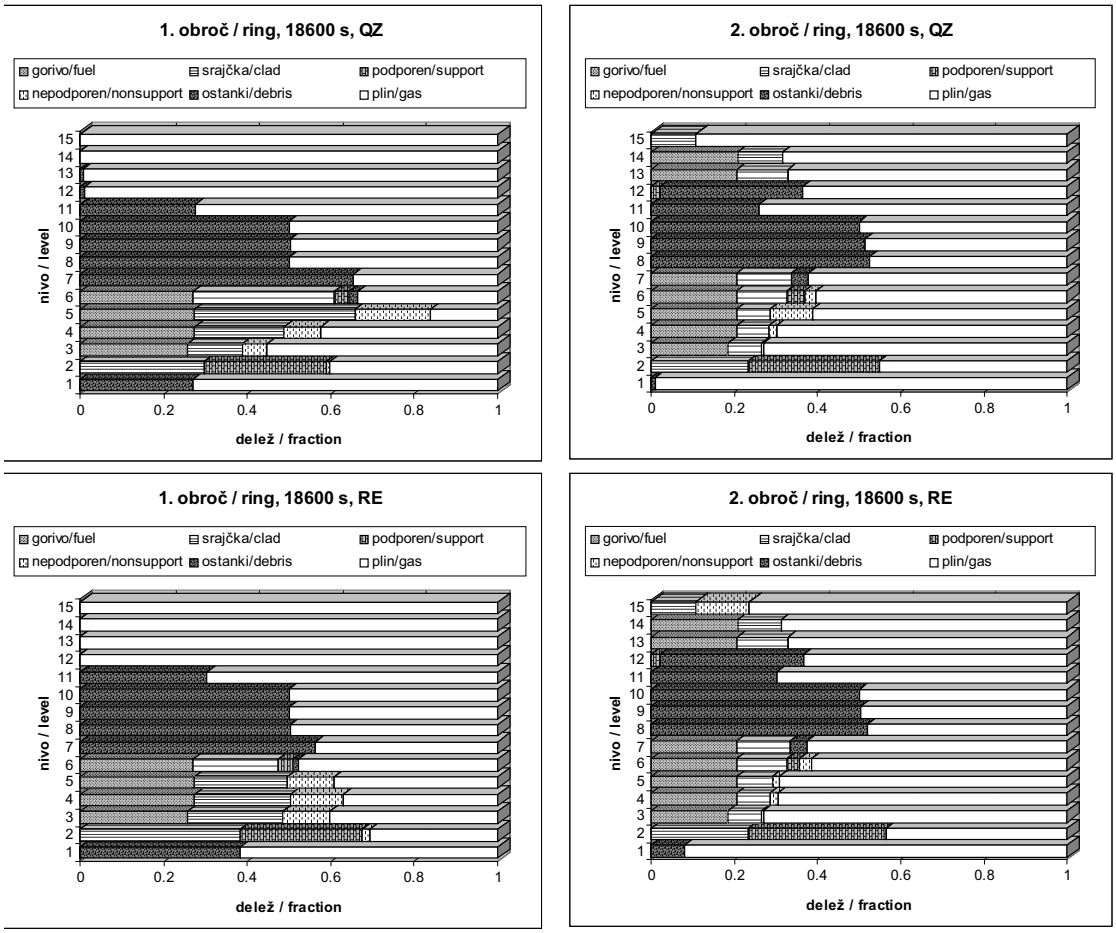

Sl. 11. *Diagrama stanj gorivnega svežnja za simuliranji QZ in RE pri času 18600 s*
Fig. 11. *Bundle state diagrams for the QZ and RE simulations at time 18600 s*

Na sliki 11 sta za obe simuliranji prikazana diagrama stanj gorivnega svežnja ob koncu faze degradacije sredice. Stanji gorivnega svežnja sta prikazani s prostorskimi deleži različnih komponent sredice (gorivo, srajčka, podporna struktura, nepodporna struktura in ostanki) v vseh osnih vozliščih obeh prečnih obročev. Zaradi omejitve uporabljenega programa za risanje diagramov so vsa osna vozlišča narisana enakomerno. Prave velikosti celic sredice so prikazane na sliki 5. V modulu MELCOR sredice (COR) so modelirani vsi ključni postopki degradacije sredice, to so oksidacija kovinskih komponent sredice, kemijske interakcije med snovmi sredice (raztapljanje, nastanek evtektikov itn.) in porušitev sredice (deformacija, taljenje, tvorba staljenih gmot, ostanki itn.) [8]. Na sliki 11 vidimo, da sta stanji gorivnega svežnja za simuliranji QZ in RE zelo različni, čeprav so bile temperaturne razmere v svežnju pri obeh izračunih

In Fig. 11 the bundle state diagrams at the end of the degradation phase are presented for both simulations. The bundle states are presented with the volume fractions of different core components (fuel, clad, supporting structure, non-supporting structure and particulate debris) in all axial levels of both radial rings. Due to limitations of the used diagram-plotting program the axial levels had to be plotted as equidistant. The correct sizes of the core cells are presented in Fig. 5. In the MELCOR core package (COR) all the key processes of the core degradation are modelled, like the oxidation of metal core components, the core material chemical interactions (dissolution, eutectics formation, etc.) and the core relocation (deformation, candling, melting, debris formation, etc.) [8]. In Fig. 11 we see that the bundle state diagrams for the QZ and RE simulations are significantly different, despite the fact that the temperature conditions in the bundle were the same for

enake. Razlog za razlike bi bilo lahko dejstvo, da so v izboljšani izvedbi MELCOR 1.8.5 RE v modulu COR odpravili nekaj programerskih hroščev.

V simuliranjih se ostanki sredice nabirajo na višini 300 mm (sl. 11), medtem ko se pri preizkusu bazen taline oblikuje na višini 200 mm (sl. 12). Votline, ki se oblikuje v preizkusu nad bazenom taline, s programom MELCOR ni mogoče napovedati, ker se v programu MELCOR gorivne palice v zgornjih celicah sredice pomaknejo navzdol, če je pod njimi prostor in jih ne podpirajo nepoškodovane gorivne palice (ali podporna struktura) v nižjih celicah sredice.

Na sliki 13 je prikazano izračunano odlaganje joda in cezija vzdolž primarnega kroga od zgornjega predela nad preizkusnim gorivnim svežnjem (-6,78 m) do zgornjega dela uparjalnika (0,26 m). Preizkusne meritve so predstavljene le za vročo vejo uparjalnika. Odlaganje radioaktivnih snovi je obravnavano v modulu MELCOR radioaktivnih snovi (RN), kjer so modelirani vsi ključni mehanizmi odlaganja radioaktivnih snovi, to so težnostno odlaganje, Brownova difuzija, termoforeza, difuzoforeza in kondenzacija [8]. Vidimo, da so razlike med simuliranji QZ in RE pomembne, čeprav so bili izračunani izpusti podobni (sl. 10). Pri simuliranju RE je odlaganje joda kar dobro napovedano, medtem ko je odlaganje cezija

both calculations. The reason for the differences could be that in the improved MELCOR 1.8.5 RE version some core bugs were fixed.

In the simulations the debris accumulates on level 300 mm (Fig. 11), whereas in the experiment the pool forms on level 200 mm (Fig. 12). The cavity that formed in the experiment above the pool could not be reproduced with MELCOR since in MELCOR the fuel rods in the upper core cells relocate if there is place and they are not supported by intact fuel rods (or a supporting structure) in the core cells below.

In Fig. 13 the calculated depositions of iodine and caesium along the circuit from the upper plenum (-6.78 m) to the upper part of the steam generator (0.26 m) are presented. The experimental measurements are shown only for the steam generator's hot-leg region. The deposition of radio-nuclides is treated in the MELCOR radio-nuclide package (RN), where all the key radio-nuclide deposition mechanisms, like gravitational deposition, Brownian diffusion, thermophoresis, diffusiophoresis and condensation, are modelled [8]. We can see that the differences between the QZ and RE simulation are significant, despite the fact that the predicted releases are similar (Fig. 10). In the RE simulation the iodine deposition is quite well predicted, whereas the caesium deposition

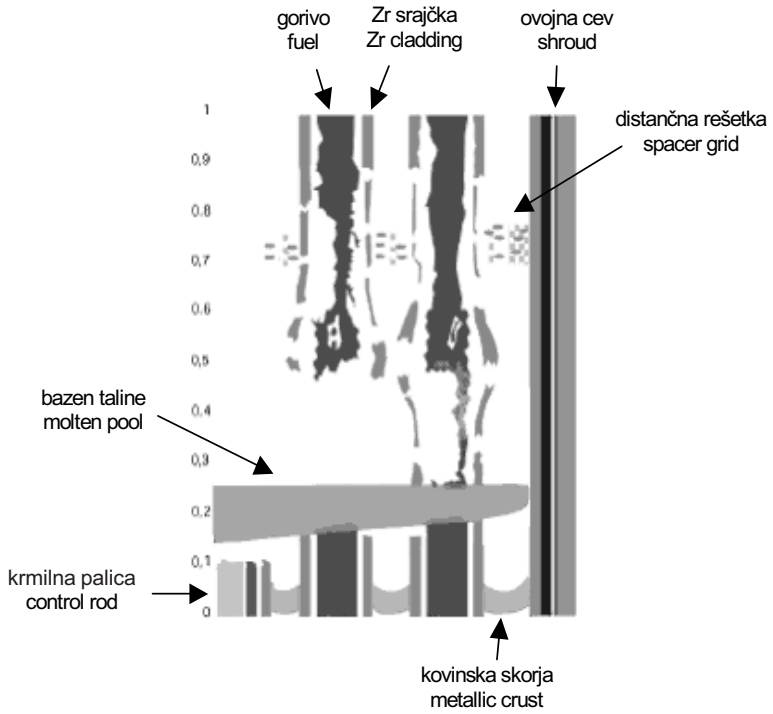

Sl. 12. *Shema na podlagi meritev ocenjenega stanja gorivnega svežnja pri času 17039 s [2]*
Fig. 12. *Scheme of the estimated state of the bundle at time 17039 s based on measurements [2]*

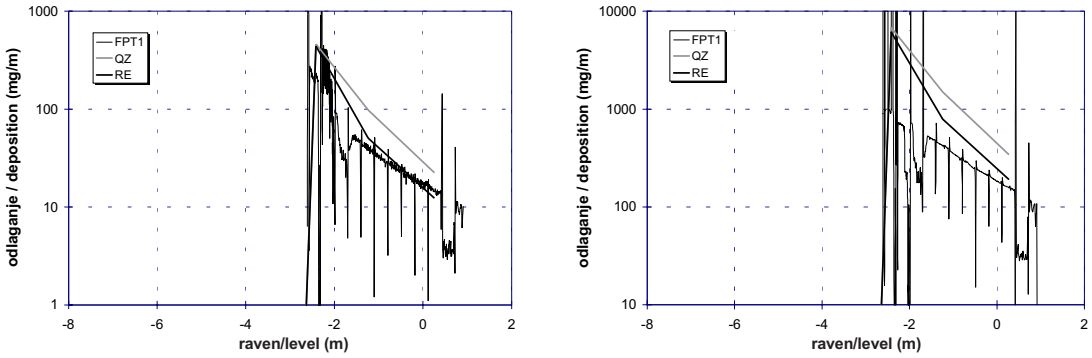

Sl. 13. *Odlaganje I (levo) in Cs (desno) v primarnem krogu*
Fig. 13. *Deposition of I (left) and Cs (right) in the circuit*

precenjeno. V splošnem je odlaganje radioaktivnih snovi v uparjalniku precenjeno.

4 SKLEP

Primerjava izračunov s preizkusnimi meritvami je pokazala, da je mogoče dobiti dobro ujemanje termohidravličnih spremenljivk v gorivnem svežnju, če pravilno upoštevamo sevanje v gorivnem svežnju in toplotne izgube skozi cev, ki obdaja gorivni sveženj. Glede izpustov radioaktivnih snovi se je izkazalo, da model CORSOR-BOOTH napove večinoma premajhne izpuste, medtem ko modela CORSOR in CORSOR-M napovesta za nekatere radioaktivne snovi kar dobre rezultate. Izpuste za nekatere radioaktivne snovi je bolje napovedal model CORSOR, medtem ko je druge bolje napovedal model CORSOR-M. Končna simuliranja smo opravili z modelom CORSOR-M, ker so rezultati v povprečju za spoznanje boljši. Izpusta strukturnih snovi, ki pomembno vplivajo na kemijo in posledično tudi na izvorni člen, ni bilo mogoče izračunati, ker v programu MELCOR 1.8.5 ni ustreznega modela za izračun izpusta strukturnih snovi.

V splošnem lahko ugotovimo, da je ujemanje termohidravličnih spremenljivk dobro, da je ujemanje končnih izpustov za večino radioaktivnih snovi zadovoljivo ter da je odlaganje radioaktivnih snovi v uparjalniku precenjeno. Ključni dogodki so napovedani ob pravih časih. Razlike med rezultati simuliranj obeh različic programa MELCOR 1.8.5 (QZ in RE) so zanemarljive za termohidravlične spremenljivke, majhne za izpuste radioaktivnih snovi in časovno pojavljanje ključnih dogodkov, vendar pomembne za odlaganje radioaktivnih snovi in degradacijo gorivnega svežnja. V splošnem se rezultati novejše izvedbe RE programa MELCOR 1.8.5 bolje ujemajo s preizkusnimi meritvami.

is overestimated. In general the depositions of radio-nuclides in the steam generator were overestimated.

4 CONCLUSION

The comparison of simulation results and experimental measurements showed that good agreement of the thermal-hydraulic variables in the bundle can be achieved if the radiation inside the bundle and the heat losses through the shroud are correctly considered. Regarding the radio-nuclide releases, it turned out that the CORSOR-BOOTH model tends to underestimate releases, whereas the CORSOR and CORSOR-M models give, for some radio-nuclide classes, relatively good results. The CORSOR model gave a better prediction for the releases of some radio-nuclide classes, whereas the CORSOR-M model gave better predictions for some others. The final simulations were performed with the CORSOR-M model, since the results are, on average, slightly better. The structural material release, which significantly influences the chemistry and consequently also the source term, could not be calculated since MELCOR 1.8.5 has no appropriate structural material release model.

In general, one can state that the agreement of the thermal-hydraulic variables is good, that the agreement of the total releases for most radio-nuclide classes is satisfactory, and that the radio-nuclide depositions in the steam generator are overestimated. The timing of the key events was relatively well predicted. The differences between the simulation results of both MELCOR 1.8.5 versions (QZ and RE) are negligible for the thermal-hydraulic variables, small for the radio-nuclide releases and the timing of key events, but significant for the radio-nuclide depositions and the bundle degradation. In general, the results of the newer MELCOR 1.8.5 version RE show better agreement with the experimental measurements.

Zahvala

Avtorja se za finančno podporo zahvaljujeta Ministrstvu za visoko šolstvo, znanost in tehnologijo (raziskovalni program številka: P2-0026) in Evropski komisiji (tematska mreža THENPHEBISP, številka pogodbe: FIKS-CT-2001-20151).

Acknowledgment

The authors gratefully acknowledge the financial support of the Ministry of Higher Education, Science and Technology of the Republic of Slovenia (research programme number: P2-0026) and the European Commission (thematic network THENPHEBISP, contract number: FIKS-CT-2001-20151).

5 LITERATURA
5 REFERENCES

[1] Schwarz, M., G. Hache, P. von der Hardt (1999) Phebus FP: A severe accident research programme for current and advanced light water reactors, *Nuclear Engineering and Design*187, pp. 47-69.
[2] Jacquemain, D., S. Bourdon, A. de Braemaeker, M. Barrachin (2000) PHEBUS FPT1 final report, IPSN/CRS/SEA/PEPF report SEA1/00, IP/00/479, *Institut de protection et de sûreté nucléaire (IPSN)*, Cadarache, France.
[3] Haste, T. (2002) Specification of international standard problem ISP-46 (PHEBUS FPT1), Note Technique SEMAR 2002/5, Rev. 1, *Institut de protection et de sûreté nucléaire (IPSN)*, Cadarache, France.
[4] Clement, B., et al. (2005) Thematic network for a Phebus FPT1 international standard problem (THENPHEBISP), *Nuclear Engineering and Design* 235, pp. 347-357.
[5] Leskovar, M. (2002) International standard problem No. 46 (Phebus FPT1), Simulation of Phebus FPT1 experiment bundle and circuit phase with the MELCOR 1.8.5 computer code, Report IJS-DP-8635, Rev.0, *Jožef Stefan Institute*, Ljubljana, Slovenia.
[6] Leskovar, M. (2002) Simulation of the PHEBUS FTP1 experiment with MELCOR 1.8.5, Proceedings, *International Conference Nuclear Energy for New Europe 2002*, Kranjska Gora, Slovenia.
[7] Kljenak, I., B. Mavko (2002) International standard sroblem No. 46 "Phebus", Simulation of FPT1 test containment phase with the CONTAIN computer code, Report IJS-DP-8614, Rev.1, *Jožef Stefan Institute*, Ljubljana, Slovenia.
[8] Gauntt, R.O., R.K. Cole, C.M. Erickson, R.G. Gido, R.D. Gasser, S.B. Rodriguez, M.F. Young (2000) MELCOR computer code manuals, Version 1.8.5 May 2000, NUREG/CR-6119, Vol.1-3, SAND2000-2417/1, *Sandia National Laboratories*, USA.
[9] Scheurer, H., B. Clement (1997) PHEBUS data book – FPT1, Document PH-PF IS/92/49, *Institut de protection et de sûreté nucléaire (IPSN)*, Cadarache, France.

Naslov avtorjev: dr. Matjaž Leskovar
prof. dr. Borut Mavko
Institut "Jožef Stefan"
Odsek za reaktorsko tehniko
Jamova 39
1000 Ljubljana
matjaz.leskovar@ijs.si
borut.mavko@ijs.si

Authors' Address: Dr. Matjaž Leskovar
Prof. Dr. Borut Mavko
Jožef Stefan Institute
Reactor Engineering Division
Jamova 39
1000 Ljubljana, Slovenia
matjaz.leskovar@ijs.si
borut.mavko@ijs.si

Prejeto: 9.7.2003
Received:
Sprejeto: 16.11.2005
Accepted:
Odprto za diskusijo: 1 leto
Open for discussion: 1 year

Strojniški vestnik - Journal of Mechanical Engineering 52(2006)3, 161-169
UDK - UDC 621.952:539.37
Izvirni znanstveni članek - Original scientific paper (1.01)

Analiza deformacij vrtal po analitični metodi in s končnimi elementi

Deformation Analysis of Boring Bars Using Analytical and Finite Element Approaches

Ahmet Taşkesen[1] - Faruk Mendi[1] - Yasin Kisioglu[2] - Mustafa Kemal Kulekci[3]
([1]Gazi University, Ankara; [2]The Ohio State University, Columbus Ohio; [3]Mersin University, Tarsus)

V prispevku obravnavamo analizo deformacij vrtal z uporabo analitične metode in metode končnih elementov. Izbrali smo tri vrste krožnih vrtal iz hitro reznega jekla in cementno-karbidnimi lastnostmi, za katera smo z uporabo obeh metod izračunali deformacije, nastale pod vplivom posrednih vrtalnih sil. Predlagali smo priporočilo izdelovalcem, s katerim lahko določijo obseg napak, ki vplivajo na odstopanje izmer in natančnost končne obdelave površine lukenj, izvrtanih vrtali, ki se upognejo zaradi vrtalnih sil. Ugotovili smo tudi, da stožčasta vrtala niso primerne oblike za vrtanje dolgih lukenj.

(Ključne besede: procesi vrtanja, analize deformacij, metode končnih elementov)

In this paper we discuss the deformation analyses of boring bars using analytical and finite-element methods. Three types of circular boring bars with HSS and cemented-carbide properties were selected, and their deformations when subjected to oblique boring forces were calculated using both methods. A guideline is proposed for the manufacturer, who can determine the extent of the errors that affect the dimensional tolerance and the surface-finish accuracy of the bored hole produced by the bar bent when subjected to the boring forces. Also, we observed that a conical bar is not an appropriate design for boring a long hole.

(Keywords: boring bars, boring processes, deformation analysis, finite element methods)

0 INTRODUCTION

Manufacturers usually select a boring process to achieve the desired dimensional accuracy when dealing with cases of large holes (e.g., diameter > 25mm) as an alternative approach to the conventional drilling and surface finishing [1]. The boring process enlarges holes previously drilled and offers straightness, parallelism, positional accuracy, size control, surface finish, improved accuracy of the dimensions and tolerance, and the elimination of any possible eccentricity. The surface quality of the bored hole, including the desired dimensional accuracy, is dependent on selecting the appropriate boring processes, including depth of cut, cutting speed, and the geometry of the boring bars. When the depth of cut and the elasticity of the material exceeds a certain limit, then the roughness of the surface of the machine components becomes unacceptable and tool breakage can occur. Usually, it is not recommended to have the ratio of the bar length, L, to the bar radius, r_b, i.e., L/r_b, larger than 10 to 12 when using steel or cemented-carbide materials [1]. Rather than using expensive experimental descriptions, the deformation of boring bars with different geometries and materials can be analyzed using both analytical and computer-aided finite-element methods to determine the appropriate shape of the bar for an acceptable process. Permissible stresses for the bars, known as design stresses, are usually low ([8] and [9]). However, the amount of deflection of the boring bar is usually high, so that boring errors occur in the dimensions of the desired hole.

The objective of this paper was to analyze the bar deformations and determine the appropriate bar design using both high-speed-steel (HSS) and cemented-carbide materials for boring bars at the recommended limit ratio (L/r_b) of 12. From the design point of view, bar deflection is one of the most troublesome elements for boring bars. When it exceeds the allowed limit [2], dimensional tolerance errors can occur on the diameter of the bored hole.

1 DEFORMATION ANALYSIS OF THE BORING BAR

Boring bars are usually made in three geometrical shapes: the square shank, the round shank, and the solid-carbide round shank [1]. Round-shank boring tools find wide application in industry, while the other two, because of manufacturing difficulties, have very limited applications. For this reason, in this paper, round-shank boring bars are discussed. The boring process is an oblique metal-cutting process, in which the tool is considered stationary and the workpiece is rotating about its axis [8]. Some of the procedures for dealing with boring-bar deformation analysis are described below.

1.1 Selecting Geometrical Models

Three types of geometrical models selected for boring bars, corresponding to the rules of the manufacturing and design processes, are shown in Figure 1. Each model was selected in accordance with possible geometrical conditions and the mechanical design methodologies. The three selected models shown in the figure have the same length and bar diameter: Model A is a traditional straight bar with a shoulder, but without a fillet. Model B has a variable front-end radius (r) and a constant rear-end radius (r_b), the ratio (r/r_b) of which ranges from 0.5 to 1. And finally, Model C has a shoulder with a large fillet radius, which enables it to be more flexible and resistant to the stress concentration and deformation due to notch effects.

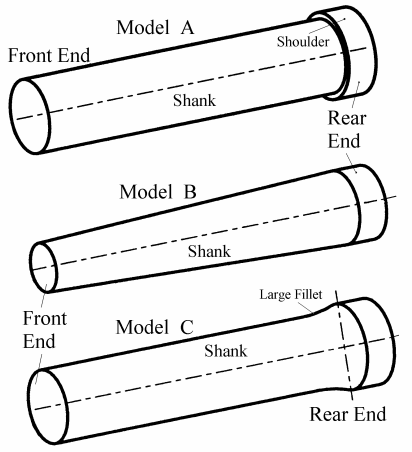

Fig. 1. *Selected circular geometrical models of boring bars*

1.2 Analytical Approach

Our goal is to derive a formulation that accurately describes the shank deformation of the boring bar due to oblique boring forces (OBFs), depending on certain variables such as the depth of cut (chip thickness), cutting edge angle, length and diameter of the bar, geometrical variables, and material properties. Figure 2 shows a boring tool consisting of a boring bar, an inserted cutter tip, and adjustment and set screws. The cutter tip is usually inserted onto the boring bar with an angle of 53°08' [1]. The boring bar can be clamped in any position in the turret (support). With this type of boring tool, the bar can be extended beyond the holder just far enough to reach the length of the hole to be bored, which makes the tool very rigid. In analytical deformation analysis, the values of the specific shear pressure, K_s, of each of the HSS-steel and carbide-steel material couples for the boring process [1] are considered. When we consider a constant cutting speed of 30 m/min for the boring process and the feed per revolution of 0.2 mm, the values of the specific cutting pressures are selected from the appropriate tables [1] as 2000 MPa and 2800 MPa for the HSS-steel and the carbide-steel material couples, respectively. In addition, the depth of cut is selected, ranging from 1 mm to 3 mm. The Young's Modulus is also selected from tables as 200 GPa and 400 GPa for the HSS and carbide materials, respectively [3].

The OBF at the front end of the boring tool creates torsion and bending moments during the

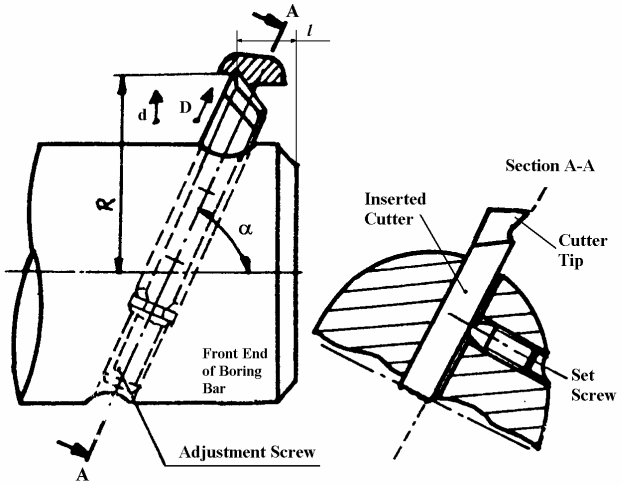

Fig. 2. *The components of a boring tool*

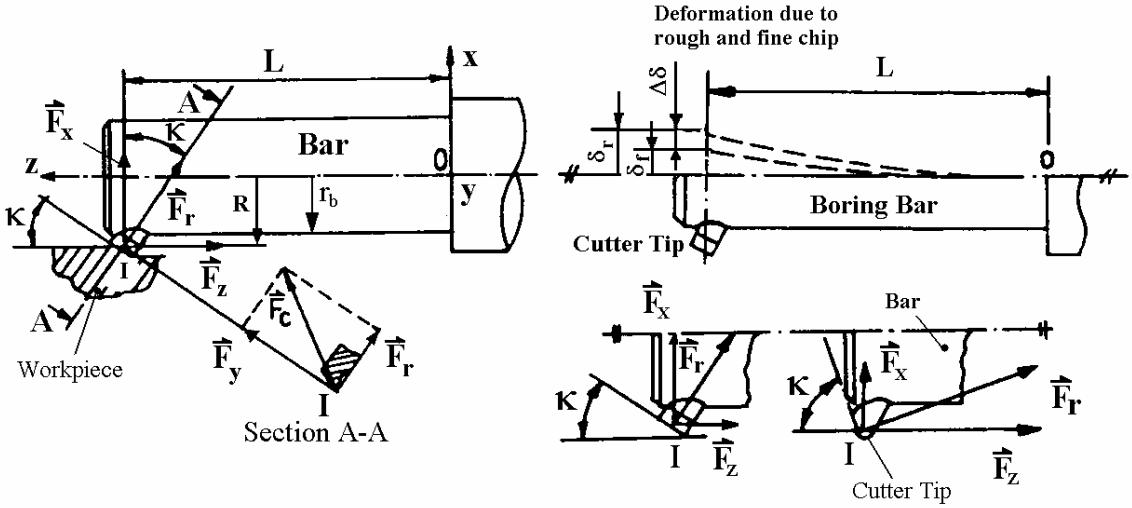

Fig. 3. *Distribution of the OBF and deflection due to the rough- and fine-chip processes*

boring process in such a way that the moments create deflection on the boring bar. A rigid bar subjected to the OBF at the interaction point 'I' of the cutter and workpiece and their resultants are shown in Figure 3. The radial and axial forces in the x-z projection plane have a resultant force, F_r. The distribution of the OBF on a single-point cutting tool is not a constant but depends on the cutting edge angle, κ, as shown in Figure 3. Experiments have shown that if κ is 45°, then the boring forces can be distributed as F_x, F_y, and F_z components, in the ratio 1:5:2 [1]. The three forces, F_x, F_y, and F_z, acting on the boring bar will do the bending, torsion, and compression, respectively. As shown in the equations below, the OBFs depend on the cutting-edge angle, the chip thickness, and the feed per revolution. Indeed, the three components of the OBF, F_x, F_y, and F_z, affect the boring bar through the tip of the cutting tool during the operation process. The tangential, radial, and axial forces within the corresponding directions, respectively, can be found using the following equations:

$$F_y = t_c \cdot s \cdot K_s \tag{1}$$

$$F_x = F_r \cdot \sin\kappa \tag{2}$$

$$F_z = F_r \cdot \cos\kappa \tag{3}.$$

Where: $F_r = 2 \cdot F_y / 3$ when $30^o < \kappa < 70^o$ [1]
$F_r = F_y / 3$ when $70^o < \kappa < 90^o$ [1]
t_c : chip thickness (mm)
s : feed per revolution (mm/rev)
K_s : specific shear pressure of the material (MPa)
κ : cutting edge angle.

1.3 Quantitative Description of the Boring Bar Deformation

The boring bars, considered as a cantilever beam, must be capable of deflection under the OBF. In the case of analytical deflection analysis, the most popular approach, strain energy by Castigliano's theorem, is applied instead of the many other available approaches. The strain energy for a combined, loaded boring bar is a nonlinear function of the OBF and the bending moment [7]. In applying Castigliano's second theorem in this application, the strain energy for a circular boring bar subjected to the OBF, such as the axial forces F_z, pure bending moment $M = F_x \cdot L$, shearing due to bending V, and the torque $T = F_y \cdot r_b$, can be rewritten in terms of the OBF and the bending moments as follows:

$$U = \int \frac{F^2 \cdot dz}{2A \cdot E} + \int \frac{M^2 \cdot dz}{2E \cdot I} + \int \frac{\alpha_s \cdot V^2 \cdot dz}{2A \cdot G} + \int \frac{T^2 \cdot dz}{2J \cdot G} \tag{4}.$$

Generally, the translational (δ_i) and rotational (θ_i) displacements of the boring bar can be performed by partial derivation of the strain-energy equation (4) with respect to the general OBF (F_i) and general torsional couple (T_i), respectively. Therefore, the translational and rotational displacements of the circular boring bar can be obtained using the following convenient form of equations, in the corresponding x, y, and z directions. Here, the integration is carried out over the boring-bar length to calculate the bar deflection in the related directions, i.e.:

$$\delta_x = \left(\frac{\partial U}{\partial F}\right)_z = \int \frac{\alpha \cdot V}{A \cdot G} \cdot \frac{\partial V}{\partial F} \cdot dz + \int \frac{M}{E \cdot I_y} \cdot \frac{\partial M}{\partial F} \cdot dz - \int \frac{M}{E \cdot I_x} \cdot \frac{\partial M}{\partial F} \cdot dz \tag{5}$$

$$\delta_y = \left(\frac{\partial U}{\partial F}\right)_z = \int \frac{\alpha \cdot V}{A \cdot G} \cdot \frac{\partial V}{\partial F} \cdot dz + \int \frac{M}{E \cdot I_y} \cdot \frac{\partial M}{\partial F} \cdot dz + \int \frac{T}{G \cdot J} \cdot \frac{\partial T}{\partial F} \cdot dz \quad (6)$$

$$\delta_z = \left(\frac{\partial U}{\partial F}\right)_z = \int \frac{F_z}{A \cdot E} \cdot \frac{\partial F_z}{\partial F} \cdot dz - \int \frac{M}{E \cdot I_y} \cdot \frac{\partial M}{\partial F} \cdot dz + \int \frac{M}{E \cdot I_x} \cdot \frac{\partial M}{\partial F} \cdot dz \quad (7),$$

by the same token, the rotational displacement (twist angle), δθ, which occurs only about the 'z' axis, can be written as follows:

$$\delta_\theta = \int_0^L \frac{T}{2J \cdot G} \cdot \frac{\partial T}{\partial T} \cdot dz \quad (8),$$

from which the boring-bar deflections in both the translational and rotational directions can be written as follows:

$$\delta_x = \frac{F_x \cdot L}{G \cdot A_2} + \frac{F_x \cdot L^3}{3E \cdot I_x} - \frac{F_z \cdot r_b \cdot L^2}{2E \cdot I_y} \quad (9)$$

$$\delta_y = \frac{F_y \cdot L}{G \cdot A_1} + \frac{F_y \cdot L^3}{3E \cdot I_x} + \frac{F_y \cdot r_b^2 \cdot L}{G \cdot J} \quad (10)$$

$$\delta_z = \frac{F_z \cdot L}{E \cdot A} - \frac{F_x \cdot r_b \cdot L}{3E \cdot I_x} + \frac{F_z \cdot r_b^2 \cdot L}{2E \cdot I_y} \quad (11)$$

$$\delta_\theta = \frac{F_y \cdot r_b \cdot L}{G \cdot J} \quad (12).$$

Where: $\delta_{x,\ y,\ and\ z}$: translational deflections in the direction of the x, y and z-axes,

δθ: rotational deflection about the z-axis,

E: Young's modulus of the boring bar material

G: shear modulus of the boring-bar material

$I_x = I_y = \pi \cdot r_b^4/4$: moment of inertia

$J = \pi \cdot r_b^4/4$: polar moment of inertia

$A = \pi \cdot r_b^2$: cross-sectional area of the boring bar

$A_1 = A_2 \cong 0.9A$: shearing area [1]

α_s: shear form factor.

The resultant deflection of the boring bar in 3-D can be calculated as follows:

$$\delta = \sqrt{\delta_x^2 + \delta_y^2 + \delta_z^2} \quad (13).$$

When changing the condition of the boring process during the operation, the deflection of the boring bar does not remain constant. For instance, in the transition from the rough to the fine chip process during the operation, the bar deflection is variable. This variation, as shown in Figure 3, causes the dimensional tolerance errors in the bored-hole dimensions. Considering the deflection δ_r due to the rough chip and δ_f due to the fine-chip processes, the variation of the deflection can be defined as follows:

$$\Delta\delta = \delta_r - \delta_f \quad (14)$$

From this we can say that Δδ causes the dimensional accuracy of the bored hole, which can be determined in the following equation:

$$D_{bh} = D_{dh} - 2 \cdot \Delta\delta \quad (15),$$

where D_{bh} and D_{dh} are the bored and desired hole diameters, respectively.

As a result, from Equation (15), the D_{bh} would be made much bigger than D_{dh} without dimensional tolerances. For this reason, it is highly recommended to avoid the transition from the rough-chip to the fine-chip process during the boring operations.

1.4 Finite-Element Analysis (FEA) Approach

The bending deflections for all types of boring bars are carried out with FEA using the ANSYS computer-code software. The results from the simulations are compared with the corresponding analytical results for the validation of our boring-bar models.

1.4.1 FEA mesh generation and boundary conditions

It is very important to select the mesh generation that is characterized by a structural solid element to enable us to describe the boring-bar behavior because of the difficulties in dealing with the geometrical model. The structural solid element provides us with information about the degrees of freedom (DOFs) related to the translational and the rotational displacements. Basically, the element is defined by four nodes, each node has six DOFs, i.e., three of them are translational in the x, y, and z directions, the other three are rotational about the x, y, and z-axes [4]. Besides the mesh generation, suitable boundary conditions are applied for each type of every bar model by using these FEA mesh generations, as shown in Figure 4. Considering the conditions of the boring process, the boring bars have free rotational DOFs about the axis of rotation, the z-axis, but all the nodes are restricted to rotations about the x- and y-axes. On the other hand, all other nodes have free translational DOFs in the three axes, except the clamped area at the rear end, and the OBFs are applied at point 'I'.

1.4.2 Deflections of the boring bars

By applying the different amounts of OBF as a function of the chip thickness using Equations (1),

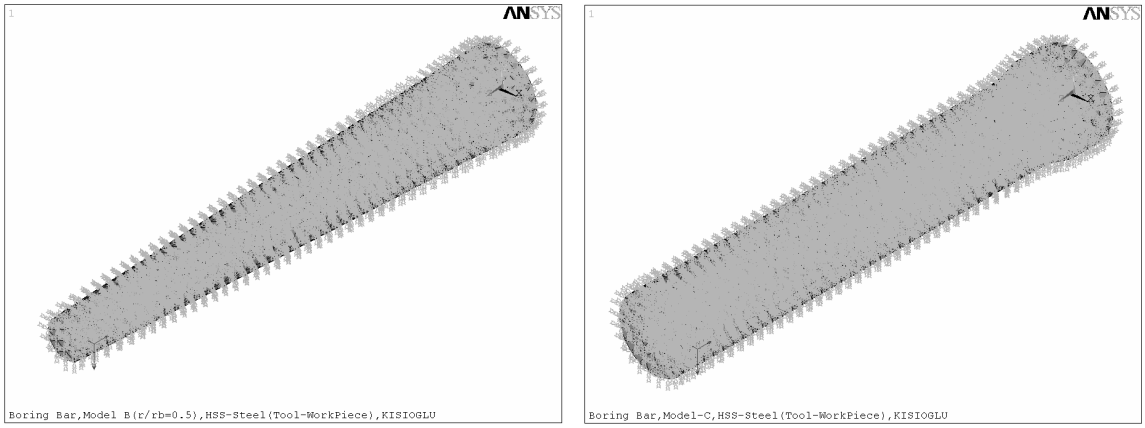

Fig. 4. *FEA mesh generation and boundary conditions for Models B (0.5), and C*

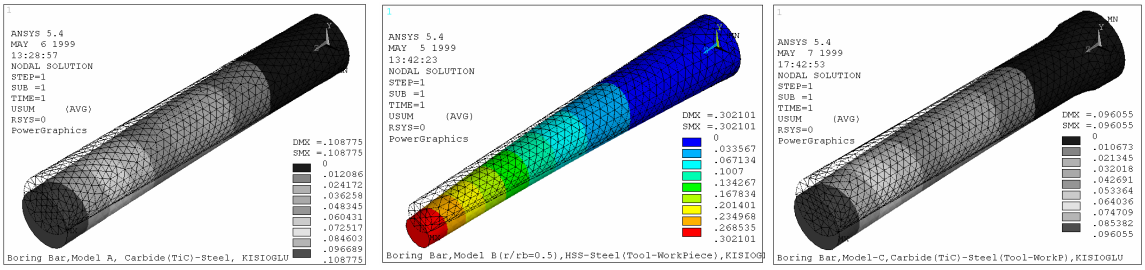

Fig. 5. *Contour plots of the translational deflections for three types of bar Models*

(2) and (3), the FEA models are simulated and some results are obtained. The translational deflections for Models A, B, and C are shown in Figure 5. For all the simulation-pictures, the dashed and solid lines show the undeformed and deformed geometries of the bar, respectively. On the other hand, the rotational deflections of the three models are also obtained. The rotational deflections, however, are very small, and do not cause the manufacturing errors mentioned in the literature as well. For this reason, the rotational deflection of the boring bars is not demonstrated in detail as contour plots from the simulations.

1.4.3 Experimental Investigation

Experiments have been conducted to further examine the validity of the analytical and FE methods. The boring tests were carried out without lubricant. A dynamometer with high sensitivity was set up to measure the cutting forces and the deflections. A specifically designed tool holder mechanically locked in the front of the dynamometer was used to hold the ANSI TPN 431 carbide tools. The cutting conditions were appropriately selected to obtain continuous chip flow. The chip thickness was set to be: 1.2, 1.4, 1.6, 1.8, 2, 2.2, 2.4, 2.6, 2.8, and 3 mm. The cutting speed was chosen as 30 m/min. The data are shown in Table 1.

1.4.4 Data and results

Table 1, below, shows the translational deflection data for all types of boring bars, having properties of the HSS-steel material couples. These values of the deflections are obtained from bending tests under the OBF of the boring bars by applying both the analytical and FEA approaches. The first column shows the depth of cut in mm. In the second column, the magnitude of the bar deflections as a function of depth of cut is given by applying Equation (13) of the analytical approach. The rest of the columns show the translational deformations of all types of boring bars by applying the FEA approach. The numbers in the brackets in columns 3 to 6 show the ratia (r/r_b) of Model B. Likewise, Table 2, below, shows the translational deflection data for all types of boring bars, having the properties of the cemented carbide-steel material couple by applying both analytical and FEA approaches. Figure 6, below, shows the relationship between the translational and rotational deflections for all types of boring bars as

Table 1. Translational deflections of the boring bar using the HSS-steel material couple from both analytical and FEA approaches

Boring Bar Deflection (USUM) Using HSS-Steel Couple Materials						
t_c(mm)	Analyt. Model	Model A & B(1)	Model B (0.5)	Model B (0.67)	Model B (0.83)	Model C
1	0.117751743	0.129492	0.251674	0.182973	0.154614	0.114348
1.2	0.141302092	0.155291	0.302101	0.229481	0.185538	0.137219
1.4	0.164852441	0.181291	0.352589	0.268149	0.216481	0.16009
1.6	0.188402789	0.207194	0.40305	0.306501	0.247391	0.182964
1.8	0.211953138	0.233091	0.4535075	0.344884	0.278725	0.205833
2	0.235503487	0.258988	0.5039691	0.383283	0.309743	0.228701
2.2	0.259053836	0.284903	0.5544307	0.4244896	0.340694	0.251574
2.4	0.282604184	0.310811	0.6048923	0.464093	0.371726	0.274445
2.6	0.306154533	0.336719	0.6553539	0.503696	0.402757	0.297316
2.8	0.329704882	0.362627	0.7058155	0.543299	0.433789	0.320187
3	0.35325523	0.388535	0.7562771	0.582902	0.464821	0.343058

Table 2. Translational deflections of the boring bars with the cemented carbide-steel material couple from both analytical and FEA approaches

Total Deflection (USUM) Using Carbide-Steel Couple Materials						
t_c (mm)	Analyt. Model	Model A & B(1)	Model B (0.5)	Model B (0.67)	Model B (0.83)	Model C
1	0.082617129	0.090646	0.175914	0.133865	0.108231	0.080073
1.2	0.099140555	0.108775	0.211097	0.160638	0.129879	0.096055
1.4	0.115663981	0.12691	0.24665	0.187042	0.151532	0.112069
1.6	0.132187407	0.145034	0.281929	0.214184	0.173171	0.128073
1.8	0.148710833	0.163166	0.317245	0.240962	0.194822	0.144085
2	0.165234259	0.181291	0.352558	0.268127	0.216463	0.16009
2.2	0.181757685	0.1994225	0.3879265	0.2947454	0.238113	0.1760921
2.4	0.198281111	0.2175517	0.4232677	0.3215861	0.259759	0.1920972
2.6	0.214804537	0.2356809	0.4586089	0.3484268	0.2814055	0.2081023
2.8	0.231327962	0.2538101	0.4939502	0.3752675	0.303052	0.2241074
3	0.247851388	0.2719393	0.529291	0.4021081	0.3246985	0.2401125

a function of the depth of cut when using the properties of the HSS-Steel material couple for the boring process. As the figure shows in the first graphics using data from Table 1, the translational deflections of Model C using both the analytical and FEA approaches are consistent. In the second graphics, the rotational deflections for all types of bar models are not consistent. The results from the FEA approaches are obtained higher than the analytical approach. The data for the rotational deflections are obtained using Equation (12) for the analytical approach. The data table of the rotational deflections is not shown here. Similarly, the graphical relationships of the translational and rotational deflections of all types of boring bars are shown in Figure 7 using the data in Table 2, taking into consideration the properties of the cemented carbide-steel material couples for the boring process. As can be seen in the first graphics using the data from Table 2, the translational deflections of Model C using both the analytical and FEA approaches are also consistent. In the second graphics, the rotational deflections for all types of bar models are not consistent. The results from the FEA approaches are found higher than the analytical approach. The data for the rotational deflections are obtained using Equation (12) for the analytical results. The data table of the results is not shown here. Indeed, in general, the rotational displacement is not sufficient to cause the boring errors in the bar, nor is it considered seriously in the related literature. Figure 8, below, illustrates the variation of the bar deflection in both the translational and rotational directions as a function of the ratio r/r_b of Model B. The figure shows a rapid decrease in the bar deformation, whereas 'r' increases, as explained above. The

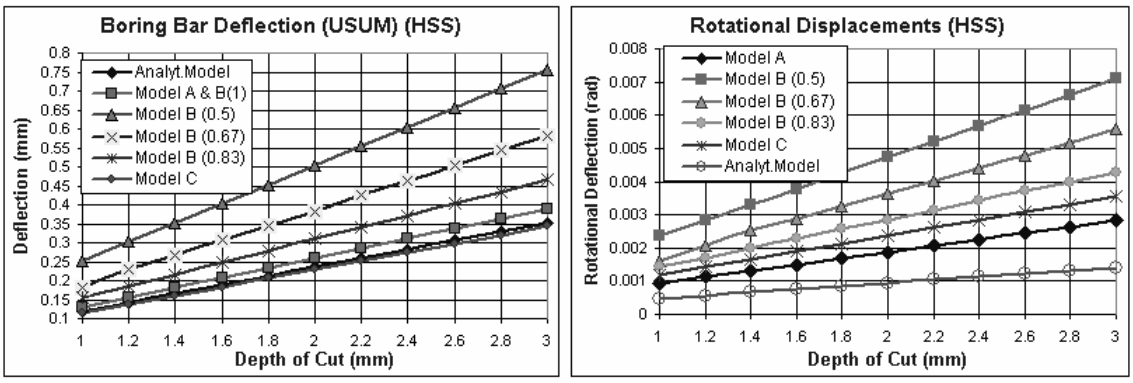

Fig. 6. *Graphical results of bar deflections in translational and rotational directions from both the analytic and the FEA approaches (material: HSS-steel couple)*

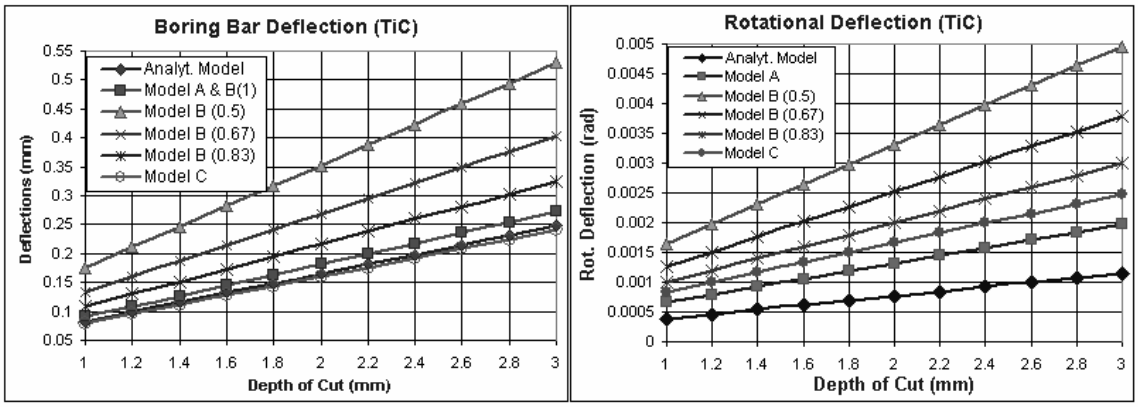

Fig. 7. *Graphical results of bar deflections in translational and rotational directions from both the analytical and the FEA approaches (material: cemented carbide-steel couple)*

variation in the rotational deflection as a function of conical ratio is found to be more than the variation of the translational deflection. The trends of both variations are also different.

1.5 Qualitative Description of Bar Deformation

Considering the deflections in the x, y, and z directions, the δ_z deflection is very small, whereas the δ_x and δ_y are bigger, as mentioned above. In this case, the δ_x and δ_y are especially important. In particular, if the δ_x exceeds the allowable limit, then it causes tolerance errors on the surface finish. However, if the δ_y exceeds the permissible limit, which causes a certain error "*e*", as shown in Figure 9, then the desired size control and the dimensional accuracy of the desired bored hole may not be obtained. Thus, we can find the error '*e*', as given by Equation (16) below. The δ_y will specify the degree of surface roughness. In this situation, '*e*' can be treated as an error and can be calculated using the Pythagorean theorem, knowing that it is related to the size of the bored hole and the deflection, δ_y, in the vertical direction in the case of the analytical model, as is given by Equation (10), above. In other words:

$$e = R - (R^2 - \delta_y^2)^{1/2} \tag{16}$$

where $R = r_b + (l \cdot \tan\alpha)$ (see Figure 1.)

The magnitude of the translational deflection's errors of the boring bars Models A, B (0.83) and C as a function of the depth of cut are shown in Figure 10 when considering the properties of both HSS-steel and cemented-carbide-steel material couples and using both analytical and FEA approaches. Both graphics illustrate that the smallest errors are obtained when Model C, with any type of material properties, is considered as the bar geometry for the boring process. Both solution approaches, the analytical and the FEA analysis, showed that the magnitude of the errors for Model C is consistent with both graphics in Figure 10.

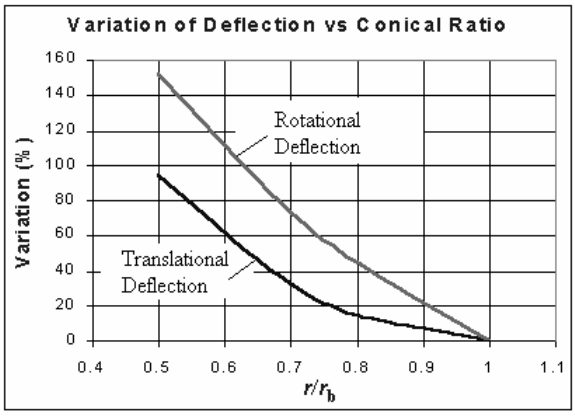

Fig. 8. *The boring bar deformation vs. the conical ratio of Model B*

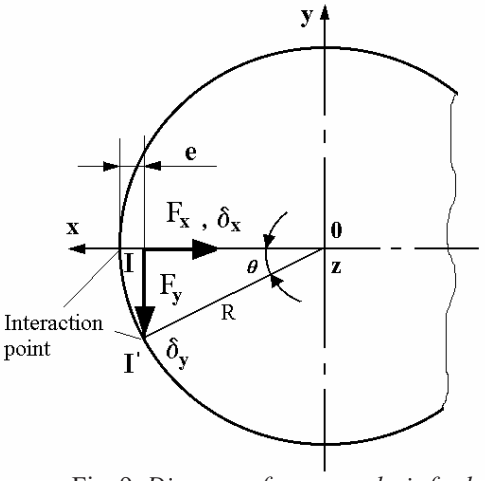

Fig. 9. *Diagram of error analysis for bar deformation*

2 DISCUSSION AND CONCLUSIONS

The deformation of the boring bar is modeled accurately by the driven analytical equations and validated by a computer-code finite-element method. Both the analytical and the FEA approaches confirm that Model C is an appropriate boring-bar design. From Figures 6 and 7 it is clear that the deflections of boring bars for both the analytical and FEA models are increasing with the depth of cut. But generally, the trends are the same. From the figures we can conclude that the twisting angle is very small, and that the rotational deformation is not important in the case of bar-design considerations and a bored hole with the desired characterizations. Figure 8, on the other hand, shows that the deflection is inversely proportional to the conical ratio (r/r_b), so that reducing r increases the deflection. Therefore, using a conical shape in the design of the boring bar is not appropriate for a long hole. On the other hand, the results found for Models A, B (0.83) and C, as shown in Figure 10, may be used by manufacturers as guidelines to determine the boring errors that affect the bored hole's dimensional tolerance and surface-finish accuracy according to the depth of cut.

Finally, the main purpose in the boring process with a boring bar is to reduce the tangential force F_y by making the cutting edge angle κ and the diameter of the bar as large as possible. For the same reason, the length of the bar L must be chosen to be as small as possible. In order to design a boring bar in the form of Model C, certain criteria must be followed. The amount of deformation must be restricted to a certain value and, on the other hand, the vibration must be absorbed and the effects of the notch between the shoulder and the bar must be reduced by a large fillet. Generally, if we change the boring process conditions like the chip thickness, the feet rate, etc. during the operation, the bar deformation becomes variable. This will create dimensional errors in the desired bored hole (size control, surface finish etc.). Indeed, the constant deformation is a special case that leads to dimensional tolerance errors in the size control.

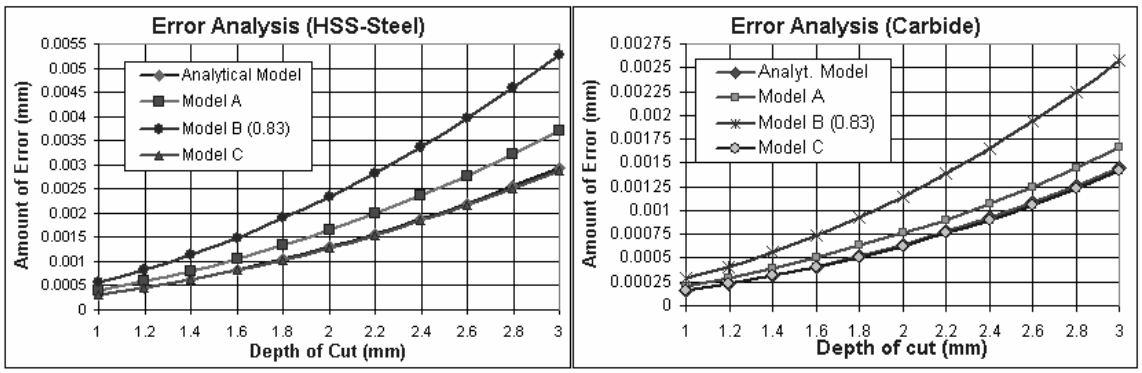

Fig. 10. *The magnitude of the error on the boring-bar deflections*

3 REFERENCES

[1] F. Mendi, T. Tezgahlari (1996) Teori ve Hesaplari, *72 TDFO Ltd. Sti.*, Ankara, Turkey.
[2] S.T. Nagano, T. Koizumi, T. Fujii, N. Tsujiuchi, H. Ueda, and K. Steel (1997) Development of a composite boring bar, *Composite Structures*, 38 (1997) 531-539.
[3] E. A. Avallone, T. Baumeister (1987) Marks' standard handbook for mechanical engineers, *McGraw-Hill Inc*.
[4] ANSYS User Manual (1998) ver. 5.4.
[5] T. Tyan, W.H. Yang (1992) Analysis of orthogonal metal cutting processes, *International Journal for Numerical Methods in Engineering*, 34 (1992) 365-389.
[6] A.J. Shih (1995) Finite element simulation of orthogonal metal cutting, *Journal of Engineering for Industry*, 117(1995) 84-93.
[7] A.C. Ugural, S.K. Fenster (1995) Advanced strength and applied elasticity, *Prentice Hall*.
[8] P.F. Oswald, J. Munoz (1997) Manufacturing processes and systems, *John Wiley & Sons*.
[9] M.C. Shaw (1996) Metal cutting principles, *Oxford University press*.

Authors' Addresses: Dr. Ahmet Taşkesen
Dr. Faruk Mendi
Gazi University
Technical Education Faculty
Besevler, Ankara, 06503
Turkey

Dr. Yasin Kisioglu
The Ohio State University
Industrial, Welding and
Systems Engineering
Columbus Ohio 43210
U.S.A.

Dr. Mustafa Kemal Kulekci
Mersin University
Tarsus Technical Education
Faculty
33480 Tarsus
Turkey
mkkulekci@mersin.edu.tr

Prejeto: 1.6.2005
Received:
Sprejeto: 16.11.2005
Accepted:
Odprto za diskusijo: 1 leto
Open for discussion: 1 year

Strojniški vestnik - Journal of Mechanical Engineering 52(2006)3, 170-180
UDK - UDC 658.562:621.313.13
Pregledni znanstveni članek - Review scientific paper (1.02)

Izvedba sistema za avtomatsko končno kontrolo kakovosti elektromotorjev za sesalnike

Implementation of a System for the Automatic End-Quality Assessment of Vacuum-Cleaner Motors

Bojan Musizza[1] - Janko Petrovčič[1] - Dejan Tinta[1] - Jože Tavčar[2] - Gregor Dolanc[1] - Janez Koblar[2] - Đani Juričić[1]
([1]Institut Jožef Stefan, Ljubljana; [2]Domel, Železniki)

V prispevku je predstavljen diagnostični sistem za končno kontrolo kakovosti elektromotorjev za sesalnike. Sistem temelji na novih mehatronskih rešitvah, ki združujejo posebno načrtovano strego testiranih enot, lasersko vibrometrijo, vibroakustične in elektromehanske meritve ter sodobne metode obdelave signalov. Rezultat obdelave izmerjenih signalov so značilke, na podlagi katerih sistem zazna in lokalizira tudi najmanjše napake v električnem ali mehanskem delu motorja. Natančni, zanesljivi in občutljivi diagnostični postopki zagotavljajo popolnoma brezhibne končne izdelke.

(Ključne besede: kontrola kakovosti, odkrivanje napak, avtomatizacija, elektromotorji majhni)

In this paper we present a diagnostic system for the end-quality assessment of vacuum-cleaner motors. The system relies on innovative mechatronic solutions, which combine custom-designed handling of the units under test, vibro-acoustic measurements and electrical measurements as well as advanced signal processing. Processing of the measured signals results in the so-called features, which serve to detect and localize even the tiniest faults, in either the electrical or mechanical parts of the motor. Thus the accurate, reliable and sensitive diagnostic procedure allow for entirely fault-free final products.

(Keywords: quality assessment, fault diagnosis, automation, small electric motors)

0 UVOD

Konkurenčne razmere na trgu malih elektromotorjev silijo proizvajalce k nenehnemu zniževanju stroškov proizvodnje in izboljševanju kakovosti svojih izdelkov. Domel d.d. Železniki je eden izmed vodilnih evropskih proizvajalcev elektromotorjev za sesalnike. Ena izmed možnosti za dvig konkurenčnosti - predvsem v primerjavi s proizvajalci z daljnjega vzhoda in njihovimi nizkimi cenami - je v nadaljnjem dvigu kakovosti izdelkov in učinkovitosti proizvodnje skozi zmanjševanje proizvodnih stroškov. Pomemben korak v tej smeri pomeni modernizacija sistema nadzora kakovosti, in sicer predvsem v smislu popolne avtomatizacije končne kontrole z namenom zagotavljanja 100-odstotno brezhibnih dobavljenih motorjev.

Na trgu obstaja nekaj ponudnikov avtomatskih testnih postaj za manjše elektromotorje, npr. [1] do [3]. Glavni problem je

0 INTRODUCTION

Continuously increasing competition on the market for small electrical motors is forcing manufacturers to reduce production costs while increasing the quality of their final products. Domel Ltd Železniki ranks among the leading manufacturers of vacuum-cleaner motors in Europe. As a way of coping with market competitors, particularly those from the Far East that gain market share by offering low prices, the company is working hard to improve quality and raise the efficiency of production by lowering production costs. A step towards achieving this goal is related to improving the process of quality assurance and, as part of this, fully automated end-quality assessment of the products. In this way, maximum quality and almost 100% fault-free final products are guaranteed.

There are several manufacturers in the market that offer automatic test stands for the end-quality assessment of vacuum-cleaner motors, e.g. [1] to [3].

Sl. 1. *Elektromotor za sesalnike*
Fig. 1. *Vacuum-cleaner motor*

ta, da omenjeni sistemi le delno rešujejo specifični problem kontrole kakovosti Domelovih sesalnih enot. Na primer, sistem Vogelsang & Benning omogoča merjenje vibracij le v eni točki, kar pa ne ustreza zahtevam kupcev. Podobno je s Schenckovim sistemom. Zato z njihovo uporabo ne bi v celoti odpravili potrebe po ročni kontroli.

Izgled elektromotorja za sesalnike, ki ga je treba testirati, je prikazan na sliki 1.

Rešitev, ki jo predlagamo v pričujočem prispevku, ima namen zagotoviti popolnoma avtomatsko končno kontrolo elektromotorjev, tj.:

- natančno ugotavljanje ključnih parametrov kakovosti sesalne enote,
- identifikacijo vseh parametrov kakovosti, ki odstopajo od predpisanih meja ter
- lokalizacijo napake v primeru, da je enota neprimerne kakovosti.

Rezultat omenjenih funkcionalnih lastnosti je zmanjšanje stroškov proizvodnje, ker potreba po dodatnih "ročnih" testih povsem odpade.

Glavni namen prispevka je predstaviti avtomatski diagnostični sistem za sesalne enote, ki je uveden na proizvodnji liniji v Domelu. Prispevek je organiziran takole. V sledečem poglavju je najprej prikazana zgradba diagnostičnega sistema, sledi opis merilnih celic. V četrtem poglavju je prikazano delovanje obravnavanega sistema, na koncu pa so podani sklepi.

1 ZGRADBA DIAGNOSTIČNEGA SISTEMA

Diagnostični sistem (sl. 2) je sestavljen iz petih glavnih modulov (sl.3):

- treh merilnih in diagnostičnih celic,

These systems, however, are only able to fulfil some of the requirements set by Domel. For example, the system of Vogelsang & Benning [1], and that of Schenk, only allows the measurement of vibrations at a single point. According to the quality standards of Domel, as well as the requirements imposed by various customers, vibration measurements should be carried out at three different points on the motor's body. Therefore, if installed, these systems would only partly solve the problem of full quality assessment and hence additional (manual) measurements would still be needed.

The device to be tested is shown in Figure 1.

The solution presented in this paper attempts to provide fully automatic quality-assessment tests that comprise:

- determination of the key quality parameters for vacuum-cleaner motors,
- identification of all the parameters of the motor's quality, which exceed pre-defined thresholds,
- fault localization once a motor of improper quality is identified.

These features lead to a reduction of production costs as no additional manual checks are needed.

The main purpose of the paper is to present a system for the automatic end-quality assessment of vacuum-cleaner motors at the end of the assembly line. The paper is organized as follows. In the section to follow the structure of the diagnostic system is described first. After that the diagnostic cells are explained. In the fourth section the performance of the system is presented and, finally, concluding remarks are given.

1 SYSTEM ARCHITECTURE

The system (Fig. 2) is composed of five major parts (Fig. 3):

- three measurement and diagnostic cells,

Sl. 2. *Diagnostični sistem za sesalne enote*
Fig. 2. *End-quality assessment system installed on the assembly line*

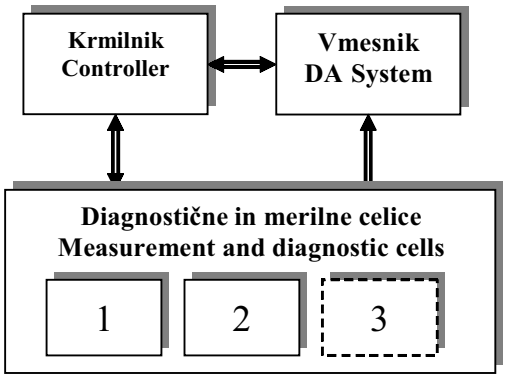

Sl. 3. *Zgradba diagnostičnega sistema*
Fig. 3. *Architecture of the diagnostic system*

- krmilnika za strego in
- računalnika s karticama za zajem podatkov.

Diagnostični sistem temelji na neposrednem merjenju devetih fizikalnih veličin, in sicer: napajalne napetosti na motorju, toka, podtlaka, moči, hitrosti vrtenja, in vibracij, za korekcijo meritev pa še temperaturo zraka, vlažnost in atmosferski tlak. Pozneje bo mogoča še meritev zvoka, ki ga za zdaj merimo le v preizkusne namene.

Glavni testi kakovosti se opravijo na treh merilnih modulih, ki delujejo vzporedno. Vzporednost je v tem primeru potrebna iz dveh razlogov:

a) zaradi razmeroma velikega števila različnih testov, ki jih je treba izvesti ter
b) zato, da se ujame takt proizvodnje, ki znaša 9 s.

Za usklajeno delovanje vseh operacij diagnostičnega sistema in strego skrbi zmogljiv Mitsubishijev krmilnik MELSEC-Q. Le-ta daje takt diagnostičnemu sistemu, ki mora ustrezati taktu preostalega dela proizvodne linije. Z uporabo informacij, ki jih dobi s pozicijskih zaznaval na liniji, ter pnevmatskih izvršilnih organov skrbi za pravilno vmeščanje in vklapljanje testiranih sesalnih enot v različnih fazah testiranja. Obenem pa skrbi tudi za transport enot skozi diagnostični sistem.

Sistem za zbiranje podatkov temelji na merilnih karticah NI 6220 in NI 6221, ki sta namenjeni za vzorčenje merjenih veličin. Zbrani podatki se predhodno obdelajo in potem pošljejo skozi algoritme za izračun značilk, od koder sledi vektor značilk. Vsaka značilka odraža nek vidik kakovosti tako, da s preverjanjem, ali je le-ta v predpisanem območju, sklepamo o tem, ali naprava ustreza zahtevanim standardom kakovosti. Če ne ustreza,

- a control unit for mechanical handling of the motors,
- a data-acquisition system.

The system operation relies on the direct measurements of nine electrical and mechanical quantities, i.e., power-supply voltage, motor current, air-pressure drop on the motor, speed of revolution, electric power, vibrations, as well as air temperature and humidity (needed for data conditioning). This set of measurements will soon be complemented by sound measurement.

The key assessment tasks are performed within three measurement modules running in parallel. The parallelism was needed in this case for two reasons:

a) a relatively large number of different tests that need to be performed,
b) to ensure the 9 s production cycle.

The control unit is built around a Mitsubishi MELSEC-Q PLC, which takes care of the mechanical handling and the tasks synchronization. The cycle of the diagnostic system is adapted to the cycle of other parts of the assembly line. Based on information from position sensors located on the line and pneumatic actuators, the control system generates signals for motor positioning as well as motor start-up and shut-down during the test. In addition, it takes care of transport of the motors through the diagnostic system.

The data-acquisition system is based upon the National Instruments NI 6220 and NI 6221 data-acquisition modules. The acquired data are first pre-processed and then passed to the feature-extraction algorithms that calculate a vector of features. Each feature (reflecting a particular aspect of quality) is checked in order to verify whether the device meets

Sl. 4. *Operaterski vmesnik*
Fig. 4. *Control panel*

potem algoritem ugotovi izvor napake. Vsa programska oprema je izdelana v grafičnem okolju LabVIEW.

Uporabljeni krmilnik je prek vodila RS 232 povezan z računalnikom. Slika 4 prikazuje operaterski vmesnik za upravljanje s celotnim diagnostičnim sistemom.

2 DIAGNOSTIČNE CELICE IN NJIHOVE FUNKCIJE

Prva merilna celica je namenjena preverjanju karakterističnih veličin sesalnih enot in kakovosti komutacije. Karakteristika motorja je definirana z naslednjimi podatki: električni tok motorja, električna moč, podtlak in hitrost vrtenja. Ob tem se nadzirajo tudi merilni pogoji, in sicer napajalna napetost, temperatura okolice, vlažnost ter atmosferski tlak. Pri tem se podtlak najprej korigira glede na atmosferski tlak in temperaturo okolice, nato pa se vse karakteristične veličine korigirajo še glede na razliko med nazivno (230 V) in dejansko napajalno napetostjo.

Kakovost komutacije se preverja na podlagi merjenja korena povprečja kvadratov (KPK - RMS), vrednosti toka v 12 frekvenčnih področjih širine 2,5 kHz. V ta namen tok vzorčimo s frekvenco 60 kHz, izračunamo njegov frekvenčni spekter in iz tega določimo vrednosti KPK posameznih pasov (sl. 5).

to the quality requirements. If this is not so, detection and localization of the tentative defects are performed. The entire application software is realized in LabVIEW.

The data-acquisition system is connected to the controller unit via an RS 232 communication line. Fig. 4 shows the control panel.

2 DIAGNOSTIC MODULES AND THEIR FUNCTIONS

The first diagnostic module serves for measuring the characteristic parameters of the motor on the one hand, and for assessing the quality of commutation, on the other. The motor's characteristic is defined by the following data: the electrical current, the electrical power, the pressure difference and the speed of revolution. As it is very important that these data are obtained under a nominal supply voltage, the measurement conditions are fully supervised in order to compensate for possible fluctuations. Based on a sampled actual voltage as well as the air temperature and humidity, the system is able to provide corrected values of the characteristic parameters, i.e., normalized to the nominal supply voltage (230V) and standard atmospheric conditions.

The quality of the commutation is verified by calculating the root-mean-square (RMS) values of the current signal in 12 consecutive frequency bands that are 2.5 kHz wide. The current signal is sampled with 60 kHz and the Fourier spectrum is calculated from the samples (Fig. 5).

Druga merilna celica, ki je prikazana na sliki 6, je namenjena merjenju vibracij. Le-te je na zahtevo kupca treba pomeriti v treh točkah, in sicer: na turbini v osni smeri, na turbini v radialni smeri in na ohišju sesalne enote zopet v radialni smeri.

Meritev vibracij poteka takole. Najprej posebne klešče primejo sesalno enoto (sl. 7). S tem jo vibracijsko ločijo od okolice (palete) in tako preprečijo, da bi na meritev vplivale vibracije, ki jih povzroča proizvodna linija. Vibracije enot se merijo z laserskim merilnikom Ometron VQ-500-D. Le-ta je pritrjen na vmeščalni mehanizem, ki omogoča njegovo navpično premikanje, in meri vibracije v vodoravni smeri. Meritev v osni smeri enote (navpični smeri) se izvede z uporabo zrcala, ki laserski žarek preusmeri v omenjeno smer. Nato pozicionirni mehanizem premakne laserski merilnik v še dve točki, tako da se lahko izmerijo še vibracije v radialni smeri, in sicer na turbini ter na ohišju. Po končanih meritvah se laserski merilnik vrne v začetno lego, klešče pa izpustijo sesalno enoto.

Vibracije sesalne enote se ovrednotijo na podlagi njihovih vrednosti KPK v 15 frekvenčnih pasovih širine 1 kHz, in sicer od 0

The second measurement and the diagnostic cell shown in Figure 6 serve for the vibration measurements. According to the customer's requirements the vibration must be measured at three points: on the cover, in the axial direction; on the cover, in the radial direction; and on the housing of the vacuum-cleaner motor, again in the radial direction.

The vibration measurement is carried out as follows. First, specially designed tongs grip the motor under test (see Fig. 7). In this way the motor is vibrationally isolated from the environment (i.e., transportation pallet) and so the vibration originating from the assembly line cannot affect the vibration measurement of the motor itself. The vibrations are acquired with an Ometron VQ-500-D laser vibrometer. The vibrometer is fixed on a positioning mechanism, which allows for movement of the vibrometer in the vertical direction, thus allowing measurement of the vibration in the radial direction. The measurement in the axial direction of the motor (in the vertical direction) is carried out by using a mirror, which redirects the laser beam in the appropriate direction. Then the positioning mechanism moves the vibrometer in another two points in order to measure the vibrations in the radial direction, i.e., on the cover and on the housing. As soon as the measurements are finished the vibrometer returns to its initial position and the tongs release the motor.

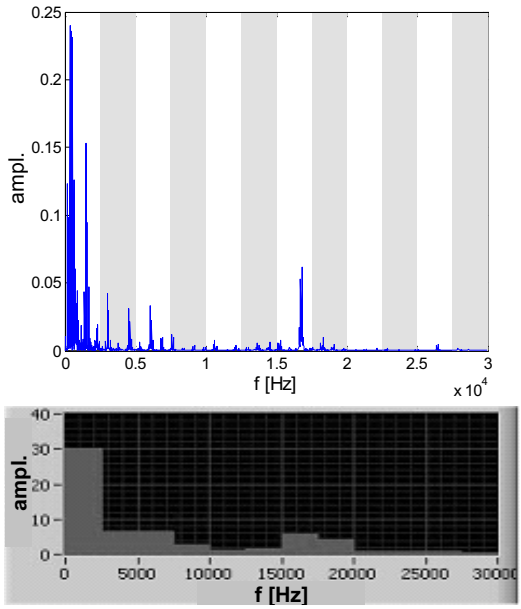

Sl. 5. *Primer frekvenčnega spektra toka (zgoraj) in pripadajočih značilk oz. vrednosti KPK posameznih pasov (spodaj)*

Fig. 5. *An example of the current frequency spectrum (above) and the corresponding features, i.e., RMS values of the individual bands (below)*

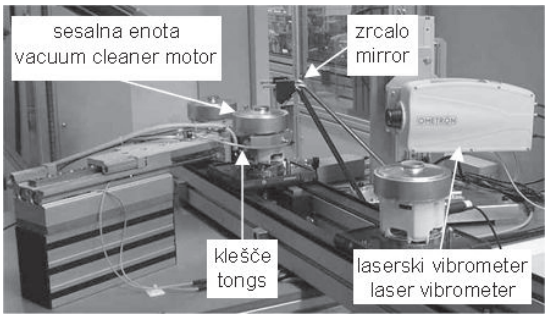

Sl. 6. *Merjenje vibracij*
Fig. 6. *Vibration measurement*

Sl. 7. *Prijemalo za motor*
Fig. 7. *A motor gripped by tongs*

do 15 kHz. V ta namen se signal vibracij vzorči s frekvenco 60 kHz, izračuna njegov frekvenčni spekter in iz tega določi vrednosti KPK posameznih pasov (sl. 8).

Tretja merilna celica, ki je v fazi uvajanja, bo namenjena merjenju zvoka sesalnih enot pri majhnih hitrostih vrtenja (okrog 40 vrtljajev na minuto). Zaradi nizke jakosti zvoka pri omenjenih vrtljajih bo treba meritve izvajati v akustično izolirani komori, s čimer se bo zmanjšal vpliv motilnega hrupa iz okolice.

Pri majhnih hitrostih vrtenja sesalnih enot pridejo v signalu zvoka do izraza značilni vzorci,

The vibrations of the vacuum-cleaner motor are evaluated with the RMS values of 15 1 kHz wide frequency bands in the range from 0 to 15 kHz. For this purpose the vibration signal is sampled at 60 kHz. Then its frequency spectrum is calculated, and from this the RMS values of the individual bands are defined (Fig. 8).

The third measuring cell, which is still in the implementation phase, is intended for measuring the sound emitted by vacuum-cleaner motors at low rotational speeds (app. 40 revolutions per minute). Due to the low intensity of the sound at these revolutions the measurements have to be carried out in an anechoic chamber in order to cut down the influence of disturbing noise from the environment.

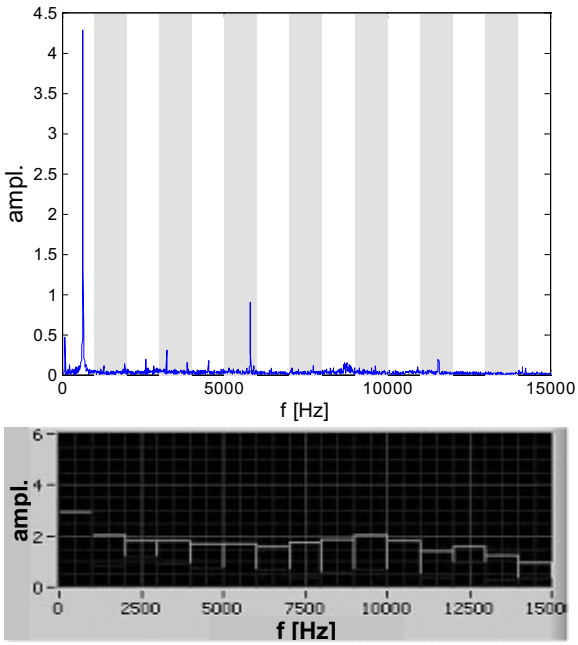

Sl. 8. *Primer frekvenčnega spektra vibracij (zgoraj) in pripadajočih značilk oz. vrednosti KPK posameznih pasov (spodaj)*
Fig. 8. *Example of vibration frequency spectrum (above) and the corresponding features, i.e., RMS values of the individual bands (below)*

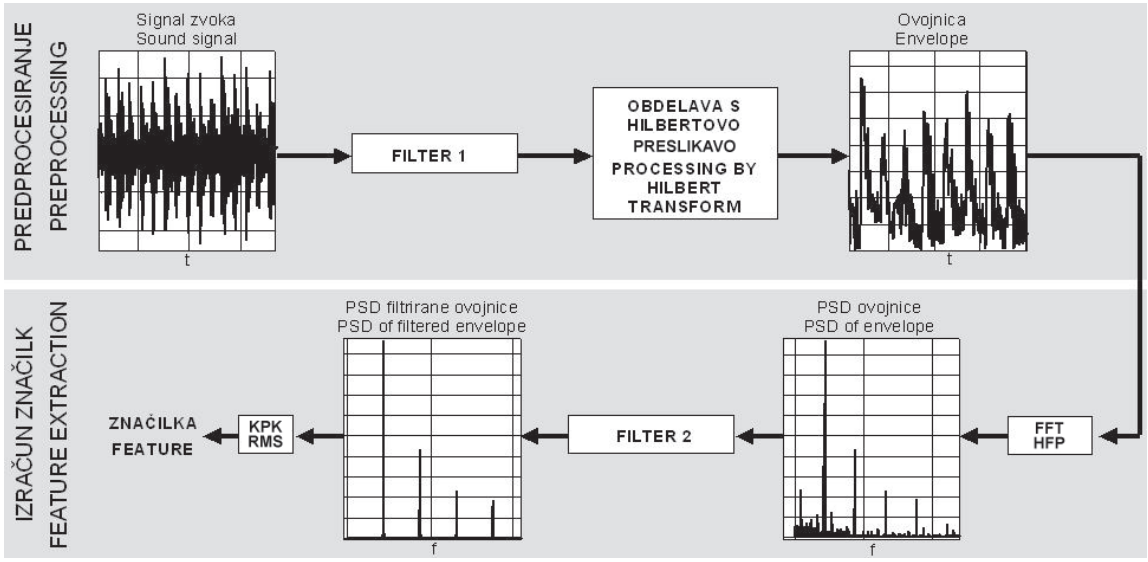

Sl. 9. *Obdelava signala zvoka*
Fig. 9. *Processing of the sound signal*

ki so posledica napak v ležajih ali drgnjenja med vrtečimi se in mirujočimi deli. Ti vzorci imajo obliko izbruhov, katerih pogostost pojavljanja je v primeru napake v ležaju odvisna od izmer ležaja in hitrosti vrtenja enote, v primeru drgnjenja pa ustreza frekvenci vrtenja enote oz. njenim večkratnikom [7]. S Hilbertovo preslikavo najprej določimo ovojnico signala zvoka, nato pa izračunamo njen frekvenčni spekter [8]. Določena napaka se kaže v vrednosti KPK ovojnice v ustreznih frekvenčnih pasovih, ki so značilni za posamezno napako. Postopek prikazuje slika 9.

3 DELOVANJE DIAGNOSTIČNEGA SISTEMA

Na vhodu v diagnostični sistem se najprej prebere številka palete, na katero je postavljena sesalna enota. Pod to številko se nato v računalniku shranjujejo diagnostični rezultati določene sesalne enote. S tem se zagotovi sledenje enoti medtem, ko le-ta potuje skozi posamezne merilne celice diagnostičnega sistema. Številka palete se ponovno prebere na izhodu sistema in primerja s tisto v računalniku. Če se številki ujemata, pomeni, da je bilo testiranje opravljeno uspešno. V nasprotnem primeru se sproži ustrezni alarm. V zadnji operaciji diagnostičnega sistema se v čip na paleti testirane sesalne enote vpiše, ali je le-ta brezhibna oz. ustrezno kodo morebitne napake.

At low rotational speeds of vacuum-cleaner motors typical patterns occur due to bearing faults or rubbing between rotating and static parts of the motor. They are shaped like bursts. The frequency of bursts depends on the dimensions of the bearing and on the rotational speed of the motor in the case of a bearing fault, while in the case of rubbing it depends on the rotational frequency of the motor or on its higher harmonics [7]. First, the envelope of the sound signal is obtained by using the Hilbert transform. Next, the frequency spectrum of the envelope is calculated [8]. The presence of a certain fault is reflected in the RMS value of the envelope in corresponding frequency bands, which are typical for an individual fault. The procedure is illustrated in Figure 9.

3 DIAGNOSTIC SYSTEM PERFORMANCE

Each vacuum-cleaner motor in the production line is associated with a label. First, the code of the transporting pallet is read at the entrance of the diagnostic system. Then, the diagnostic results of the particular vacuum-cleaner motor are saved in the computer under this code. In that way the tracking of the motor through the individual measuring cells of the diagnostic system is ensured. At the exit of the system the pallet code is read again and it is compared with the code in computer. If the two codes match, it means that the testing was performed successfully. In the opposite case, the appropriate alarm is triggered. In the last operation of the diagnostic system the condition of the tested vacuum-cleaner motor is recorded on the chip mounted on the pallet. The record contains information on the motor's health; if the

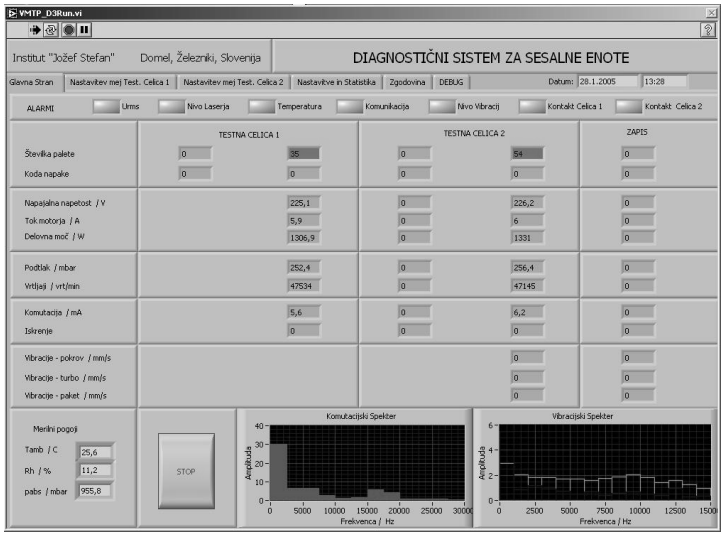

Sl. 10. *Uporabniški vmesnik*
Fig. 10. *User interface*

Uporabniški vmesnik obravnavanega sistema (sl. 10) je namenjen prikazu diagnostičnih rezultatov testiranih sesalnih enot. Poleg tega omogoča še nastavitev mejnih vrednosti značilk v obeh merilnih celicah, izračun nekaterih statističnih parametrov na izmerjenih vrednostih in pregled preteklih rezultatov testiranj.

Na sliki 11 je prikazana porazdelitev vrednosti KPK signalov tokov v frekvenčnem področju od 0 do 2,5 kHz za poskusno serijo sesalnih enot, ki so bile izdelane v fazi testiranja proizvodne linije. Vidimo, da je pri večini sesalnih enot kakovost motor is not fault-free, the appropriate code of the eventual fault is provided.

The user interface of the system (Fig. 10) is used to display all the essential diagnostic results of the tested vacuum-cleaner motors. In addition, it makes it possible to set the thresholds of the features in both measuring cells, to calculate some statistical parameters of the measured values and to review past results of the tests.

Figure 11. shows a distribution of the RMS values of current signals in the frequency band from 0 to 2.5 kHz obtained on a series of vacuum-cleaner motors. It can be seen that the commutation quality of almost all of the motors falls within the required

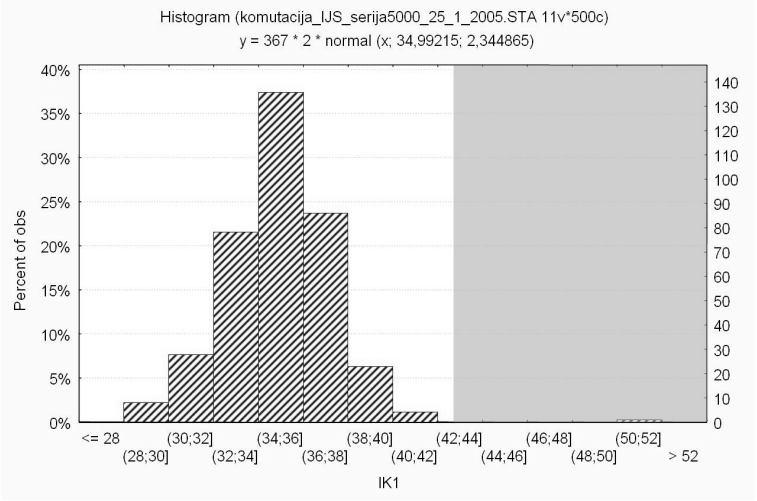

Sl. 11. *Porazdelitev značilke kakovosti komutacije za serijo 367 sesalnih enot*
Fig. 11. *Distribution of the commutation quality feature for a series of 367 vacuum-cleaner motors*

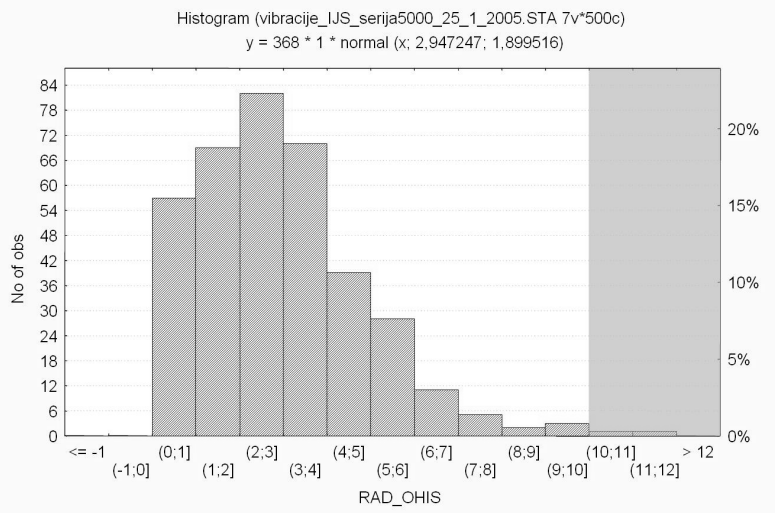

Sl. 12. *Porazdelitev značilke vibracij za serijo 368 sesalnih enot*
Fig. 12. *Distribution of the vibration feature for a series of 368 vacuum-cleaner motors*

komutacije ustrezna. Le pri nekaterih značilka preseže še dopustno mejo (osenčeno področje na grafu).

Slika 12 prikazuje porazdelitev značilke vibracij, tj. vrednosti RMS signalov vibracij v frekvenčnem pasu v okolici frekvence vrtenja sesalnih enot (600 do 800 Hz) za serijo 368 enot. Predstavljene so vibracije na ohišju v radialni smeri. Vibracije večine enot so v še dopustnih mejah (pod 10 mm/s), le pri nekaterih enotah jo prekoračijo (osenčeno področje na grafu). Pri tem je treba omeniti, da je srednja vrednost vibracij precej pod postavljeno mejo.

Oba primera kažeta dobro kakovost postopka montaže na liniji kakor tudi stabilno kakovost sestavnih delov, ki jih izdelujejo poddobavitelji.

4 VREDNOTENJE DIAGNOSTIČNEGA SISTEMA

Diagnostični sistem je po naravi podoben običajnemu merilnemu inštrumentu, saj ga lahko obravnavamo kot navidezni inštrument, ki "meri" stanje motorja. Zaradi tega lahko diagnostični sistem vrednotimo podobno kakor običajne merilne inštrumente. Slednje običajno vrednotimo na podlagi primerjave z odzivi vzorcev. V primeru diagnostičnega sistema žal ni vzorca, na katerega "referenčno" vrednost bi se lahko oprli. Zato je edina "referenčna" vrednost mnenje operaterjev. Žal so mnenja operaterjev subjektivna in zato včasih protislovna, predvsem v primerh, ko napaka ni

band (the forbidden band is displayed in grey). Only in a few cases does the feature exceed the threshold (shaded area in the graph).

Figure 12 shows the distribution of vibration feature, i.e., RMS values of the vibration signals in the frequency band around the rotational frequency of the vacuum-cleaner motors (600-800 Hz) for a series of 368 motors. In this figure the vibrations on the housing in the radial direction are presented. The vibrations of most of the motors are below the threshold (10 mm/s); just in some cases the threshold is exceeded (shaded area in the graph). It should also be noted that the mean value of the vibration features is, generally, well below the threshold.

Both examples reflect the high quality of the assembly process and the stable quality of the assembly parts delivered by subcontractors.

4 DIAGNOSTIC SYSTEM EVALUATION

The performance of the diagnostic system is closely analogous to the performance of any classical instrumentation. Indeed, the former can be viewed merely as a virtual instrument that "senses" the motor's condition. Therefore, it could be evaluated in the same way as classical measuring instruments, i.e., according to the reference value from the ethalon device. In this case, however, the ethalon device, which would give the reference value for the motor's condition, does not exist. The only available "reference" is the operators' judgements. Unfortunately, the operators' judgements happen to be non-uniform in some "grey" cases in which

izrazita. Problem uglaševanja diagnostičnega sistema smo rešili tako, da smo uporabili iterativni postopek v fazi preizkusne proizvodnje elektromotorjev. Pragovne vrednosti so bile izbirane upoštevajoč naslednje vidike:

- skladnost z uporabnikovimi zahtevami,
- enotno mnenje operaterjev, ki so zadolženi za nadzor kakovosti,
- izkušnje iz preteklosti, ki se nanašajo na podobne motorje,
- statistika, dobljena v fazi preizkusne proizvodnje.

5 SKLEP

V prispevku je predstavljen sistem za avtomatsko končno kontrolo sesalnih enot, ki omogoča ovrednotenje vseh njihovih najpomembnejših parametrov kakovosti. Njegova odlika je neprimerno večja zanesljivost in natančnost v primerjavi z ročno kontrolo. Sistem daje tudi globlji vpogled v stanje sesalne enote. Spremljanje trendov kakovosti pa omogoča hitre reakcije na proizvodni liniji.

Popolna avtomatizacija končne kontrole in zagotavljanje visokih standardov kakovosti posledično omogočata zmanjšanje stroškov postopka zagotavljanja kakovosti ter dvig zaupanja kupcev.

ZAHVALA

Avtorji se zahvaljujemo za podporo Ministrstvu za visoko šolstvo, znanost in tehnologijo ter družbi Domel d.d.

a defect is not particularly obvious. The reason for this is the operators' subjectivity and the limitations of human perception. Therefore, the diagnostic system was tuned and evaluated in an iterative procedure during the test production of the motors. In this phase the feature thresholds were set in deference to several aspects:

- full compliance with customers' requirements,
- consensus of opinion between the operators responsible for quality control,
- past experience on quality assessment with similar motors,
- available statistics obtained during the test production.

5 CONCLUSION

In this paper a system for the automatic end-testing of vacuum-cleaner motors is presented. It makes it possible to evaluate all of the most important quality parameters of the motor. Much better reliability and accuracy are its main advantages, compared to manual testing. The system also gives us a better insight into the condition of the vacuum-cleaner motor. Moreover, tracking the quality trends means that early corrective actions can be taken on the production line.

Complete automation of the end-test and high-quality standard assurance consequently make it possible to reduce the costs of the quality-assurance process and to raise customers' confidence.

ACKNOWLEDGEMENTS

The financial support of the Ministry of Higher Education, Science and Technology of the Republic of Slovenia as well as of Domel Ltd. is gratefully acknowledged.

6 LITERATURA
6 REFERENCES

[1] Vogelsang & Benning (2005). Routine test systems, URL: www.vogelsangbenning.de/intro.html.
[2] Schenck (2005). Schenck motor test systems, URL: www.schenck-usa.com/prod_motor_test.html.
[3] Artesis (2005). Motor quality monitor, URL: www.artesis.com/mqm.asp.
[4] Tinta, D., J. Petrovčič, U. Benko, Đ. Juričić, A. Rakar, M. Žele, J. Tavčar, J. Rejec in A. Stefanovska (2005). Fault diagnosis of vacuum cleaner motors. *Control Engineering Practice*, 13, 177-187.
[5] Edwards, S., A.W. Lees in M.I. Friswell (1998). Fault diagnosis of rotating machinery. *Shock and Vibration Digest*, 30, 1, 4-13.
[6] Yang, D. M. in J. Penman (2000). Intelligent detection of induction motor bearing faults using current and vibration monitoring. *Proceedings of COMADEM 2000*, Houston, 461-470.
[7] Benko, U., J. Petrovčič, Đ. Juričič, J. Tavčar in J. Rejec (2005). An approach to fault diagnosis of vacuum cleaner motors based on sound analysis. *Mech. Syst. Signal Process*, 19, 427-445.

[8] Randall, R.B. (2002). State of the art in monitoring rotating machinery. *Proceedings of ISMA 2002*, 4, 1457-1477.

Naslova avtorjev: Bojan Musizza
dr. Janko Petrovčič
dr. Gregor Dolanc
mag. Dejan Tinta
doc.dr. Đani Juričić
Institut Jožef Stefan
Jamova 39
1000 Ljubljana
bojan.musizza@ijs.si
janko.petrovcic@ijs.si
gregor.dolanc@ijs.si
dejan.tinta@ijs.si
dani.juricic@ijs.si

doc.dr. Jože Tavčar
Janez Koblar
Domel d.d.
Otoki 21
4228 Železniki
joza.tavcar@domel.si
janez.koblar@domel.si

Authors' Addresses: Bojan Musizza
Dr. Janko Petrovčič
Dr. Gregor Dolanc
Mag. Dejan Tinta
Doc.Dr. Đani Juričić
Jožef Stefan Institute
Jamova 39
1000 Ljubljana, Slovenia
bojan.musizza@ijs.si
janko.petrovcic@ijs.si
gregor.dolanc@ijs.si
dejan.tinta@ijs.si
dani.juricic@ijs.si

Doc.Dr. Jože Tavčar
Janez Koblar
Domel Ltd.
Otoki 21
4228 Železniki, Slovenia
joza.tavcar@domel.si
janez.koblar@domel.si

Prejeto: 13.8.2005
Received:
Sprejeto: 16.11.2005
Accepted:
Odprto za diskusijo: 1 leto
Open for discussion: 1 year

Strojniški vestnik - Journal of Mechanical Engineering 52(2006)3, 181-194
UDK - UDC 510.5:004.42
Strokovni članek - Speciality paper (1.04)

Uporaba gladilnih funkcij za glajenje podatkov podanih v diskretni obliki

Using Spline Functions to Smooth Discrete Data

Igor Emri - Robert Cvelbar
(Fakulteta za strojništvo, Ljubljana)

V prispevku je predstavljen algoritem za izračun gladilnih funkcij, uporabljen v programskem paketu "SPLINE", razvitem v Centru za eksperimentalno mehaniko na Fakulteti za strojništvo v Ljubljani. Podana je podrobna analiza vpliva števila izbranih podintervalov in števila diskretnih vrednosti na natančnost približka. Uporabnost algoritma je prikazana na eksperimentalnih podatkih za realno in imaginarno komponento modula lezenja poli-izobutilena. Podatki, ki smo jih analizirali, so povzeti iz objave [5].

(Ključne besede: funkcije gladilne, glajenje podatkov, algoritmi, paketi programski, SPLINE)

In this paper we present an algorithm for calculating spline functions. This algorithm is integrated into the software package "SPLINE". The influence of the number of pre-selected sub-intervals and the number of datum points per sub-interval on the accuracy of the approximation was analyzed. The power of the algorithm was demonstrated on the shear storage and the loss-compliance data for an uncrosslinked poly-isobutylene. The experimental data were measured and discussed by [5].

(Keywords: spline functions, smoothing splines, algorithms, software packages, SPLINE)

0 UVOD

Rezultat meritev je po navadi množica točk, ki podaja odvisnost med dvema fizikalnima veličinama, recimo x in y. Zelo pogosto želimo izmerjeno množico točk nadomestiti (približati) z množico diskretnih točk, ki pomenijo "gladko" krivuljo. Ena izmed možnosti, ki jo v praksi pogosto uporabljamo, je približek s polinomom ustreznega reda. Ta postopek bo praviloma dal zadovoljivo rešitev samo v tistih primerih, pri katerih je odvisnost med fizikalnima veličinama x in y v resnici potenčnega tipa. V vseh drugih primerih (tj., ko je odvisnost eksponentna ali trigonometrična) je omenjeni postopek po navadi nesprejemljiv. V takih primerih najučinkoviteje opravimo postopek glajenja z uporabo zlepkov polinomov tretjega reda.

V prispevku je predstavljen algoritem, ki omogoča interaktivno spreminjanje širine posameznega zlepka, kar omogoča kakovostnejše glajenje eksperimentalnih podatkov z večjim raztrosom. Algoritem je bil uporabljen v programskem paketu 'SPLINE', ki smo ga razvili v Centru za eksperimentalno mehaniko na Fakulteti za strojništvo v Ljubljani za potrebe vrednotenja časovno odvisnega obnašanja polimernih in kompozitnih materialov.

0 INTRODUCTION

The results of measurements are usually given as a set of datum points, which defines the relation between the two measured physical quantities, i.e., x and y. Very often we want to replace the set of measured data points with a set of discrete data points representing a smooth curve. One of the possible choices we often use in practice is an approximation with polynomials of the appropriate order. This approach would only result in a satisfying solution when the relationship between the physical quantities x and y is indeed polynomial. In all other cases (i.e., when the relation is exponential or trigonometric) the polynomial approach can be unacceptable. In such cases, the most effective procedure for smoothing the data is the use of so-called "spline" functions.

We present an algorithm that was used in the development of the "SPLINE" computer program at the Center for Experimental Mechanics, Faculty of Mechanical Engineering, University of Ljubljana. The algorithm was used to evaluate the time-dependent behavior of polymers and composite materials.

0.1 Definicija problema

V ravnini $x - y$ naj bo podanih N parov diskretnih vrednosti:

$$\mathcal{F} = \{x_i, y_i;\ i = 1,\ 2,\ ....,\ N;\ N > 3\} \quad (1),$$

ki podajajo odvisnost med izmerjenima fizikalnima veličinama x in y. Diskretne vrednosti naj bodo urejene tako, da bo izpolnjen pogoj:

$$x_i < x_{i+1} \quad (2)$$

za vsak i, ki zadosti pogoju:

$$1 \le i \le N - 1 \quad (3).$$

Cilj, ki si ga zastavljamo, je določitev 'gladke' krivulje, ki bo najbolje približala omenjeno odvisnost ne glede na to, kakšna je oblika te odvisnosti.

1 TEORETIČNE OSNOVE

Gladilna funkcija je v bistvu krivulja, ki je sestavljena iz množice polinomov tretjega reda. Zaprto območje na osi x, znotraj katerega so podane diskretne vrednosti x_i in y_i, razdelimo na ustrezno število korakov. Znotraj vsakega koraka izvedemo nato približek podanih diskretnih vrednosti s polinomom tretjega reda. Ker zahtevamo, da je približna krivulja zvezna in zvezno odvedljiva, morajo polinomi na stičišču dveh korakov imeti enaki funkcijski vrednosti ter enak prvi in drugi odvod.

1.1 Definicija vozlišč

Zaprto območje:

$$I\left[x_1, x_N\right] \quad (4)$$

razdelimo na K–1 korakov:

$$I_j = \left[t_j, t_{j+1}\right];\quad j = 1, 2, 3, ..., K - 1 \quad (5),$$

kjer sta t_j in t_{j+1} spodnja in zgornja meja j-tega koraka. Velikost j-tega koraka je potem:

$$l_j = t_{j+1} - t_j \quad (6).$$

Meje korakov podaja množica točk:

0.1 Problem statement

In the plane $x - y$ we have a set of N discrete data pairs:

$$\mathcal{F} = \{x_i, y_i;\ i = 1,\ 2,\ ....,\ N;\ N > 3\} \quad (1),$$

which defines the relationship between the two measured physical quantities, x and y. Let the discrete values be ordered such that

$$x_i < x_{i+1} \quad (2)$$

for every i, which fulfills the condition

$$1 \le i \le N - 1 \quad (3).$$

The goal is to obtain a smooth curve that would faithfully represent the actual relationship between the two physical variables independently of the shape of the underlying relation.

1 THEORETICAL BACKGROUND

The spline function is essentially a curve assembled from a number of third-order polynomials. The closed interval on the x-axis, within which the discrete values x_i and y_i are given, is divided into an appropriate number of sub-intervals. Within each of the sub-intervals an approximation of the given discrete values is achieved with the third-order polynomials. The approximation curve has to be continuous and continuously derivative. Thus, the value of the polynomials, and their first and second derivatives in the connection points of the two neighboring sub-intervals should have the same values.

1.1 Definition of the connection points

The closed interval:

$$I\left[x_1, x_N\right] \quad (4)$$

we divide into K–1 sub-intervals,

$$I_j = \left[t_j, t_{j+1}\right];\quad j = 1, 2, 3, ..., K - 1 \quad (5),$$

where t_j and t_{j+1} are the lover and the upper boundary of the j-th sub-interval. Thus, the size of the j-th sub-interval is:

$$l_j = t_{j+1} - t_j \quad (6).$$

The boundaries (connection points) of the sub-intervals are given with the set of data points

$$T = \{t_j;\ j = 1, 2, ..., K\} \tag{7},$$

ki morajo izpolnjevati naslednje pogoje:

which must fulfill the following conditions:

$$3 \le K \le N \tag{8}$$

$$t_1 = x_1\ ;\ t_K = x_N \tag{9}$$

$$l_j > 0; \quad j = 1, 2, ..., K-1 \tag{10}.$$

Točke t_j bomo imenovali vozlišča.

Points t_j are denoted as connection points.

1.2 Izpeljava algoritma ([1] do [3])

Znotraj vsakega koraka:

1.2 Outline of the algorithm ([1] to [3])

Within each of the sub-intervals:

$$I_j = \left[t_j, t_{j+1}\right]; \quad j = 1, 2, 3, ..., K-1$$

uporabimo polinom tretjega reda:

we utilize the third-order polynomial:

$$f_j(x) = A_j x^3 + B_j x^2 + C_j x + D_j \tag{11},$$

ki naj na meji s sosednjima korakoma, tj., v j-tem in j+1 vozlišču, izpolnjuje naslednje pogoje:

which at the borders of the sub-interval, i.e., at the connection points j and j+1, fulfills the conditions:

$$f_j(t_j) = f_{j-1}(t_j) = F_j; \qquad f_j(t_{j+1}) = f_{j+1}(t_{j+1}) = F_{j+1} \tag{12}$$

$$f'_j(t_j) = f'_{j-1}(t_j) = P_j; \qquad f'_j(t_{j+1}) = f'_{j+1}(t_{j+1}) = P_{j+1} \tag{13}$$

$$f''_j(t_j) = f''_{j-1}(t_j) = H_j; \qquad f''_j(t_{j+1}) = f''_{j+1}(t_{j+1}) = H_{j+1} \tag{14}.$$

Iz linearnosti drugega odvoda gladilne funkcije (sl. 1) izhaja:

From the linearity of the second derivative of the smoothing function, Fig. 1, follows:

$$\frac{t_{j+1} - x}{x - t_j} = \frac{H_{j+1} - f''_j(x)}{f''_j(x) - H_j} \tag{15}$$

in od tod:

and

$$f''_j(x) = H_j \frac{t_{j+1} - x}{l_j} + H_{j+1} \frac{x - t_j}{l_j} \tag{16}.$$

Dvakratno integriranje enačbe (16) da:

Double integration of Eq. (16) yields:

$$f'_j(x) = -\frac{H_j}{2l_j}\left(t_{j+1} - x\right)^2 + \frac{H_{j+1}}{2l_j}\left(x - t_j\right)^2 + E_1 \tag{17}$$

$$f_j(x) = \frac{H_j}{6l_j}\left(t_{j+1} - x\right)^3 + \frac{H_{j+1}}{6l_j}\left(x - t_j\right)^3 + E_1 x + E_2 \tag{18},$$

kjer integracijski stalnici E_1 in E_2 določimo iz pogoja (12):

where the integration constants E_1 and E_2 can be obtained from the conditions (12):

$$E_1 = \frac{F_{j+1} - F_j}{l_j} - \frac{l_j\left(H_{j+1} - H_j\right)}{6} \tag{19}$$

$$E_2 = t_{j+1}\left(\frac{F_j}{l_j} - \frac{l_j H_j}{6}\right) - t_j\left(\frac{F_{j+1}}{l_j} - \frac{l_j H_{j+1}}{6}\right) \tag{20}.$$

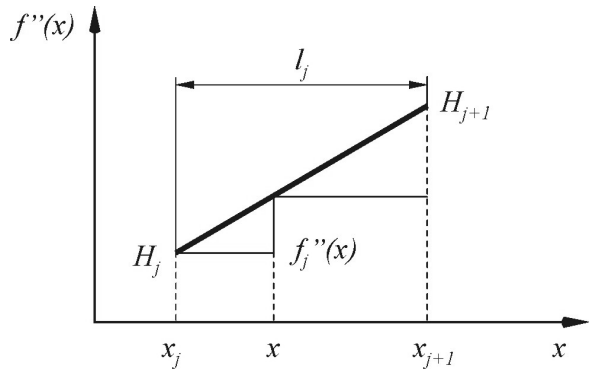

Sl. 1. *Drugi odvod približne funkcije znotraj j-tega koraka*
Fig. 1. *Second derivative of the approximation function inside the j-th sub-interval*

Iz razmerij (18) do (20) bi sedaj lahko izračunali stalnice A_j, B_j, C_j in D_j, definirane z enačbo (11). Iz praktičnih razlogov bomo stalnice polinoma ohranili izražene v odvisnosti od F_j, P_j, H_j in l_j (glej enačbe (12) do (14) in sliko1). Enačbi (17) in (18) sedaj lahko zapišemo kot:

The constants of the polynomials within each sub-interval, A_j, B_j, C_j and D_j, Eq. (11), can be calculated from the relations (18) through (20). For practical reasons the constants will be expressed in terms of F_j, P_j, H_j and l_j, (see Eqs. (12) to (14) – and Fig. 1). Equations (17) and (18) can now be rearranged as:

$$f_j'(x) = -H_j\left[\frac{(t_{j+1}-x)^2}{2l_j} - \frac{l_j}{6}\right] + H_{j+1}\left[\frac{(x-t_j)^2}{2l_j} - \frac{l_j}{6}\right] - \frac{F_j}{l_j} + \frac{F_{j+1}}{l_j} \tag{21}$$

$$f_j(x) = H_j\left[\frac{(t_{j+1}-x)^3}{6l_j} - l_j\frac{t_{j+1}-x}{6}\right] + H_{j+1}\left[\frac{(x-t_j)^3}{6l_j} - l_j\frac{x-t_j}{6}\right] + F_j\left[\frac{t_{j+1}-x}{l_j}\right] + F_{j+1}\left[\frac{x-t_j}{l_j}\right] \tag{22}.$$

Iz pogoja (13) izhaja:

From the condition (13) it follows:

$$H_j\frac{l_j}{6} + H_{j+1}\left[\frac{l_j+l_{j+1}}{3}\right] + H_{j+2}\frac{l_{j+1}}{6} - \frac{F_j}{l_j} + F_{j+1}\left(\frac{1}{l_j}+\frac{1}{l_{j+1}}\right) - \frac{F_{j+2}}{l_{j+1}} = 0 \tag{23},$$

kjer je $j = 1, 2, ..., K–2$. Dobili smo sistem $K–2$ enačb z $2K$ neznankami, H_k in F_k, kjer je $k = 1, 2, ..., K$. Za enolično rešitev problema potrebujemo še dodatnih $K+2$ enačb.

where $j = 1, 2, ..., K–2$. We obtained the system of $K–2$ equations with $2K$ unknowns, i.e., H_k and F_k, where $k = 1, 2, ..., K$. Hence, in order to solve the problem, we need additional $K+2$ equations.

Določitev F_i

Naslednjih K dodatnih enačb lahko dobimo na dva načina:
a) V primeru, ko je število izbranih vozlišč enako številu podanih diskretnih točk, $K = N$ in $x = t_j$, se bodo vozlišča ujemala s podanimi diskretnimi vrednostmi. V tem primeru je:

Determination of F_i

There are two ways of obtaining the next K additional equations:
a) When the number of connection points is the same as the number of given data points, $K = N$ and $x = t_j$, then the connection points coincide with the given set of discrete values. Hence:

$$\{F_j = y_j; \quad j = 1, 2, \cdots, K\} \tag{24}.$$

V tem primeru gre izračunana krivulja natanko skozi vse diskretne vrednosti, kar pomeni, da dobimo interpolacijsko krivuljo množice točk $\mathcal{F}$, podane z izrazom (1). Ta postopek pomeni poseben primer metode, opisane v nadaljevanju.

In this case the calculated curve goes exactly through all the discrete values, meaning that we obtain an interpolation curve for the set of discrete datum points $\mathcal{F}$, Eq. (1). This case is a special case of the method described below.

b) Drugi, splošnejši postopek imamo, ko je število izbranih vozlišč manjše od števila podanih diskretnih vrednosti, $K < N$. V tem primeru določimo funkcijske vrednosti v vozliščih $\{F_j; j = 1, 2, ..., K\}$z metodo najmanjših kvadratov. Vozlišča $\{t_j; j = 1, 2, ..., K\}$ moramo izbrati tako, da bo vsak od korakov $\{l_j; j = 1, 2, ..., K\}$ vseboval vsaj en x_i.

V nadaljevanju bomo analizirali samo metodo b), ki je splošnejša.

Vsota kvadratov odstopkov med vrednostmi, izračunanimi iz gladilne funkcije, $f_j(x_i)$, in izmerjenimi diskretnimi vrednostmi y_i znotraj j-tega koraka, je:

b) We have a more general case when the number of selected connection points is smaller than the number of given discrete datum points, i.e., $K < N$. In this case the values at the connection points $\{F_j; j = 1, 2, ..., K\}$ are determined with the least-squares method. The set of connection points $\{t_j; j = 1, 2, ..., K\}$ should be selected such that each of the sub-intervals $\{l_j; j = 1, 2, ..., K\}$ includes at least one x_i.

Here we will discuss only case b), as it is more general.

The sum of the squares of the deviations between the values computed from the spline function, $f_j(x_i)$, and the measured discrete values y_i within the j-th sub-interval is:

$$s_j = \sum_{i=v_{j-1}+1}^{v_j} \left[f_j(x_i) - y_i \right]^2 \tag{25}$$

Pri tem je v_j številec zadnje točke v koraku v_j. Seštevanje prek vseh K–1 korakov da skupno napako približka:

Here v_j is the index of the last data point within the sub-interval v_j. Summation over all K–1 sub-intervals yields the sum of the approximation errors:

$$\mathcal{S} = \sum_{j=1}^{K-1} s_j = \sum_{j=1}^{K-1} \sum_{i=v_{j-1}+1}^{v_j} \left[f_j(x_i) - y_i \right]^2 \tag{26}$$

Z minimiziranjem skupne napake dobimo:

Minimizing the sum errors we obtain:

$$\frac{\partial \mathcal{S}}{\partial F_k} = 2 \sum_{j=1}^{K-1} \sum_{i=v_{j-1}+1}^{v_j} \left[f_j(x_i) - y_i \right] \frac{\partial f_j(x_i)}{\partial F_k} = 0 \tag{27}$$

$$\sum_{j=1}^{K-1} \sum_{i=v_{j-1}+1}^{v_j} f_j(x_i) \frac{\partial f_j(x_i)}{\partial F_k} = \sum_{j=1}^{K-1} \sum_{i=v_{j-1}+1}^{v_j} y_i \frac{\partial f_j(x_i)}{\partial F_k} \tag{28}$$

Za vsak F_k, kjer je k = 1, 2, ..., K, dobimo enačbo oblike (28), kar pomeni naslednjih K enačb. Parcialne odvode $\partial f_j(x_i)/\partial F_k$ izračunamo z odvajanjem enačbe (22):

For each F_k, where $k = 1, 2, ..., K$, an equation of the form of Eq. (28) is obtained. This yields the next K equations. The partial derivatives $\partial f_j(x_i)/\partial F_k$ can be obtained from the Eq. (22):

$$\frac{\partial f_j(x_i)}{\partial F_k} = \begin{cases} \dfrac{(t_{j+1} - x)}{l_j}; & \text{za/for} \quad k = j \\ \dfrac{(x - t_j)}{l_j}; & \text{za/for} \quad k = j+1 \\ 0; & \text{za/for} \quad j \neq k \neq j+1 \end{cases} \tag{29}$$

Z upoštevanjem razmerij (29) preide enačba (28) v obliko:

Using the relations (29), Eq. (28) can be rearranged as:

$$\sum_{i=v_{k-2}+1}^{v_{k-1}} f_{k-1}(x_i) \frac{x_i - t_{k-1}}{l_{k-1}} + \sum_{i=v_{k-1}+1}^{v_k} f_k(x_i) \frac{t_{k+1} - x_i}{l_k} = \sum_{i=v_{k-2}+1}^{v_{k-1}} y_i \frac{x_i - t_{k-1}}{l_{k-1}} + \sum_{i=v_{k-1}+1}^{v_k} y_i \frac{t_{k+1} - x_i}{l_k} \tag{30}$$

Če sedaj upoštevamo še enačbo (22), dobimo:

Utilizing Eq. (22) we obtain:

$$\begin{aligned} &\sum_{i=v_{k-2}+1}^{v_{k-1}} \left\{ H_{k-1} \left[\frac{(t_k - x_i)^3}{6 l_{k-1}} - l_{k-1} \frac{t_k - x_i}{6} \right] + H_k \left[\frac{(x_i - t_{k-1})^3}{6 l_{k-1}} - l_{k-1} \frac{x_i - t_{k-1}}{6} \right] + F_{k-1} \left[\frac{t_k - x_i}{l_{k-1}} \right] + F_k \left[\frac{x_i - t_{k-1}}{l_{k-1}} \right] \right\} \left(\frac{x_i - t_{k-1}}{l_{k-1}} \right) + \\ &+ \sum_{i=v_{k-1}+1}^{v_k} \left\{ H_k \left[\frac{(t_{k+1} - x_i)^3}{6 l_k} - l_k \frac{t_{k+1} - x_i}{6} \right] + H_{k+1} \left[\frac{(x_i - t_k)^3}{6 l_k} - l_k \frac{x_i - t_k}{6} \right] + F_k \left[\frac{t_{k+1} - x_i}{l_k} \right] + F_{k+1} \left[\frac{x_i - t_k}{l_k} \right] \right\} \left(\frac{t_{k+1} - x_i}{l_k} \right) = \\ &= \sum_{i=v_{k-2}+1}^{v_{k-1}} y_i \frac{x_i - t_{k-1}}{l_{k-1}} + \sum_{i=v_{k-1}+1}^{v_k} y_i \frac{t_{k+1} - x_i}{l_k} \end{aligned} \tag{31}$$

oziroma

$$\mathcal{A}H_{k-1} + \mathcal{B}H_k + \mathcal{C}H_{k+1} + \mathcal{D}F_{k-1} + \mathcal{E}F_k + \mathcal{G}F_{k+1} = \mathcal{H}_{k+1} \tag{32},$$

kjer so:

$$\mathcal{A}_k = \sum_{i=v_{k-2}+1}^{v_{k-1}} \left[\frac{(t_k - x_i)^3}{6l_{k-1}} - l_{k-1}\frac{t_k - x_i}{6} \right] \left(\frac{x_i - t_{k-1}}{l_{k-1}} \right) \tag{33}$$

$$\mathcal{B}_k = \sum_{i=v_{k-2}+1}^{v_{k-1}} \left[\frac{(x_i - t_{k-1})^3}{6l_{k-1}} - l_{k-1}\frac{x_i - t_{k-1}}{6} \right] \left(\frac{x_i - t_{k-1}}{l_{k-1}} \right) + \sum_{i=v_{k-1}+1}^{v_k} \left[\frac{(t_{k+1} - x_i)^3}{6l_k} - l_k\frac{t_{k+1} - x_i}{6} \right] \left(\frac{t_{k+1} - x_i}{l_k} \right) \tag{34}$$

$$\mathcal{C}_k = \sum_{i=v_{k-1}+1}^{v_k} \left[\frac{(x_i - t_k)^3}{6l_k} - l_k\frac{x_i - t_k}{6} \right] \left(\frac{t_{k+1} - x_i}{l_k} \right) \tag{35}$$

$$\mathcal{D}_k = \sum_{i=v_{k-2}+1}^{v_{k-1}} \frac{(t_k - x_i)(x_i - t_{k-1})}{l_{k-1}^2} \tag{36}$$

$$\mathcal{E}_k = \sum_{i=v_{k-2}+1}^{v_{k-1}} \frac{(x_i - t_{k-1})^2}{l_{k-1}^2} + \sum_{i=v_{k-1}+1}^{v_k} \frac{(t_{k+1} - x_i)^2}{l_k^2} \tag{37}$$

$$\mathcal{G}_k = \sum_{i=v_{k-1}+1}^{v_k} \frac{(x_i - t_k)(t_{k+1} - x_i)}{l_k^2} \tag{38}$$

$$\mathcal{H}_k = \sum_{i=v_{k-2}+1}^{v_{k-1}} y_i \frac{x_i - t_{k-1}}{l_{k-1}} + \sum_{i=v_{k-1}+1}^{v_k} y_i \frac{t_{k+1} - x_i}{l_k} \tag{39}.$$

Enačbi (23) in (31) pomenita skupaj (2*K*–2) enačb, kar pomeni, da manjkata še dve enačbi. Zadnji dve enačbi dobimo iz robnih pogojev.

1.3 Robni pogoji

Manjkajoči enačbi dobimo iz zahteve o ukrivljenosti krivulje na obeh koncih množice $\mathcal{F}$, tj. H_1 in H_K, ki ju zapišemo kot linearni funkciji ukrivljenosti v sosednjih točkah t_2 in t_{K-1}:

Eqs. (23) and (31) together represent (2*K*–2) equations. Two more equations are needed. These are obtained from the boundary conditions.

1.3 Boundary Conditions

The missing two equations can be obtained from the condition that the curvatures on both ends of the set $\mathcal{F}$, i.e., H_1 and H_K, can be expressed as linear functions of the curvatures at the two neighboring points t_2 in t_{K-1}. Hence:

$$H_1 = \lambda_1 H_2 + \lambda_2 \tag{40}$$

$$H_K = \lambda_3 H_{K-1} + \lambda_4 \tag{41}.$$

Z izbiro stalnic λ_1 do λ_4 lahko prilagajamo ukrivljenost krivulje na obeh koncih. V primeru $\{\lambda_i = 0;\ i = 1, ..., 4\}$ bosta, recimo, oba konca krivulje ravna.

Največkrat seveda nimamo informacij o obnašanju podatkov $\mathcal{F}$, ki jih analiziramo, na robovih. V tem primeru se izkaže kot najprimernejše, da H_1 in H_K določimo z minimizacijo integrala kvadratov ukrivljenosti krivulje:

With the selection of the constants λ_1 to λ_4 the curvature of the function at both ends can be adjusted as required. For example, when $\{\lambda_i = 0;\ i = 1, ..., 4\}$ both ends of the curve will be straight.

Usually, we do not have information about the behavior of the analyzed data, $\mathcal{F}$, at both ends. In such a case it is most appropriate to determine H_1 and H_K by minimizing the integral of the squares of the curve's curvatures:

$$\{U\}_{\min} = \left\{ \int_{t_1}^{t_k} \left[f''(x) \right]^2 dx \right\}_{\min} \tag{42}.$$

Z upoštevanjem razmerja (16) dobimo:

Using relation (16) we obtain:

$$U = \sum_{j=1}^{K-1} \int_{t_j}^{t_{j+1}} \left[H_j \frac{t_{j+1} - x}{l_j} + H_{j+1} \frac{x - t_j}{l_j} \right]^2 dx \tag{43}$$

in po integraciji

and after integration

$$U = \frac{1}{3} \sum_{j=1}^{K-1} \left(H_{j+1}^2 + H_j H_{j+1} + H_j^2 \right) l_j \tag{44}.$$

Minimizacijski postopek izvedemo z odvajanjem funkcije U po H_1 in H_K:

The minimization of the function U is obtained through a derivation with respect to H_1 and H_K:

$$\frac{\partial U}{\partial H_1} = \frac{l_1 \left(H_2 + 2H_1 \right)}{3} = 0 \tag{45}$$

$$\frac{\partial U}{\partial H_K} = \frac{l_{K-1} \left(2H_K + H_{K-1} \right)}{3} = 0 \tag{46}.$$

Iz (45) in (46) izhaja:

From (45) and (46) it follows that:

$$H_1 = -\frac{H_2}{2} \tag{47}$$

$$H_K = -\frac{H_{K-1}}{2} \tag{48}.$$

V primeru, ko izberemo na abscisi (osi x) en sam korak, bo $K = 2$ in $H_1 = H_2 = 0$, kar pomeni, da bo v tem primeru izveden približek podatkov s premico. K temu problemu se bomo ponovno vrnili v razpravi.

When on the abscissa (x-axis) we select only one interval, then $K = 2$ and $H_1 = H_2 = 0$, which means that the data will be approximated by a straight line. We will address this problem again later in the discussion.

Izraza (47) in (48) sta manjkajoči dve enačbi. Skupaj z enačbami, ki ju definirata izraza (23) in (31), imamo sedaj sistem $2K$ linearnih enačb z $2K$ neznankami:

Expressions (47) and (48) represent the missing two equations. Together with the expressions (23) and (31) we have now a system of $2K$ linear equations with $2K$ unknowns:

$$H_k \frac{l_k}{6} + H_{k+1} \left[\frac{l_k + l_{k+1}}{3} \right] + H_{k+2} \frac{l_{k+1}}{6} - \frac{F_k}{l_k} + F_{k+1} \left(\frac{1}{l_k} + \frac{1}{l_{k+1}} \right) - \frac{F_{k+2}}{l_{k+1}} = 0 \ , \ k = 1, 2, \cdots, K-2 \tag{49}$$

$$\mathcal{A}_k H_{k-1} + \mathcal{B}_k H_k + \mathcal{C}_k H_{k+1} + \mathcal{D}_k F_{k-1} + \mathcal{E}_k F_k + \mathcal{G}_k F_{k+1} = \mathcal{H}_{k+1}, \quad k = 1, 2, \cdots, K \tag{50}$$

$$H_1 + \frac{H_2}{2} = 0 \tag{51}$$

$$H_K + \frac{H_{K-1}}{2} = 0 \tag{52}.$$

Stalnice $\mathcal{A}_k$, $\mathcal{B}_k$, $\mathcal{C}_k$, $\mathcal{D}_k$, $\mathcal{E}_k$, $\mathcal{G}_k$ in $\mathcal{H}_k$ so podane z enačbami (33) do (39). Dobljeni sistem enačb (49) do (52) rešimo numerično z eno izmed znanih metod za reševanje sistemov linearnih enačb.

The constants $\mathcal{A}_k$, $\mathcal{B}_k$, $\mathcal{C}_k$, $\mathcal{D}_k$, $\mathcal{E}_k$, $\mathcal{G}_k$ and $\mathcal{H}_k$ are given by Eqs. (33) to (39). The obtained system of Equations (49) to (52) can be solved numerically using one of the existing methods for solving systems of linear equations.

Rešitev sistema linearnih enačb so funkcijske vrednosti interpolacijske krivulje v vozliščih $\{F_j, t_j; j = 1, 2, ..., K\}$, ter vrednosti pripadajočih drugih odvodov $\{H_j, t_j; j = 1, 2, ..., K\}$. Poljubno število diskretnih vrednosti interpolacijske krivulje lahko sedaj izračunamo z enačbo (23). V primeru, da nas zanimajo tudi vrednosti prvega in drugega odvoda, lahko te izračunamo z enačbama (21) in (16).

The solutions of the system of linear equation are the values of the interpolation curve at the connection points $\{F_j, t_j; j = 1, 2, ..., K\}$, and the corresponding second derivatives $\{H_j, t_j; j = 1, 2, ..., K\}$. Any number of discrete data along the interpolation curve can be calculated using Eq. (23). To determine the corresponding values of the first and second derivative, Eqs. (21) and (16) can be used.

2 RAZPRAVA

Uporabnost izpeljanega algoritma za glajenje diskretno podanih krivulj bomo prikazali na treh primerih. V prvih dveh primerih smo diskretne vrednosti ustvarjali iz analitično podanih krivulj. Uporabili smo preprosto trigonometrično funkcijo $y = 50 + 40\sin x$ in ustvarili dve množici „eksperimentalnih" podatkov. Prva množica:

$$\{\mathbf{A}\} = \{0 \le x_i \le 10,\ y_i = 50 + 40\sin x;\ i = 1, 2, \cdots, 41\} \tag{53}$$

je znotraj natančnosti računalnika brez napake. Druga množica:

$$\{\mathbf{B}\} = \{0 \le x_i \le 10,\ y_i = 50 + 40\sin x - 4.5 + 9 \cdot RND;\ i = 1, 2, \cdots, 41\} \tag{54}$$

pa vsebuje z dodatnimi členi (–4,5+9*RND*), kjer je *RND* ime vira naključnih števil od 0 do 1, numerično ustvarjeno 10% naključno napako. Množici sta v obliki polne črte in kvadratkov prikazani na sliki 2. Ta primera bosta namenjena za prikaz vpliva izbranega števila korakov na natančnost glajenja diskretnih podatkov.

V tretjem primeru bomo uporabili "prave" eksperimentalne podatke za realno $J'(\omega)$ in imaginarno $J''(\omega)$ komponento dinamične funkcije lezenja, ki smo jih poprej uporabili v okviru študija obrnjenega problema pri karakterizaciji materialnih funkcij viskoelastičnih materialov ([4] do [7]). Ta analiza je zahtevala predhodno „glajenje"' izmerjenih materialnih funkcij, kar je vodilo do nastanka tega prispevka. Eksperimentalni podatki obeh materialnih funkcij so prikazani na sliki 3.

2.1 Minimalno število korakov

Za določitev minimalnega števila korakov, oziroma minimalnega števila vozlišč, smo uporabili podatke {**A**}, ki so brez napake. Diskretne vrednosti na gladilnih krivuljah, izračunanih za različno število korakov, smo primerjali z analitičnimi vrednostmi. Kakovost približka je bila ocenjena s povprečno relativno napako $\mathcal{N}$:

$$\mathcal{N} = \frac{1}{N}\sum_{i=1}^{N}\frac{\sqrt{\left(y_{i,apr} - y_{i,teor}\right)^2}}{y_{i,teor}} \tag{55}.$$

Z N smo označili število diskretnih podatkov, uporabljenih v izračunu približne krivulje, z $y_{i,apr}$ diskretne vrednosti na približni krivulji in z $y_{i,teor}$ pripadajoče funkcijske vrednosti brez napake.

2 DISCUSSION

The power of the proposed algorithm will be demonstrated on three different sets of discrete data. In the first two cases we will use the synthetic discrete data generated from the analytical function $y = 50 + 40\sin x$. The first set of "experimental" data:

is within the accuracy of the computer without an error, while the second set:

with the additional terms (–4.5+9*RND*), where *RND* represents a random generator of numbers between 0 and 1, incorporates a generated random 10% error. The two sets of data are shown in Fig. 2 as a solid line and diamonds, respectively. These two sets of data will be used to analyze the influence of the selected number of sub-intervals on the precision of smoothing discrete data.

In the third example we will use "true" experimental data on the real $J'(\omega)$ and the imaginary $J''(\omega)$ component of the creep-compliance function of poly-isobutylene. These data were used previously for studying inverse problems in the characterization of viscoelastic materials ([4] to [7]). In this analysis we had to smooth the data, which resulted in the paper presented here. Experimental data for both material functions are shown in Fig. 3.

2.1. Minimum number of sub-intervals

To determine the minimum required number of sub-intervals we used the first set of discrete data, {**A**}, which are within the resolving power of a computer without an error. Discrete values of the smoothing curve calculated for a different number of sub-intervals were compared with the corresponding analytical values. The accuracy of the approximation was evaluated with the average relative error, $\mathcal{N}$:

Here N denotes the number of discrete data used in the calculation of the approximation curve, $y_{i,apr}$ denotes the discrete values on the approximation curve, and $y_{i,teor}$ denotes the corresponding function-values without an error.

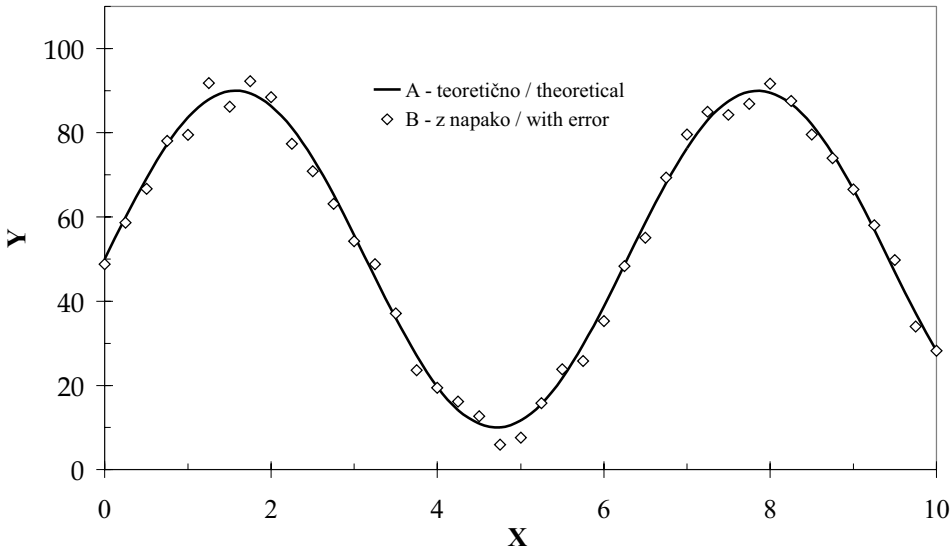

Sl. 2. *Ustvarjeni "eksperimentalni" podatki brez {**A**} in z naključno 10% napako {**B**}*
Fig. 2. *Generated "experimental" data without, {**A**}, and with a random 10% error, {**B**}*

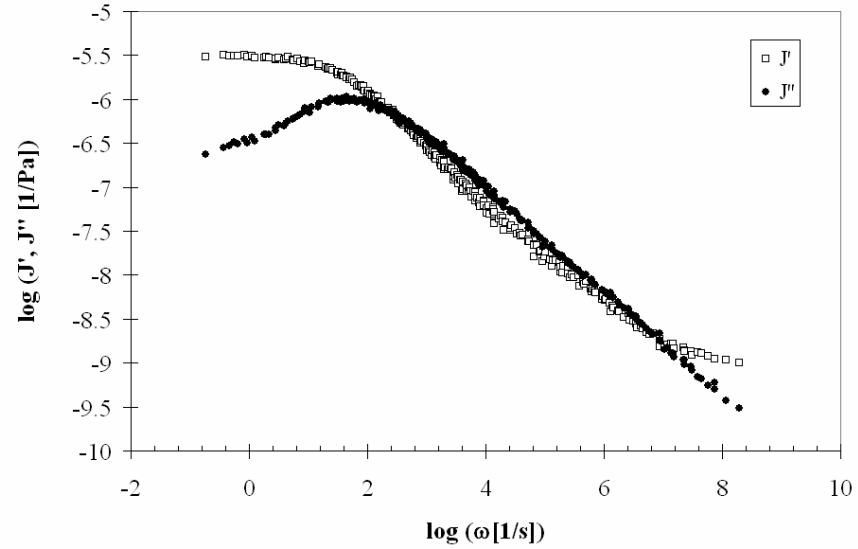

Sl. 3. *Izmerjene diskretne vrednosti skupnih krivulj za realno, J'(ω), in imaginarno, J''(ω) komponento funkcije lezenja poli-izobutilena*
Fig. 3. *Measured discrete values of master curves for real, J'(ω), and imaginary, J''(ω), component of the creep compliance of poly-isobutylene*

Rezultat te analize je prikazan kot krivulja A v diagramu na sliki 4. Krivulja B je za podatke {**B**}, ki jih bomo analizirali pozneje. Zaradi boljše preglednosti je v notranjosti diagrama prikazan povečani del območja med 0 in 10% napake.

Primeri gladilnih krivulj izračunanih za različno število korakov, so prikazani na sliki 5. Zaradi preglednosti je prikazanih samo pet približnih krivulj, izračunanih za 1, 2, 3, 5 in 15 korakov.

The result of this analysis is shown as curve A in Fig. 4. Curve B shows the results for the set of data {**B**}, which will be discussed later. For reasons of clarity the enlarged segment of the curve between 0 and 10% of error is shown as an enclosure.

Examples of smoothing curves calculated for a different number of sub-intervals are shown in Fig. 5. For reasons of clarity we show only five approximation curves calculated for 1, 2, 3, 5 and 15 sub-intervals.

V primeru, ko izberemo en sam korak, bo približna krivulja premica. Ta lastnost krivulj zlepkov izhaja iz enačb (47) in (48). Ukrivljenosti na obeh koncih koraka sta namreč enaki nič, $H_1 = H_2 = 0$, kar pomeni, da je približna krivulja premica.

Če izberemo dva koraka, bosta ukrivljenosti gladilne krivulje na obeh koncih za polovico manjši od ukrivljenosti na stičišču obeh korakov, v skladu z enačbama (51) in (52). Gladilna krivulja bo v tem primeru parabolične oblike.

Sprejemljivo približno (gladilno) krivuljo dobimo šele pri petih korakih oziroma šestih vozliščih. Napaka približka je v tem primeru okrog 3,5%. S povečevanjem števila vozlišč se napaka približka hitro zmanjšuje, kakor to nazorno prikazuje krivulja A na sliki 4. Če izberemo 15 korakov, je relativna napaka že manjša od 0,2%. Z nadaljnjim povečevanjem števila vozlišč pridemo v mejni primer, ko je število vozlišč enako številu diskretnih podatkov. V tem primeru dobimo interpolacijsko krivuljo, ki povezuje vse točke. Ker so diskretni podatki {**A**} brez eksperimentalne napake, bo gladilna krivulja v bistvu enaka pripadajoči teoretični.

In the case when we choose only one sub-interval the approximation curve will be a straight line. This property of the spline curves results from the conditions (47) and (48). The curvatures at both ends of the sub-interval are equal to zero, i.e., $H_1 = H_2 = 0$, which means that the approximation curve is a straight line.

If we select two sub-intervals, the curvatures of the smoothing curve at both ends are half of the curvature in the connecting point of the two sub-intervals, in accordance with Equations (51) and (52). In this case, the shape of the smoothing curve will be parabolic.

An acceptable approximation (smoothing) curve is obtained only after five sub-intervals, i.e., six connecting points. In this case the error of the approximation is about 4.5%. The error of the approximation will decrease with the increased number of sub-interval, as shown with the curve A in Fig. 4. If we choose 15 sub-intervals the relative error will be less than 0.2%. With a further increase in the number of sub-intervals we approach the limiting case when the number of connecting points is equal to the number of datum points. In such a case we obtain an interpolation curve, which connects all the datum points. Since the discrete data {**A**} are without experimental error, the smoothing curve will be essentially identical to the underlying theoretical curve.

2.2 Optimalno število korakov

Množica izmerjenih podatkov, ki jih želimo v praksi približati, vsebuje zmeraj določeno napako. V

2.2 Optimum number of sub-intervals

Measured data, which we want to approximate, always contain some experimental error. In such cases

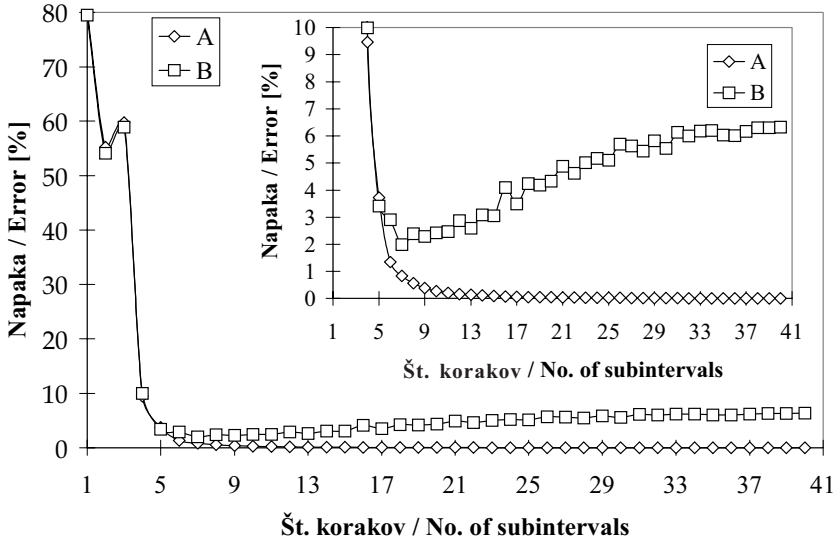

Sl. 4. *Napaka približka v odvisnosti od števila korakov, A – za približek krivulje brez naključne napake, B – približek krivulje z ±10% naključno napako*

Fig. 4. *Error of the approximation as a function of the number of sub-intervals, A – for the approximation of the theoretical curve, B – for the approximation of the curve with the added ±10% random error*

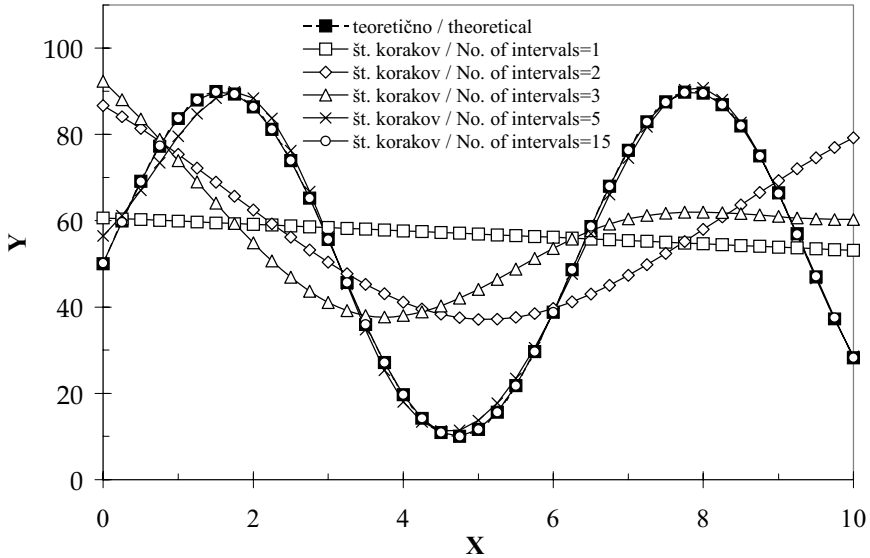

Sl. 5. *Približne krivulje z različnim številom korakov*
Fig. 5. *Approximation curves with a different number of sub-intervals*

teh primerih uporabimo gladilne funkcije za določitev gladkih približnih krivulj. Število korakov mora biti torej manjše od števila diskretnih podatkov. Sedaj stojimo pred pomembnim vprašanjem: Kolikšno je optimalno število korakov?

Da bi dobili odgovor na to vprašanje, smo uporabili množico podatkov {**B**}, enačba (54), ki vsebujejo naključno 10-odstotno napako. Diskretne vrednosti so v obliki kvadratkov prikazane na sliki 2. Podobno kakor v prejšnjem primeru, smo tudi tokrat napako glajenja ocenjevali v skladu z enačbo (55), tj. vrednosti dobljene z glajenjem smo primerjali s teoretičnimi funkcijskimi vrednostni, ki ne vsebujejo napake. Rezultat te analize je prikazan na sliki 4 kot krivulja B. Iz diagrama je razvidno, da je napaka približka v primeru, ko je število korakov enako ali manjše od 5, praktično enaka kakor v primeru, če podatki ne vsebujejo „eksperimentalne“ napake. S povečevanjem števila korakov se bo napaka najprej zmanjšala, nato pa se bo ponovno začela zvečevati. V trenutku, ko je število vozlišč enako številu diskretnih podatkov (krivulja gre v tem primeru natančno skozi vse diskretne vrednosti), bo napaka približka enaka povprečni eksperimentalni napaki, ki jo vsebuje množica diskretnih vrednosti {**B**}, v tem primeru približno 6 odstotkov.

S slike 4 je razvidno, da bomo dobili najboljši rezultat glajenja podatkov {**B**}, če izberemo 7 korakov. Na sliki 6 je ta primer približka prikazan v obliki trikotnikov, povezanih s polno črto. V istem diagramu je s polno črto prikazan tudi približek s 40

we use spline functions to obtain smooth continuous curves. Therefore, the number of selected sub-intervals should be smaller than the number of datum points. This raises an important question: What is the optimum number of sub-intervals?

To answer this question we have used the set of data {**B**}, Eq. (54), with a 10% random error. The data are shown as diamonds in Fig. 2. As in the previous case the quality of the smoothing was evaluated according to Eq. (55), i.e., discrete values predicted with the spline function were compared to the underlying theoretical values. The result of this analysis is presented in Fig. 4 as curve B. From the diagram it is clear that the error of splining the data with a 10% random error is about the same as for the data with no “experimental” error, if the selected number of sub-intervals is equal to or less than five. If we increase the number of sub-intervals the error of smoothing will first decrease and then start to increase again. We reach the limiting case when the number of connecting points is the same as the number of datum points. In this case the smoothing curve goes through all the datum pints, and the error of the approximation becomes equal to the average relative error of the set of data, {**B**}, which in this case is approximately 6%.

As seen from Fig. 4 we will get the best smoothing of the set of data {**B**} if we choose six sub-intervals. The result of this smoothing is shown in Fig. 6 as a line with triangles. In the same figure the approximation with 40 sub-intervals, i.e., 41 connecting points, is also shown as a solid line. In this case the

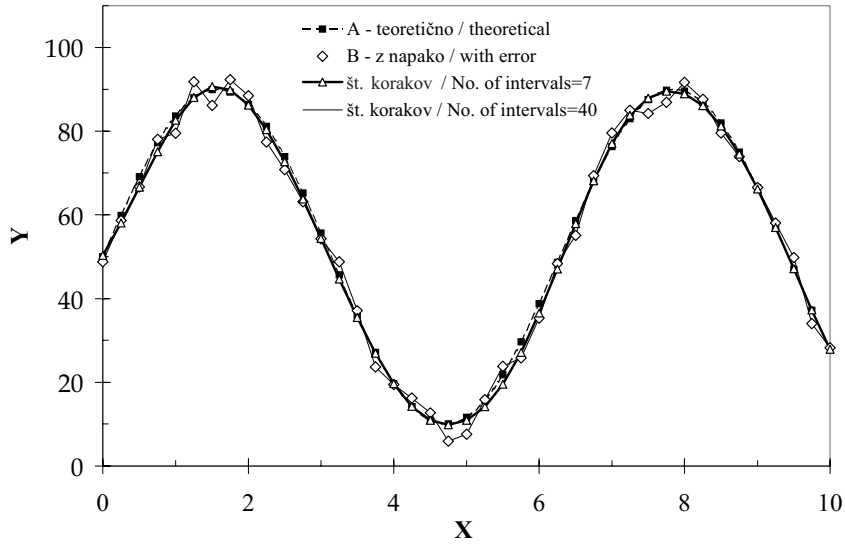

Sl. 6. *Približek funkcije, podane z 10-odstotno napako*
Fig. 6. *Approximation of function given with a 10% error*

koraki oziroma 41 vozlišči. V tem primeru gladilna krivulja povezuje diskretne vrednosti, kar pomeni, da v resnici glajenja ni.

Znotraj posameznega koraka je povprečna relativna napake približka odvisna od števila diskretnih vrednosti v tem koraku. Diagram na sliki 7 prikazuje takšno analizo za primer glajenja podatkov {**B**} z 10 koraki. Velikost napake glajenja se zmanjšuje s povečanim številom podatkov znotraj koraka in se stabilizira pri približno 30 podatkih na korak, kar se ujema s tistim, kar vemo iz statistike. Nadaljnje povečevanje števila točk na korak bistveno ne bo prispevalo h kakovosti glajenja.

2.3 Glajenje viskoelastičnih materialnih odvisnosti

Kot zadnji primer si oglejmo sedaj še uporabo predstavljenega algoritma na eksperimentalnih podatkih za realno, $J'(\omega)$, in imaginarno, $J''(\omega)$, komponento funkcije lezenja za nezamrežen poliizobutilen. Te eksperimentalne podatke smo pred tem analizirali v okviru študija obrnjenega problema pri analizi viskoelastičnih materialnih funkcij [6]. Podatki so bili povzeti iz [8], kjer so v preglednični obliki podani odseki krivulj za različne temperaturne razmere. Na podlagi časovno-temperaturnega superpozicijskega načela smo konstruirali skupni krivulji za temperaturo $T = 20$ °C, po postopku, ki je opisan v [6]. Skupni krivulji sta predstavljeni v obliki polnih krogcev in kvadratkov na sliki 3.

Krivulji, ki ju dobimo z interpolacijo z uporabo gladilne funkcije, sta predstavljeni v obliki polne črte

smoothing curve connects the discrete values, which essentially means that there is no smoothing.

The average relative error of smoothing depends on the number of datum points within each sub-interval. Figure 7 shows such an analysis for the case of smoothing the set of data {**B**} with 10 sub-intervals. The error of smoothing decreases with the number of datum points per sub-interval, and it stabilizes at about 30 datum points per sub-interval, which is in agreement with what we know from the statistics. Further increasing the number of datum points per sub-interval will not lead to substantially improved smoothing.

2.3 Smoothing of the viscoelastic material functions

The final demonstration of the power of the presented algorithm will be executed on the experimental data on the real, $J'(\omega)$, and the imaginary, $J''(\omega)$, components of the creep-compliance function of an uncrosslinked poly-isobutylene. We have used these data before [6] for studying the inverse problem of viscoelastic materials functions. The experimental data were taken from [8], where they are given in a tabular form as segments of the creep curve measured at different temperatures. Using the time-temperature superposition principle we have constructed the master curves for the reference temperature T = 20°C, as described in [6], which are shown as filled circles and squares in Fig. 3.

The two curves obtained after the smoothing with spline functions are shown in Fig. 8 as solid lines.

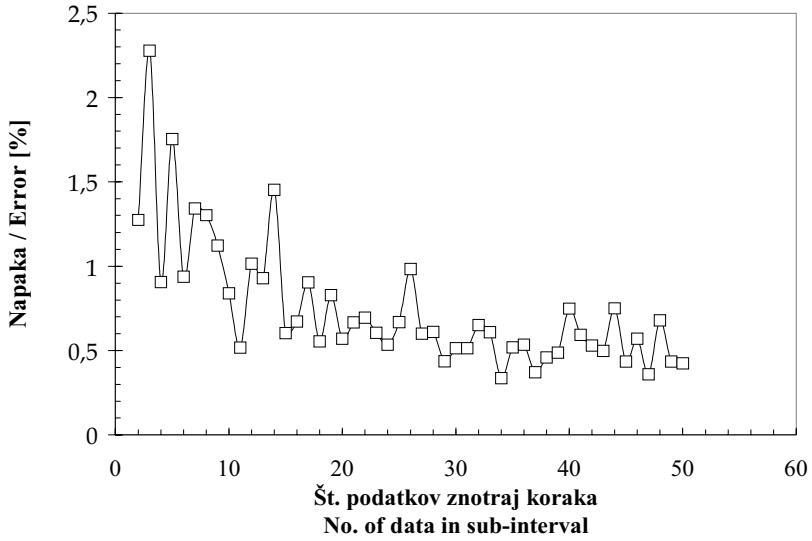

Sl. 7. *Napaka približka v odvisnosti od števila podatkov znotraj koraka*
Fig. 7. *Error of the approximation as a function of the number of datum points per sub-interval*

na sliki 8. Glajenje je bilo izvedeno z 10 koraki. Z gladilno funkcijo lahko preberemo poljubno število diskretnih vrednosti, kar je pomembno za nadaljnjo numerično analizo izmerjenih podatkov, posebno v primeru reševanja obrnjenih problemov. V tem primeru smo izračunali 10 diskretnih vrednosti na dekado vzdolž logaritemske frekvenčne koordinate.

The smoothing procedure was executed with 10 sub-intervals. Using spline functions one can calculate as many discrete datum points as necessary, which is very important for any further numerical analysis of the experimental data, in particular for solving the inverse problems. In this case we have calculated 10 values per-decade along the logarithmic frequency axis.

3 SKLEP

Na temelju izvedene analize lahko ugotovimo, da ni enoličnega odgovora na vprašanje: "Katero

3 CONCLUSION

From the presented analysis we can conclude that there is no unique answer to the question: "What

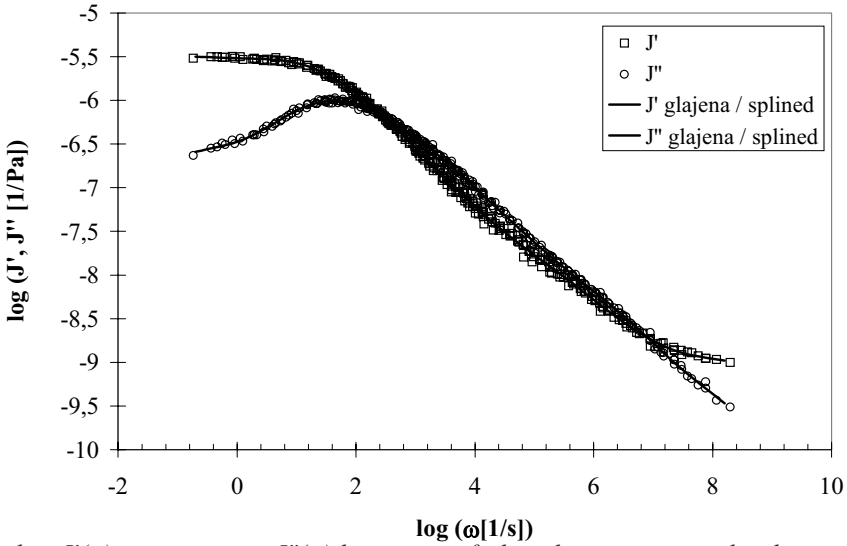

Sl. 8. *Realna, J'(ω) in imaginarna, J''(ω) komponenta funkcije lezenja po postopku glajenja z gladilno funkcijo*
Fig. 8. *The real, J'(ω), and the imaginary, J''(ω), component of the creep compliance function after smoothing with the spline functions*

število korakov moramo izbrati za optimalno glajenje diskretnih podatkov?" Izbira števila korakov je in zmeraj bo "stvar osebne odločitve uporabnika". To si velja še posebej zapomniti v primerih, ko uporabljamo tržne programe, pri katerih nimamo vpogleda v algoritem uporabljen za glajenja diskretnih podatkov. V določenih primerih lahko tak postopek glajenja vodi tudi do neustrezne razlage meritev [9].

number of subintervals should be selected for optimum smoothing of discrete data?" Selection of the number of sub-intervals is, and will always be, a "personal decision by the user". This should be remembered when we are using commercial software packages where we have no information on the algorithm used for the process of smoothing discrete data. In some cases, such an approach may lead to an inappropriate interpretation of measurements [9].

4 LITERATURA
4 REFERENCES

[1] de Boor C. (1978) A practical guide to splines, *Springer Verlag*.

[2] Press, W.H., Flannery, B.P., Teukolsky, S.A., Vetterling, W.T. (1986) Numerical recepies, *Cambridge University Press*, pp. 86-89.

[3] J.H. Ahlberg, E.N. Nielsen, J.T. Walsh (1967) The theory of splines and their application, *Academic Press*.

[4] Emri I., Tschoegl, N.W. (1993) Generating line spectra from experimental responses. 1. Relaxation modulus and creep compliance, *Rheol. Acta*, 32, 311 –321, 1993.

[5] Tschoegl, N.W., Emri I. (1993) Generating line spectra from experimental responses. 2. Storage and loss functions, *Rheol. Acta*, 32, 322 – 327, 1993.

[6] Emri I., Tschoegl, N.W. (1994) Generating line spectra from experimental responses. 4. Application to experimental – data, *Rheol. Acta*, 33, 60 – 70, 1994.

[7] Emri I., Tschoegl, N.W. (1997) Generating line spectra from experimental responses. 5. Time – dependent viscosity', *Rheol. Acta*, 36, 303 – 306, 1997.

[8] Ferry J.D., Grandine L.D., Fitzgerald R.E (1953) Dynamic mechanical properties of Polyisobutylene, *J. Applied Phys*, 24, 650-655, 1953.

[9] Emri I., Pindera J.T. (1993) On the use of spline functions in evaluation of experimental data, *1993 SEM Spring Conf. on Experimental Mechanics*, Dearborn, Michigan, USA, Jun. 7 – 9, 1993, 1196 – 1205.

Naslov avtorjev: prof.dr. Igor Emri
mag. Robert Cvelbar
Univerza v Ljubljani
Fakulteta za strojništvo
Aškerčeva 6
1000 Ljubljana
ie@fs.uni-lj.si
robert.cvelbar@fs.uni-lj.si

Authors' address: Prof.Dr. Igor Emri
Mag. Robert Cvelbar
University of Ljubljana
Faculty of Mechanical Eng.
Aškerčeva 6
1000 Ljubljana, Slovenia
ie@fs.uni-lj.si
robert.cvelbar@fs.uni-lj.si

Prejeto: 14.6.2005
Received:

Sprejeto: 16.11.2005
Accepted:

Odprto za diskusijo: 1 leto
Open for discussion: 1 year

Strojniški vestnik - Journal of Mechanical Engineering 52(2006)3, 195-203
UDK - UDC 711.1(4):65.011.8
Strokovni članek - Speciality paper (1.04)

Regionalni vidiki inoviranja kot osnova konkurenčnosti podjetja znotraj države in EU

Regional Aspects of Innovation as a Cornerstone of the Competitiveness of a Company within the State and the EU

Mirko Markič - Borut Likar
(Fakulteta za management, Koper)

Lizbonska strategija, ki jo je Evropski svet sprejel leta 2000, predstavlja dolgoročno strategijo s ciljem, da postane Evropa do leta 2010 najbolj konkurenčno, dinamično ter na znanju temelječe gospodarstvo na svetu. Ker je EU stičišče držav z različnimi stopnjami gospodarske in raziskovalne razvitosti, jeziki, socialnimi razmerami, zgodovino, kulturo itn., je poleg celovitega načina vodenja zveze treba nujno ohraniti in razvijati močno regionalno komponento. To velja tako za države kakor tudi za regije. Hkrati je EU v svojih strateških dokumentih postavila spodbujanje inovativnosti med prednosti. Zato želimo s prispevkom prikazati možnosti za Slovenijo na tem izredno pomembnem delu – regionalne usmeritve inovativnih procesov.

Na podlagi analize inovativnih procesov v Sloveniji in v EU smo izdelali model inovativnih procesov v treh korakih. V prvem definiramo, kaj mora regija doseči, če želi postati inovativna. Osnovno vodilo za razvoj je posodobitev razmišljanja in usklajenost delovanja vseh udeležencev glede inoviranja, ki je podlaga za izboljšanje konkurenčnosti ter hkrati boljšo kakovost življenja njenih prebivalcev in družbe kot celote. V drugem koraku določimo, kako naj v regionalnih razmerah ravnamo, upoštevajoč dialektični sistem pogojev za dosego inovacije v podjetju ali drugi organizaciji in lastnosti regije v širšem merilu. V tretjem koraku regijo in njene dejavnosti povežemo na eni strani s podjetjem in drugo organizacijo, na drugi strani pa z državnimi in evropskimi razvojnimi smernicami ter vzpostavimo povezavo z inovacijskim podpornim okoljem.

(Ključne besede: konkurenčnost podjetij, procesi inovacijski, modeli, okolje podporno, strategije regijske)

In 2000 the European Council approved the Lisbon strategy, which represents a long-term strategy with the aim to make the EU the most competitive, dynamic knowledge-driven economy in the world by 2010. Since Europe is a group of countries with different degrees of economic and research development, languages, social conditions, history, culture, etc., it is thus essential to preserve and develop a strong regional component together with a comprehensive approach to managing the EU. This is true not only for the states but also for the regions. At the same time, in its documents the EU set fostering innovativeness among its priorities. In this paper we thus wish to describe the opportunities for Slovenia in this extremely important segment – regional orientation of the innovative processes.

On the basis of an analysis of the innovative processes in Slovenia and the EU we created a model of innovation processes in three steps. In the first one we define what the region has to achieve in order to become innovative. Fundamental guidance for the development is the modernization of deliberation and the performance reconciliation of all participants regarding innovation, which is the foundation for an improvement of competitiveness as well as a better quality of life of its inhabitants and society as a whole. In the second step we define how we should act within specific regional circumstances, taking into consideration a dialectic system of conditions for achieving innovation within the company or other organisations and the characteristics of the region in broader criteria. In the third step we connect on one side the region and its activities with a company and other organisations, and on the other side with Republic and European development guidelines and establish a connection with an innovation support environment.

(Keywords: company competitiveness, innovative processes, models, supporting environment, regional strategy)

0 UVOD

Analiza in model obravnavata predvsem regije v Sloveniji ob upoštevanju slovenskega podpornega okolja. Čeprav smo pri analizi izhajali iz poznavanja problemov v določenih regijah, pa se pri izdelavi modela nismo omejevali na katerokoli od njih. Razlike med njimi seveda obstajajo, vendar je model zasnovan tako, da ponuja enakovredna izhodišča za prehod v inovativno regijo vsaki od njih.

V zadnjih desetletjih raziskovalci ([1] do [12]), podjetniki in zaposleni vedno izraziteje spoznavajo, da je dolgoročno preživetje vsakega podjetja ali druge organizacije odvisno od njegove celovite zmožnosti, da zadovolji povpraševanje kupca oziroma odjemalca bolje kakor drugi.

Inoviranje je ustvarjanje in koristno uvajanje novih zamisli ([4] in [12]). Nove zamisli se nanašajo na inoviranje tehnologij (nove tehnične izume, stroje ali izdelke), inoviranje proizvodnih procesov (nove storitve, programi ali načini proizvajanja), ali izvedbeno inoviranje ([14], [30], [32] in [34]).

Če hoče biti organizacija uspešen usmerjevalec sprememb, mora razviti politiko načrtne inovativnosti. Glavno izhodišče za snovanje te politike so "agenti sprememb" (tako jih je poimenoval [12]), ki naj bi bili vseskozi inovativni. Še pomembnejši razlog je ta, da politika načrtne inovativnosti ustvarja miselnost ustvarjalca koristnih sprememb. Načrtna inovativnost spodbuja celotno organizacijo, da v spremembah išče priložnosti [15]. Podjetništvo zahteva menedžment, drugačen od sedanjega [16].

Zamisli (še niso inovativne, so le faza na poti k njim) za reorganiziranje, znižanje stroškov, vzpostavitev novega modela financiranja, izboljšanje komuniciranja ali skupinsko sestavljanje izdelkov ali storitev so inovacije, če in ko dajo koristne rezultate. Inoviranje je nastajanje, sprejem in uvajanje novih zamisli, procesov, izdelkov ali storitev.

0.1 Stanje na področju inoviranja v Sloveniji

Povprečna stopnja razvojne zahtevnosti izdelkov je 5,24, tehnološka zahtevnost proizvodnih procesov pa 4,9 (lestvici od 1 do 15) [17]. V vrhunski tehniki je samo 1,5 odstotka vseh zaposlenih in v višjevredni tehniki 9,1 odstotkov, medtem ko je 89,4 odstotkov zaposlenih v podjetjih z razvojno nezahtevno tehniko [17]. Podjetja investirajo / vlagajo v RiR samo 1,4 odstotka prihodka, medtem ko investira nemška industrija 4 odstotke, pri čemer pa je njihov vložek v RiR 6745 EUR (po izvirnih podatkih 13.220 DEM) na nemškega zaposlenega proti slovenskemu vložku 759 EUR (po izvirnih podatkih 1.487 DEM) 8,9-krat večji [18].

Z vidika inovacijske zmožnosti in tehnološke ravni slovenskega gospodarstva ugotavljajo [18] naslednje zaostanke in primanjkljaje na ravni države in podjetij:

- primanjkljaj uporabnih tehnološko usmerjenih raziskav,
- poudarjanje tehnične razsežnosti inovacijskega procesa in prenosa tehnologije ter zanemarjanje upravljalskega, organizacijskega in marketinškega vidika inoviranja,
- zapostavljanje regionalne razsežnosti v razvijanju državnega inovacijskega sistema,
- slabo izkoriščanje mreže institucij za prodiranje inovacij in prenos tehnologije,
- nepreglednost dosedanjega modela in nepovezanost posameznih mehanizmov za spodbujanje inovacijske dejavnosti,
- nejasno opredeljena prednosti vlade na področju raziskav in razvoja

Nova tehnološka in inovacijska politika v obdobju 2001 do 2006 pa naj bi ob upoštevanju smernic EU za pospešen razvoj inovativnosti, ki bo z ukrepi na ravni EU podpirala državno delovanje, poleg že omenjenih nalog, upoštevala v zasnovi tehnološke politike še naslednje:

- Vzpostavitev inoviranju naklonjene inovacijske kulture. Številne organizacije ne zmorejo slediti tehničnemu napredku zaradi neustrezne organiziranosti sestav in procesov, slabega menedžmenta in nerazvitih metodologij za uporabo novega znanja.
- Obstaja nevarnost, da bodo ukrepi za vzpostavitev kulture inoviranja usmerjeni le k podpiranju tehničnega napredka in s tem preveč enostranski.
- Razširjanja uporabe nove tehnologije; zajeli naj bi čim širši krog podjetij, od tehnološko naprednejših do podjetij v običajnih, delovno zahtevnih panogah, tudi podjetja v različnih stopnjah življenjskega kroga.
- Promoviranje mrežnega povezovanja in vzpostavljanja industrijskih grozdov.
- Posebno pozornost naj bi namenili vzpostavljanju in razvoju industrijskih grozdov s posebnimi spodbudami za izmenjavo znanja, informacij in baz podatkov.
- Posebne spodbude za RiR [17].

0.2 Stanje na področju inoviranja v razvitem tržnem gospodarstvu

V veliki meri je sprejeto izhodišče, da so srednje velika in majhna podjetja tista, ki imajo največjo zmožnost inoviranja. Od leta 1994 obstaja skoraj 100 evropskih regij, ki načrtno izvajajo ali so začele razvijati regionalne strategije, ki se nanašajo na spodbujanje inoviranja.

Politika inoviranja v zahodno evropskih regijah naj bi se posebej ukvarjala s temi ključnimi značilnostmi:

- Uspešnost inoviranja v Evropski zvezi je zelo različna. Razlikuje se po posameznih državah, regijah, podjetjih in dejavnostih.
- Ustaljeni načini delovanja in podpora Evropske zveze na področju inoviranja za zdaj še niso zadovoljivi. Podobno je tudi v podjetjih in drugih organizacijah, v katerih neradi tvegajo.
- Inovatorje doživljajo kot motnjo ustaljenega načina ravnanja.
- Izrablja naj Evropske razsežnosti s pomočjo medregijskega sodelovanja [19].

Določene smeri delovanja so ([12] in [34]):
1. Razvoj spremljanja tehnologije in njenega napovedovanja. 2. Večja usmerjenost raziskovanj v inoviranja. 3. Povezava vseživljenjskega izobraževanja z inoviranjem na vseh stopnjah. 4. Gibljivost študentov in raziskovalcev. 5. Predstavljanje prednosti inoviranja. 6. Izboljšanje financiranja inoviranja. 7. Vzpostavitev proračunskega obvladovanja koristi od inoviranja. 8. Promoviranje intelektualne in industrijske lastnine. 9. Poenostavljane administrativnih postopkov. 10. Inoviranju naklonjen zakonodajni in uredbeni okvir. 11. Razvoj »gospodarskega razumevanja« inoviranja. 12. Spodbujanje inoviranja v podjetjih, posebej v majhnih, in krepitev regionalne razsežnosti inoviranja. 13. Posodabljanje javne predstavitve inoviranja.

1 PODPORNO OKOLJE V SLOVENIJI

Z namenom, da bi vsaj del omenjenih 'zaostankov' odpravili in upoštevali začrtane smernice inovacijske politike ter povečali možnost za vzpostavitev učinkovitih inovacijskih procesov, je v Sloveniji v zadnjem desetletju zrasla vrsta podpornih centrov in programov (ministrstva, uradi, razvojni centri, regionalne agencije, informacijski centri, skladi tveganega kapitala, tehnološki parki, zametki univerzitetnih inkubatorjev itn.), ki ponujajo različne oblike pomoči. Dejstvo je, da slovensko podporno okolje zaradi marsikdaj ne najbolj usklajenega in učinkovitega ter v mlade usmerjenega delovanja inovacijskim projektom še vedno ne daje zadostne podpore ([20] in [21]). Delni vzrok, da so omenjene dejavnosti dale šele delne želene rezultate, je treba iskati tudi v razvoju podpornega okolja ([22] in [28]), ki se je od državne podpore šele v zadnjih letih močneje usmerilo na regionalni in lokalni nivo. Pomembnost regionalnega dejavnika postaja še posebno očitna v zadnjih letih. V svojih strateških dokumentih, ki veljajo podobno za velike kakor za majhne države, jih poudarja EU [30] kot tudi Slovenija [31].

S podobnim problemom so se srečevali tudi v Južni Koreji in Nemčiji. Kljub osrednje usmerjenemu korejskemu podpornemu okolju, kjer so bili programi razmeroma homogeni, pa so bili ti premalo regionalno usmerjeni. V tem primeru je prevelika osrednja (navpična) spodbuda zmanjšala možnosti regionalne spodbude [23]. Čeprav je Južna Koreja bistveno večja od Slovenije in na prvi pogled neprimerljiva, pa smo jo za primerjavo ob upoštevanju navedenih smernic EU [30] izbrali namenoma. Gre za to, da so strukturne lastnosti podpornega okolja podobne v Sloveniji, poleg tega pa je v primeru majhne države in s tem velikega števila majhnih in srednjih podjetij odvisnost od podpornega okolja še toliko večja. Kljub veliki podobnosti korejskega in nemškega modela je bil navedeni problem v Nemčiji uspešno rešen. Ta je boljše rezultate dosegla s sicer osrednjim podpornim sistemom, ki pa je uravnotežen z regionalnimi spodbudami [24]. Če primerjamo Slovenijo, lahko rečemo, da se regionalne spodbude v zadnjih letih pospešeno razvijajo, centralne pa so še vedno neusklajene in so odsev trenutnih političnih interesov. To je tudi eden temeljnih razlogov teze, da je regionalna usmerjenost za Slovenijo izredno pomembna.

Predhodne ugotovitve lahko strnemo v ključne točke, ki predstavljajo pomemben element pri izdelavi modela:

- Slovenija (še) nima jasnih strateških usmeritev, zaradi tega se kaže premajhna usmerjenost RR dejavnosti v potrebe gospodarstva.
- Slovensko podporno okolje ni ustrezno prilagojeno zahtevam prihajajočega EU prostora in dovolj regionalno usmerjeno, kar posledično zmanjšuje zmožnost prilagajanja podjetij novim izzivom.

- Neustrezen menedžment inovacijsko usmerjenih procesov v gospodarstvu in drugih organizacijah je pogosto vzrok počasnih sprememb.

2 MODEL INOVIRANJA PROCESOV

Model je zasnovan v treh korakih.

- V prvem koraku izdelamo pregledni model inoviranja procesov na ravni regije, v katerem definiramo, kaj hočemo.
- V drugem koraku določimo ključna področja in dejavnike spodbujanja inovativnih procesov. S pomočjo strateških nalog na področju inoviranja procesov v regiji opredelimo dejavnosti, ki bodo pomembno in trajno povečevale konkurenčne prednosti obravnavanega območja.
- V tretjem koraku regijo in njene dejavnosti povežemo na eni strani s podjetjem, na drugi strani pa z državnimi in evropskimi razvojnimi smernicami ter vzpostavimo povezavo z inovacijskim podpornim okoljem.

Model inoviranja procesov bomo izvedli iz modela vodenja politike podjetja po interesni teoriji in odlični kakovosti poslovanja. Temeljnemu modelu bomo dodali razsežnosti odličnosti poslovanja, inoviranje procesov, zmožnosti in možnosti podjetja ali druge organizacije za nenehno inoviranje ter vrednote, znanja, vednosti in čustva agentov sprememb.

Pregledni model inoviranja procesov bomo povezali v njegovo uresničitev - izdelavo strateškega načrta inoviranja procesov ter ga vpeli v dejanske razmere – v podporno okolje inovativnim procesom in s tem zaokrožili sliko o obravnavanem modelu.

1. korak - pregledni model inoviranja procesov

V prvem koraku izdelamo pregledni model inoviranja procesov na ravni regije, v katerem definiramo, kaj hočemo. Pri zasnovi modela inoviranja procesov (sl. 1.) smo na podlagi analize, predstavljene v uvodu, izhajali iz naslednjih zahtev ([25] in [26]):

Modularnost in uporabnost modela po delih. V večjem, bolj zapletenem podjetju ali drugi organizaciji so okoliščine poslovanja in razvoja zelo različne od okoliščin v majhnem podjetju ali drugi organizaciji, z različnimi možnostmi in za različne cilje. Uporabniki modela naj iz sistema / spleta sestavin inoviranja procesov izberejo tiste, ki po vsebini in globini obravnavanja ustrezajo njihovim takratnim potrebam.

Prilagodljivost in odprtost modela. Dana je možnost nabora različnih različic razrešitev, ki jih je mogoče preveriti in potem izbrati najbolj ustrezno.

Praktičnost modela inoviranja procesov vodi snovalca od stopnje zaznavanja do stopnje razreševanja zadeve in ga opominja na potrebne sprotne presoje in možne pasti.

Stopnje podrobnosti v modelu so takšne, da omogočajo izbiranje podrobnejšega načrtovanja inoviranja procesov.

Model je primeren za večpomenskost vidikov obravnave inoviranja procesov. Model inoviranja procesov je odvisen od ravni, na kateri bo potekal, zato ga bo treba obravnavati po ravneh politike, strategije, taktike in izvedbe ter bo stalen proces.

2. korak - določanje področij in dejavnikov spodbujanja inovativnih procesov

V drugem koraku določimo ključna področja in načine dejavnosti - kako (naj) v splošnem ravnamo. S strateškimi nalogami na področju inoviranja procesov v regiji opredelimo dejavnosti, ki bodo pomembno in trajno povečevale konkurenčne prednosti obravnavanega območja.

Za najbolj temeljno zadevo pri analiziranju dejavnosti, ki vplivajo na inoviranje procesov v regiji, določimo področja, ki so pomembna pri izdelavi regionalne inovacijske strategije (sl. 2).

To izbrano strateško in preostale naloge udeleženci kasneje opišejo in upoštevajo pri izdelavi regionalne inovacijske strategije, pri čemer naj bodo kar najbolj konkretni pri vsebini, smotrih, ciljih, merilih in kazalnikih uspešnosti inoviranja procesov.

Ko program zasnujemo, se odpre vprašanje, kdo ga bo uresničeval. Za ta del inoviranja procesov v regiji veljajo splošna načela izvedbe strateškega načrta in obsegajo dejavnosti koordiniranja, nadzorovanja, organiziranja, spodbujanja, načrtovanja in obveščanja. Potem ko bomo razrešili procesna vprašanja, pridejo v ospredje možnosti za izvedbo in se bodo kazale kot potrebna sredstva (materialna in nematerialna) ter določitev skrbnikov za posamezno strateško nalogo.

Pri ugotavljanju, kateri elementi kakovosti imajo največji vpliv na spodbujanje inoviranja procesov in pritegnitev sredstev zanje, navajajo v EU naslednje tri dejavnike [27]:

- kulturo spodbujanja inovacij,
- inoviranju naklonjene družbeno-ekonomske podlage,
- učinkovito povezovanje raziskav in inoviranja.

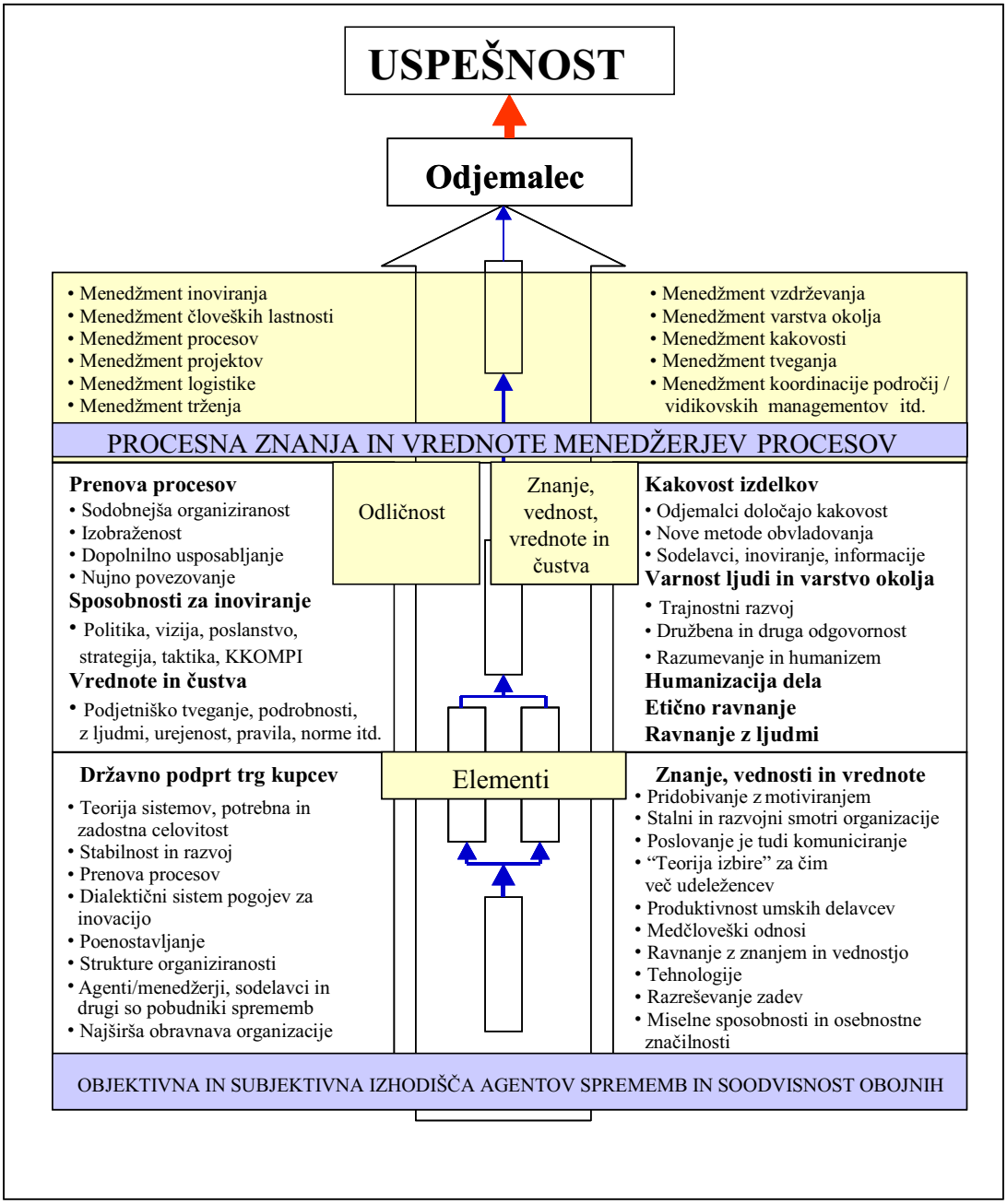

Sl.1. *Pregledni model inoviranja procesov*

Inoviranju naklonjena inovacijska kultura obsega skupne vrednote in bo temeljno sredstvo za spreminjanje procesov v regiji. Med najpomembnejšimi sredstvi za spodbujanje inovacijske kulture v regiji bodo npr. vzgoja in izobraževanje [34], pospeševanje gibljivosti prebivalcev, zavedanje prebivalcev o pomenu inoviranja za razvoj regije, usposabljanje menedžerjev in socialnih partnerjev o domiselno-inovacijskem menedžmentu, inoviranje javne uprave, spodbujanje ipd.

3.korak – povezava regije z vplivnim okoljem

V tem koraku regijo in njene dejavnosti povežemo na eni strani s podjetjem, na drugi strani pa z državnimi in evropskimi razvojnimi smernicami

Sl. 2. *Strateške dejavnosti, ki vplivajo na inoviranje proizvodnih procesov v regiji*

ter vzpostavimo povezavo z inovacijskim podpornim okoljem.

V nasprotju z različnimi osrednje (navpično) zasnovanimi modeli podpornega okolja (kar je prikazano v uvodu), bodisi na državni ali pa na regionalni ravni (ki v osredje postavljajo razvojne centre, agencije ipd., predstavljeni korak upošteva potrebe podjetja kot ključnega nosilca gospodarskega razvoja – ob upoštevanju strateških smernic Slovenije in EU. Temelji na naslednjih predpostavkah:

- Slovenija kot država si je zadala določene strateške usmeritve/področja, kjer bo ponudila različne vrste podpore.
- V vedno večji meri so te smernice povezane s strateškimi smernicami EU.
- Podjetja in druge organizacije, ki svojo poslovno strategijo gradijo v skladu s strateškimi smernicami države, bodo praviloma uspešnejša.
- Posredno (strateško) podporno okolje (vlada, ministrstva - strateške usmeritve, univerze - raziskovalno-programske smernice, RR organizacije - razvojne usmeritve ipd.) deluje predvsem v skladu s strateškimi smernicami države in se na tej ravni v manjši meri prilagaja potrebam podjetij in drugih organizacij.
- Neposredno (podjetniško) podporno okolje: uradi, razvojni centri, regionalne agencije, informacijski centri, skladi tveganega kapitala, tehnološki parki, razvojni programi RR organizacij, svetovalna in izobraževalna podpora univerz ipd. se morajo v največji meri prilagajati potrebam podjetij in drugih organizacij.
- Podjetja in druge organizacije, zlasti večje in mednarodno uspešne (tržne priložnosti) vplivajo povratno na smernice države.
- Država ima določen vpliv tudi na smernice EU. Posredno tako podjetja in druge organizacije vplivajo tudi na smernice in strateško podporno okolje EU in Slovenije.

Na vrhu piramide (sl. 3) je podjetje ali druga organizacija kot glavni tvorec dodane vrednosti gospodarstva. Vendar je smiselno, da so strategija podjetja oz. druge organizacije usklajene z usmeritvijo regije ter s strateškimi prednostmi države in posredno EU. V tem primeru lahko optimalno izkoristi podporno okolje, ki mora odražati tako smernice EU in Slovenije. Na podjetniški ravni pa se mora podporno okolje prilagajati potrebam podjetja ali druge organizacije. To še posebno velja za regionalne oblike podpore, te so praviloma podjetniško usmerjene in morajo odsevati regionalne in lokalne specifičnosti in potrebe.

3 SKLEP

Če želi biti država v svetovnem gospodarstvu uspešna, je prvi pogoj ta, da je inovacijska politika podjetja usklajena z ustrezno strateško usmeritvijo države (ki je Slovenija še nima). Naslednji korak pomeni podporno okolje, ki kaže tako strateško usmeritev države (posredno oz. osrednje podporno

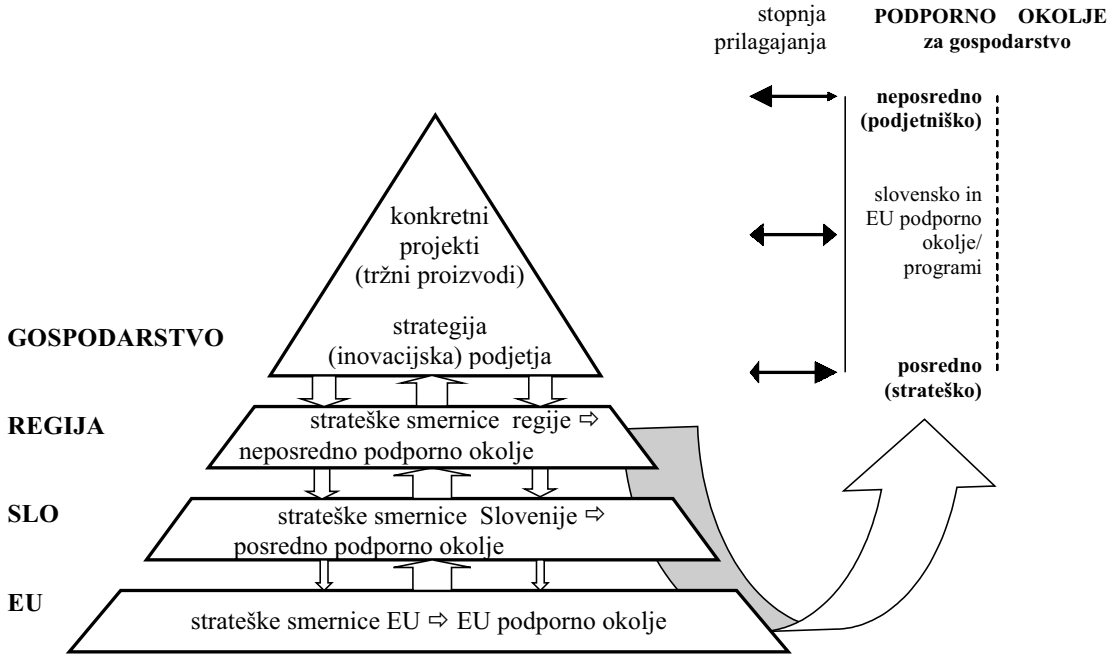

Sl. 3. *Povezava regije z vplivnim podpornim okoljem (⟷ podporno okolje se močno prilagaja gospodarskim potrebam, gospodarstvo se delno prilagaja podpornemu okolju, analogno velja za druge tipe puščic)*

okolje) kakor tudi neposredno podporno okolje, ki je v največji meri povezano z regijo. Med njimi mora potekati trajna povezava v obeh smereh, najbolj prilagodljiva mora biti na ravni podjetja oz. druge organizacije - regija, pa tudi na ravni regija - država ter država - EU. Tako bo krog sklenjen, in se bodo podjetja ter druge organizacije po eni strani usmerjali v strateško pomembna področja EU in Slovenije, po drugi strani pa bo iz tega izhajajoče podporno okolje dajalo optimalno podporo prizadevanjem in potrebam podjetij in drugih organizacij (sl. 3). V Sloveniji so te povezave še razmeroma slabo razvite, saj podporno okolje ne kaže dovolj regionalnih in lokalnih specifičnosti in potreb. Kakor ugotovimo iz modela, je problem zapleten za optimalno delovanje vsakega elementa modela (podjetja, regije, države in s tem povezanega podpornega okolja) in njihovih povezav je potreben skladen razvoj vseh dejavnikov – ob smiselni povezavi s smernicami EU. To ne pomeni, da se jim mora Slovenija slepo prilagajati (kar se v praksi pogosto dogaja), vendar jih je pametno upoštevati ob upoštevanju interesov države in gospodarstva.

Prepričani smo, da je Slovenija na dobri poti. Vendar mora previdno, a odločno, izvesti naslednji ključni korak: množico organizacij dobro postavljenega podpornega okolja spodbuditi k temu, da bodo svoje poslanstvo tudi v resnici izpolnile. Njihov prispevek mora biti jasno merljiv s kazalniki višje stopnje inovativnosti [32] in seveda z gospodarskim in socialnim napredkom slovenskih regij.

4 LITERATURA

[1] Waters, D. (1996) Operations management. *Addison-Wesley Publishers Ltd*., Belmont.
[2] Gaither, N. (1996) Production and operations management. *Duxbury Press*, Belmont.
[3] Schonberger, J. R., E. M. Knood (1997) Operations management. Customer – focused principles. Sixth edition. *Irwin*, Chicago.
[4] Mulej, M., Z. Ženko (2002) Dialektična teorija sistemov in invencijsko-inovacijski management. *Univerza v Mariboru, Ekonomsko-poslovna fakulteta*, Maribor.
[5] Hamel, G., C. L. Prahalad (1994) Competing for the future. *Harvard Business School Pres*s, Boston.

[6] Hamel, G. (2000) Leading the revolution. *Harvard Business School Press*, Boston.
[7] Peters, T. (1999) The circle of innovation. *A Division of Random House, Inc.*, New York.
[8] Pande, S. P., R. P. Newman, R. R. Cavanagh (2000) The six sigma way. *McGraw-Hill*, New York.
[9] Drucker, F. P. (2001). The essential Drucker. *HarperCollins Publishers*, New York.
[10] Moss K. R., J. Kao, F. Wiersema (1997) Innovation: breakthrough ideas at 3M, DuPont, GE, Pfizer and Rubbermaid. *Harper Collins Publishers, Inc.*, New York.
[11] Freeman, C., L. Soete (2000). The economics of industrial innovation. Third edition. *Continuum*, London in New York.
[12] Rogers M. E. (1995) Diffusion of innovations. Fourth edition. *The Free Press*, New York .
[13] http://www.cordis.lu/cordis/grnpaper.html. Green paper on innovation (1995) *European Commission* (30. 5. 2002), p.p. 38–47.
[14] Van De Ven A. (1998) Innovation. V The concise Blackwell encyclopedia of management, ur. C. L. Cooper, C. Argyris, pp. 298–300. *Blackwell Publishers Ltd.*, Oxford.
[15] Drucker, F. P. (1999) Management challenges for the 21st century. *Butterworth-Heinemann*, Oxford.
[16] Drucker, F. P. (1985) Innovation and entrepreneuership. *Harper Business*, New York.
[17] Stanovnik, P. (2000) Tehnološki razvoj kot razvojni dejavnik. Sintezno poročilo. *Inštitut za ekonomska raziskovanja*, Ljubljana.
[18] Usenik, H., M. Kos, P. Stanovnik, C. Bavec (2001) Ekspertiza: Predvidevanje tehnološkega razvoja Slovenije (PTRS). *Inštitut za ekonomska raziskovanja*, Ljubljana.
[19] Charlier, C., et. al. (2000) Pilot projects in the area of innovation promotion. *European Commission*, Brussels.
[20] Likar, B. (1999) Inovacijska in podjetniška podpora, *Naše gospod.* 45, št. 3/4, pp. 265-274.
[21] Izhodišča (2002) Izhodišča ciljnega raziskovalnega programa Konkurenčnost Slovenije 2001 – 2006.
[22] Bučar, M., M. Stare (2002) Slovenian innovation policy : underexploited potential for growth. *J. int. relat. & dev.*, 2002, vol. 5, no. 4, pp. 427-448.
[23] Hassink, R. (2001) Towards regionally embedded innovation support systems in South Korea? Case Studies from Kyongbuk–Taegu and Kyonggi. *Urban Studies*, Vol. 38, No. 8, pp. 1373–1395.
[24] Hassink, R. (2002) Regional innovation support systems: Recent trends in Germany and East Asia. *European Planning Studies*, Vol. 10, No. 2.
[25] Kralj, J. (2001). Temelji managementa in naloge managerjev. Tretja, dopolnjena izdaja. *Visoka šola za management v Kopru*, Koper.
[26] Tavčar, I. M. (1999) Razsežnosti strateškega managementa. 2. predelana izdaja. *Visoka šola za management v Kopru*, Koper.
[27] http://dbs.cordis.lu/cordis-cgi/srchidadb (19. 11. 2002).
[28] Likar, B. (2004) Mreža inovativne odličnosti mladih - model spodbujanja inovativnosti mladih = Innovative excellence for youth - creating a network to foster innovative behaviour among young Slovenes. *Stroj. vestn.*, letn. 50, št. 4, str. 239-246.
[29] Izhodišča (2002) Izhodišča ciljnega raziskovalnega programa Konkurenčnost Slovenije 2001 – 2006.
[30] Lisbon Strategy (2000) Lisbon Strategy, Reference: IP/05/338, Date: 18/03/2005. http://europa.eu.int/growthandjobs/index_en.htm, EU research maximises regional dynamics, boosts competitiveness for EU SMEs.
[31] Dolinšek, S., C. Bavec, A. Mihelič, I. Prodan (2002) Upravljanje tehnologije - ključ konkurenčnosti = The management of technology - the key to competitiveness. *Stroj. vestn.*, letn. 48, št. 3, str. 178-182.
[32] Likar, B., J. Kopač (2005) Development of innovation in modern production. V: CEBALO, Roko (ur.), SCHULZ, Herbert (ur.). *10th International Scientific Conference on Production Engineering, CIM 2005*, Lumbarda, Korčula, June 15-17, 2005. Computer integrated manufacturing and high speed machining : scientific papers. *Croatian association of production engineering*, 2005, str. VI-1-VI-6, Zagreb.
[33] Kopač, J., B. Sterle (2000) Hitra izdelava prototipov = Rapid prototyping. *Stroj. vestn.*, 2000, letn. 46, št. 2, str. 110-128.
[34] Lesjak, D., V. Sulčič, N. Trunk Širca, V. Vehovar (2004) Information and communication technology in tertiary education institutions in Slovenia : a prerequisite for e-learning. *Issues inf. syst.*, 2004, 5, 1, str. 187-193.

[35] Trček, D. (2002) Sodobne informacijske tehnologije za podporo RR dejavnosti. V: Likar B., Antunovič P., Berginc J., Černjak D. S., Demšar J., Fatur P., Križaj D., Mulej M., Pečjak V., Sitar S., Trček D., Trunk Širca N.. Uspeti z idejo! : tehnike in metode ustvarjanja, razvoja in trženja idej. *Korona plus: Pospeševalni center za malo gospodarstvo*, pp. 99-105, Ljubljana.

[36] Antončič, B., R. D. Hisrich (2003) Clarifying the intrapreneurship concept. *Journal of small business and enterprise development*, vol. 10, no. 1, str. 7-24.

Naslov avtorjev: doc.dr. Mirko Markič
doc.dr. Borut Likar
Univerza na Primorskem
Fakulteta za management
Cankarjeva 5
6000 Koper - Capodistria
mirko.markic@guest.arnes.si
borut.likar1@guest.arnes.si

Prejeto: 20.7.2004
Received:
Sprejeto: 16.11.2005
Accepted:
Odprto za diskusijo: 1 leto
Open for discussion: 1 year

Osebne vesti - Personal Events

Doktorati, magisteriji in diplome - Doctor's, Master's and Diploma Degrees

DOKTORATI

Na Fakulteti za strojništvo Univerze v Ljubljani je z uspehom zagovarjal svojo doktorsko disertacijo:

dne *14. februarja 2006*: **mag. Ciril Arkar**, z naslovom: "Parametrični model značilnic latentnega hranilnika toplote za naravno ogrevanje in hlajenje stavb".

Na Fakulteti za strojništvo Univerze v Mariboru so z uspehom zagovarjali svoje doktorske disertacije:

dne *13. februarja 2006*: **mag. Aleksander Kidrič**, z naslovom: "Vrednotenje stanja dinamičnih sistemov z uporabo genetskega programiranja";

dne *15. februarja 2006*: **mag. Sanib Bašić**, z naslovom: "Tokovne razmere v režimu mehurčkastega vrenja pri umetni tvorbi zarodnih mest";

dne *17. februarja 2006*: **mag. Filip Kokalj**, z naslovom: "Primerjava različnih turbulentnih modelov zgorevanja na primeru pilotne sežigalnice".

S tem so navedeni kandidati dosegli akademsko stopnjo doktorja znanosti.

MAGISTERIJI

Na Fakulteti za strojništvo Univerze v Mariboru so z uspehom zagovarjali svoja magistrska dela:

dne *10. februarja 2006*: **Dejan Koletnik**, z naslovom: "Analiza vpliva človeške napake na zanesljivost slovenskega prenosnega omrežja zemeljskega plina";

dne *13. februarja 2006*: **Miran Kapitler**, z naslovom: "Vpliv sosežiga odpadnih mineralnih olj na emisijo in strukturo plamena" in **Zlatko Paska**, z naslovom: "Obravnavanje hrupa v hidravličnih sistemih s frekvenčno krmiljenim pogonom";

dne *17. februarja 2006*: **Sašo Penec**, z naslovom: "Analiza kakovosti proizvodnega procesa na osnovi statističnega vrednotenja napak".

S tem so navedeni kandidati dosegli akademsko stopnjo magistra znanosti.

DIPLOMIRALI SO

Na Fakulteti za strojništvo Univerze v Ljubljani so pridobili naziv diplomirani inženir strojništva:

dne *9. februarja 2006*: Zoran BALANESKOVIĆ, Simon FINK, Robert JERIN, Uroš LOZINŠEK, Aleksander MAJDE, Igor PIRC, Adrijan PLEVNIK, Dejan TOMAŽINČIČ;

dne *14. februarja 2006*: Matjaž BREZOVAR, Lambert STRGAR.

Na Fakulteti za strojništvo Univerze v Mariboru so pridobili naziv diplomirani inženir strojništva:

dne *23. februarja 2006*: Branko HERTIŠ, Simonca ISKRAČ, Alen JAKOPIN;

dne *27. februarja 2006*: Saša TKALEC.

Strojniški vestnik - Journal of Mechanical Engineering 52(2006)3, 205-206
Navodila avtorjem - Instructions for Authors

Navodila avtorjem - Instructions for Authors

Članki morajo vsebovati:
- naslov, povzetek, besedilo članka in podnaslove slik v slovenskem in angleškem jeziku,
- dvojezične preglednice in slike (diagrami, risbe ali fotografije),
- seznam literature in
- podatke o avtorjih.

Strojniški vestnik izhaja od leta 1992 v dveh jezikih, tj. v slovenščini in angleščini, zato je obvezen prevod v angleščino. Obe besedili morata biti strokovno in jezikovno med seboj usklajeni. Članki naj bodo kratki in naj obsegajo približno 8 strani. Izjemoma so strokovni članki, na željo avtorja, lahko tudi samo v slovenščini, vsebovati pa morajo angleški povzetek.

Za članke iz tujine (v primeru, da so vsi avtorji tujci) morajo prevod v slovenščino priskrbeti avtorji. Prevajanje lahko proti plačilu organizira uredništvo. Če je članek ocenjen kot znanstveni, je lahko objavljen tudi samo v angleščini s slovenskim povzetkom, ki ga pripravi uredništvo.

VSEBINA ČLANKA

Članek naj bo napisan v naslednji obliki:
- Naslov, ki primerno opisuje vsebino članka.
- Povzetek, ki naj bo skrajšana oblika članka in naj ne presega 250 besed. Povzetek mora vsebovati osnove, jedro in cilje raziskave, uporabljeno metodologijo dela,povzetek rezulatov in osnovne sklepe.
- Uvod, v katerem naj bo pregled novejšega stanja in zadostne informacije za razumevanje ter pregled rezultatov dela, predstavljenih v članku.
- Teorija.
- Eksperimentalni del, ki naj vsebuje podatke o postavitvi preskusa in metode, uporabljene pri pridobitvi rezultatov.
- Rezultati, ki naj bodo jasno prikazani, po potrebi v obliki slik in preglednic.
- Razprava, v kateri naj bodo prikazane povezave in posplošitve, uporabljene za pridobitev rezultatov. Prikazana naj bo tudi pomembnost rezultatov in primerjava s poprej objavljenimi deli. (Zaradi narave posameznih raziskav so lahko rezultati in razprava, za jasnost in preprostejše bralčevo razumevanje, združeni v eno poglavje.)
- Sklepi, v katerih naj bo prikazan en ali več sklepov, ki izhajajo iz rezultatov in razprave.
- Literatura, ki mora biti v besedilu oštevilčena zaporedno in označena z oglatimi oklepaji [1] ter na koncu članka zbrana v seznamu literature. Vse opombe naj bodo označene z uporabo dvignjene številke[1].

OBLIKA ČLANKA

Besedilo članka naj bo pripravljeno v urejevalnilku Microsoft Word. Članek nam dostavite v elektronski obliki.

Ne uporabljajte urejevalnika LaTeX, saj program, s katerim pripravljamo Strojniški vestnik, ne uporablja njegovega formata.

Enačbe naj bodo v besedilu postavljene v ločene vrstice in na desnem robu označene s tekočo številko v okroglih oklepajih

Papers submitted for publication should comprise:
- Title, Abstract, Main Body of Text and Figure Captions in Slovene and English,
- Bilingual Tables and Figures (graphs, drawings or photographs),
- List of references and
- Information about the authors.

Since 1992, the Journal of Mechanical Engineering has been published bilingually, in Slovenian and English. The two texts must be compatible both in terms of technical content and language. Papers should be as short as possible and should on average comprise 8 pages. In exceptional cases, at the request of the authors, speciality papers may be written only in Slovene, but must include an English abstract.

For papers from abroad (in case that none of authors is Slovene) authors should provide Slovenian translation. Translation could be organised by editorial, but the authors have to pay for it. If the paper is reviewed as scientific, it can be published only in English language with Slovenian abstract, that is prepared by the editorial board.

THE FORMAT OF THE PAPER

The paper should be written in the following format:
- A Title, which adequately describes the content of the paper.
- An Abstract, which should be viewed as a mini version of the paper and should not exceed 250 words. The Abstract should state the principal objectives and the scope of the investigation, the methodology employed, summarize the results and state the principal conclusions.
- An Introduction, which should provide a review of recent literature and sufficient background information to allow the results of the paper to be understood and evaluated.
- A Theory
- An Experimental section, which should provide details of the experimental set-up and the methods used for obtaining the results.
- A Results section, which should clearly and concisely present the data using figures and tables where appropriate.
- A Discussion section, which should describe the relationships and generalisations shown by the results and discuss the significance of the results making comparisons with previously published work. (Because of the nature of some studies it may be appropriate to combine the Results and Discussion sections into a single section to improve the clarity and make it easier for the reader.)
- Conclusions, which should present one or more conclusions that have been drawn from the results and subsequent discussion.
- References, which must be numbered consecutively in the text using square brackets [1] and collected together in a reference list at the end of the paper. Any footnotes should be indicated by the use of a superscript[1].

THE LAYOUT OF THE TEXT

Texts should be written in Microsoft Word format. Paper must be submitted in electronic version.

Do not use a LaTeX text editor, since this is not compatible with the publishing procedure of the Journal of Mechanical Engineering.

Equations should be on a separate line in the main body of the text and marked on the right-hand side of the page with numbers in round brackets.

Enote in okrajšave

V besedilu, preglednicah in slikah uporabljajte le standardne označbe in okrajšave SI. Simbole fizikalnih veličin v besedilu pišite poševno (kurzivno), (npr. *v, T, n* itn.). Simbole enot, ki sestojijo iz črk, pa pokončno (npr. ms^{-1}, K, min, mm itn.).

Vse okrajšave naj bodo, ko se prvič pojavijo, napisane v celoti v **slovenskem jeziku**, npr. časovno spremenljiva geometrija (ČSG).

Slike

Slike morajo biti zaporedno oštevilčene in označene, v besedilu in podnaslovu, kot sl. 1, sl. 2 itn. Posnete naj bodo v ločljivosti, primerni za tisk, v kateremkoli od razširjenih formatov, npr. BMP, JPG, GIF. Diagrami in risbe morajo biti pripravljeni v vektorskem formatu.

Pri označevanju osi v diagramih, kadar je le mogoče, uporabite označbe veličin (npr. *t, v, m* itn.), da ni potrebno dvojezično označevanje. V diagramih z več krivuljami, mora biti vsaka krivulja označena. Pomen oznake mora biti pojasnjen v podnapisu slike.

Vse označbe na slikah morajo biti dvojezične.

Preglednice

Preglednice morajo biti zaporedno oštevilčene in označene, v besedilu in podnaslovu, kot preglednica 1, preglednica 2 itn. V preglednicah ne uporabljajte izpisanih imen veličin, ampak samo ustrezne simbole, da se izognemo dvojezični podvojitvi imen. K fizikalnim veličinam, npr. *t* (pisano poševno), pripišite enote (pisano pokončno) v novo vrsto brez oklepajev.

Vsi podnaslovi preglednic morajo biti dvojezični.

Seznam literature

Vsa literatura mora biti navedena v seznamu na koncu članka v prikazani obliki po vrsti za revije, zbornike in knjige:

[1] A. Wagner, I. Bajsić, M. Fajdiga (2004) Measurement of the surface-temperature field in a fog lamp using resistance-based temperature detectors, *Stroj. vestn.* 2(2004), pp. 72-79.

[2] Vesenjak, M., Ren Z. (2003) Dinamična simulacija deformiranja cestne varnostne ograje pri naletu vozila. *Kuhljevi dnevi '03*, Zreče, 25.-26. september 2003.

[3] Muhs, D. et al. (2003) Roloff/Matek Maschinenelemente – Tabellen, 16. Auflage. *Vieweg Verlag*, Wiesbaden.

Podatki o avtorjih

Članku priložite tudi podatke o avtorjih: imena, nazive, popolne poštne naslove in naslove elektronske pošte.

SPREJEM ČLANKOV IN AVTORSKE PRAVICE

Uredništvo Strojniškega vestnika si pridržuje pravico do odločanja o sprejemu članka za objavo, strokovno oceno recenzentov in morebitnem predlogu za krajšanje ali izpopolnitev ter terminološke in jezikovne korekture.

Avtor mora predložiti pisno izjavo, da je besedilo njegovo izvirno delo in ni bilo v dani obliki še nikjer objavljeno. Z objavo preidejo avtorske pravice na Strojniški vestnik. Pri morebitnih kasnejših objavah mora biti SV naveden kot vir.

Units and abbreviations

Only standard SI symbols and abbreviations should be used in the text, tables and figures. Symbols for physical quantities in the text should be written in italics (e.g. *v, T, n,* etc.). Symbols for units that consist of letters should be in plain text (e.g. ms^{-1}, K, min, mm, etc.).

All abbreviations should be spelt out in full on first appearance, e.g., variable time geometry (VTG).

Figures

Figures must be cited in consecutive numerical order in the text and referred to in both the text and the caption as Fig. 1, Fig. 2, etc. Pictures may be saved in resolution good enough for printing in any common format, e.g. BMP, GIF, JPG. However, graphs and line drawings sholud be prepared as vector images.

When labelling axes, physical quantities, e.g. *t, v, m,* etc. should be used whenever possible to minimise the need to label the axes in two languages. Multi-curve graphs should have individual curves marked with a symbol, the meaning of the symbol should be explained in the figure caption.

All figure captions must be bilingual.

Tables

Tables must be cited in consecutive numerical order in the text and referred to in both the text and the caption as Table 1, Table 2, etc. The use of names for quantities in tables should be avoided if possible: corresponding symbols are preferred to minimise the need to use both Slovenian and English names. In addition to the physical quantity, e.g. *t* (in italics), units (normal text), should be added in new line without brackets.

All table captions must be bilingual.

The list of references

References should be collected at the end of the paper in the following styles for journals, proceedings and books, respectively:

[1] A. Wagner, I. Bajsić, M. Fajdiga (2004) Measurement of the surface-temperature field in a fog lamp using resistance-based temperature detectors, *Stroj. vestn.* 2(2004), pp. 72-79.

[2] Vesenjak, M., Ren Z. (2003) Dinamična simulacija deformiranja cestne varnostne ograje pri naletu vozila. *Kuhljevi dnevi '03*, Zreče, 25.-26. september 2003.

[3] Muhs, D. et al. (2003) Roloff/Matek Maschinenelemente – Tabellen, 16. Auflage. *Vieweg Verlag*, Wiesbaden.

Author information

The information about the authors should be enclosed with the paper: names, complete postal and e-mail addresses.

ACCEPTANCE OF PAPERS AND COPYRIGHT

The Editorial Committee of the Journal of Mechanical Engineering reserves the right to decide whether a paper is acceptable for publication, obtain professional reviews for submitted papers, and if necessary, require changes to the content, length or language.

Authors must also enclose a written statement that the paper is original unpublished work, and not under consideration for publication elsewhere. On publication, copyright for the paper shall pass to the Journal of Mechanical Engineering. The JME must be stated as a source in all later publications.